

PUBLISHER

On Behalf of Textile and Apparel Research
Application Center

Faruk BOZDOĞAN

EDITOR IN CHIEF

Arif Taner ÖZGÜNEY
arif.taner.ozguney@ege.edu.tr

ASSOCIATE EDITORS

Mehmet KÜÇÜK
mehmet.kucuk@ege.edu.tr
Pelin SEÇİM KARAKAYA
pelinsecim@mail.ege.edu.tr

EDITORIAL BOARD

Ahmet ÇAY
Esen ÖZDOĞAN
Gözde ERTEKİN
Hale KARAKAŞ
Hüseyin Aksel EREN
Nilgün ÖZDİL

ENGLISH EDITING SERVICE

Mengü Noyan ÇENGEL

SCIENTIFIC ADVISORY BOARD

Andrej DEMŠAR
Arzu MARMARALI
Bojana VONČINA
Bülent ÖZİPEK
E. Perrin AKÇAKOCA KUMBASAR
Ender BULGUN
Hüseyin KADOĞLU
Mirela BLAGA
Oktay PAMUK
Ozan AVİNÇ
Peter J. HAUSER
Recep EREN
Rıza ATAV
Savvas G. VASSILIADIS
Turan ATILGAN

ABSTRACTING / INDEXING

Science Citation Index Expanded (SCIE)
Scopus
WOS
EBSCO
TR Dizin
Ulakbim

TYPESETTING AND PRINTING

META Basım Matbaacılık Hizmetleri
+90 232 343 64 54 / E-mail: metabasim@gmail.com
Printed Date: 30 December, 2021

Investigating the Effect of Fabric and Lamination-Foam Properties on the Air Permeability of Laminated Headrest Fabrics
Seray Aksoy, Semih Ertürk, Cemil Işlak, Diren Mecit, Semih Oylar 235

Prototype Design and Manufacture of the New Generation Highly Automated Brushing Machine in Home Textile
İlker Ertuna, Mustafa İnalöz, Nazlı Yoldaşoğlu, Fatma İpek,
Aslı Atar, Ali Küçükpetek, Ceren Göde..... 242

DSS-Based Process Control and FMEA Studies for Different Processes in the Field of Textile
Yeliz Buruk Sahin, Ezgi Aktar Demirtaş 250

Development of Multifunctional Bio-based Cotton Composite
Emine Altınkaya 264

Synthesis and Characterization of Polyvinylimidazole and Investigation of its Antipilling Effect on Different Fabrics
Burcu Büyükkoru, Ali Kara 274

Investigation of Stretch Properties of Different Stitch Types in Garments Made of Elastane Woven Fabrics
Kıvanç Geleri, Ayça Gürarda, Erhan Kenan Çeven..... 284

Study on Single Jersey Knitted Fabrics Made from Cotton/ Polyester Core Spun Yarns. Part I: Thermal Comfort Properties
Vidhya M, Parveen Banu, Vasanth Kumar, Prakash C, Subramaniam V 295

One-Bath Dyeing and Finishing Process of Polyester Fabrics
Gamze Gülşen Bakıcı, Füsün Doba Kadem..... 306

A New Objective Method for Comfort Assessment of Sportswear Knitted Fabrics
Esin Babalık, Sinem Güneşoğlu, Burçin Ütebay,
Ayşegül Çetmeli Cem Güneşoğlu 318

CONTACT

Ege Üniversitesi Tekstil ve Konfeksiyon Araştırma-Uygulama Merkezi
35100 Bornova – İzmir, TÜRKİYE
Tel: +90 232 311 38 89-83

www.dergipark.gov.tr/tekstilvekonfeksiyon
E-mail: tekstilvekonfeksiyon@mail.ege.edu.tr



Investigating the Effect of Fabric and Lamination-Foam Properties on the Air Permeability of Laminated Headrest Fabrics

Seray Aksoy¹  0000-0001-6792-6156

Semih Ertürk¹  0000-0002-0002-4075

Cemil Işılak¹  0000-0003-3677-4027

Diren Mecit²  0000-0002-3760-3417

Semih Oylar²  0000-0002-5052-7463

¹Tofaş / Yeni Yalova Yolu Cad. No:574 Bursa / Türkiye

²Martur / Nilüfer Organize Sanayi Bölgesi 302. Sok. No.1 Bursa / Türkiye

Corresponding Author: Seray Aksoy, seray.aksoy@tofas.com.tr

ABSTRACT

In the automotive industry, the interior component, which the customer first encounters is the seat. Customers have many expectations in terms of aesthetics, functionality, and comfort from the seats of the vehicle. When considering comfort in car seats, it is the backrest, cushion, headrest foam, and upholstery which are placed at the top the list. The seat upholstery in the vehicle has a composite structure including fabric, lamination foam, and backing scrim. This composite structure is combined with seat foam by using techniques such as traditional method or in-situ technology. In the traditional method, the upholstery is trimmed on the product's foam. In in-situ technology, polyurethane (PU) is injected into ready-placed upholstery. The advantage of in-situ technology is to make perfect trimming for curved foam designs. Concave shapes are more achievable with in-situ production techniques, which adds to the safety and comfort of the headrest. In this in-situ process, an overflow failure may occur on the surface of the upholstery, when foam is injected (PU) with high pressure during the process. Overflow failure is not desired by the main automobile producers, from both aesthetical and quality aspects. In this study, the effect of lamination-foam and fabric on the air permeability of composite structures used in in-situ headrests was investigated. The surface structure of the in-situ headrest was also analyzed via stereo microscope. In order to evaluate the overflow behavior of PU injected foam, the weight, peeling strength, and air permeability of fabric and lamination foam types were tested. As a result of this study, it was observed that the air permeability of the laminated fabrics has an effect on the overflow failure on the headrest.

1. INTRODUCTION

Automotive textiles have a large share in the global technical textiles market, which is comprised of seat upholstery, floor covering, headliners, door coverings, pillar coverings, safety belts, side panel coverings, airbags, tires, sound, and thermal insulators [1,2]. Automotive

interior textiles are usually made of woven, warp knitted, weft knitted, laminated and nonwoven fabrics [3,4]. The seat upholsteries are of great importance, due to their effect on the driver and passenger comfort, and also the aesthetic appeal of the interior scheme. A summary of the properties required from car seat upholsteries was shown in Table 1.

ARTICLE HISTORY

Received: 19.10.2020

Accepted: 14.09.2021

KEYWORDS

Lamination process, in-situ method, air permeability, stereo microscope, car headrest

To cite this article: Aksoy S, Ertürk S, Işılak C, Mecit D, Oylar S. 2021. Investigating the effect of fabric and lamination-foam properties on the air permeability of laminated headrest fabrics. *Tekstil ve Konfeksiyon*, 31(4), 235-241.

Car seat upholstery is generally made of different structures. The one layer of seat upholstery is the lamination foam, mostly made of PU due to the comfort and protection level served by PUs which is not achieved by any other single structure [5]. Lamination foams made of PU are generally obtained by reacting an isocyanate with polyols in the existence of blowing agents [6]. The second part is the face fabric, which is mainly a woven or knitted polyester fabric. Another part of seat upholstery is the backing scrim that is generally produced of polyester or polyamide [7,8]. Seat upholstery fabrics used as trilaminar structures were shown in Figure 1.

Table 1. Requirements on upholstery materials for car seat [4].

Seat Requirement	Important	Very Important
Optic / Aesthetic		
- Touch		⊗
- Color		⊗
- Brightness / Dullness		⊗
- Price		⊗
Resistant to wear and load		⊗
- Light fastness		⊗
- Abrasion resistance		⊗
- Pilling resistance		⊗
- Color fastness	⊗	⊗
- Tenacity / Elongation		⊗
- Dimensional stability		⊗
Resistant to ageing	⊗	⊗
- Light resistant		
- Temperature resistant	⊗	
- Industrial production (Flexibility)	⊗	
Soil resistant – easy to clean	⊗	
- Soil resistance	⊗	
- Cleaning ability	⊗	
Seat comfort		⊗
- Surface softness		
- Humidity absorption		
- Humidity transport		
- Static charge		
Recycling		

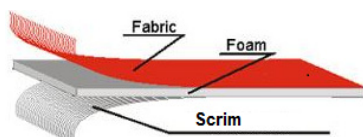


Figure 1. Trilaminar seat upholstery structure [9]

In the lamination process, PU-based lamination foams are laminated to the fabric by different methods. This process provides functionality and additional technical performance to the final composite products, which can not be achieved by using a single layer [10-12]. There are three types of

lamination processes such as flame lamination, hot-melt lamination, and powder laminating. However, the most used method in the automotive sector is flame lamination process as it has lower costs and large production volumes compared to other methods [13]. In the flame lamination process, a foam layer is exposed to an open flame around 950°C, which causes its top surface to melt. While the foam is molten, it is fed into lamination machine, and as a result, layers are combined. Thanks to this method, flexible laminated fabrics are produced [3]. Hot-melt lamination can be operated by means of an engraving roller or a nozzle in the form of slots. The hot-melt of the polymer binder (commonly copolyamides, copolyesters, PUs, and polyethylene) is fed from the extruder by means of squeegees into the grooves of the engraving cylinder [14]. In powder laminating, the foam is applied as a binder powder over the entire width by means of a sieve template or by spreading. Textiles or the foam travels to the dryer, where the powder is gelled and it combines with other textiles. This is followed by compressing and cooling processes [15, 16].

Automotive seat commonly consists of three components such as cushion, backrest and headrest. The seat upholstery (consisting of fabric, laminated foam and scrim), whose lamination process has been completed as described above, must be combined with seat foams (cushion, backrest and headrest) in order to become the final product. For combining seat headrest foam and seat upholstery either traditional methods or in-situ technology can be used. The traditional method is widely used, and it is formed by combining the seat upholstery on seat headrest foam by methods such as sewing and trimming. Unlike the traditional method in the in-situ (pour-in-place) technology the upholstery is firstly formed, afterwards the PU liquid is poured into the upholstery and the final product is produced. As in-situ technology allows production of complex shaped headrests, it is expected that this technology will replace the traditional methods [17].

The main factors effecting the properties of final in-situ headrest are the components and their characteristics used in the process and in-situ process parameters. The upholstery and poured foam are the major two components. The properties of upholstery such as permeability, porosity, elongation and trimmability influence the in-situ process performance and as a result final headrest quality.

Air permeability is one of the most important property of textile materials that ensure their comfort. The air permeability of textile fabrics depends on many parameters of fabric structure [18]. The structure of a textile contains pores between the fibers. Airflow through textiles is mainly effected by the pore characteristics of the fabrics. It is quite clear that pore dimension and distribution is a function of the fabric geometry. The yarn diameter, surface formation techniques, number of yarn for woven fabrics (yarn density), and number of loop count for knitted fabrics per unit area are the main factors affecting the porosity of

textiles. The porosity of a fabric is connected with certain important features of it, such as air permeability, water permeability, etc [19-21].

In this study, it was aimed to investigate the effect of lamination foam and fabric on the air permeability and surface structure (by evaluating the overflow) of in-situ headrests. In the first step of the study, the weight and air permeability of the seat fabric and lamination foam have been measured before and after lamination process. The peeling strength of laminated fabrics also have been measured. Afterwards PU injection has been realized. Images of final headrests have been taken by stereo microscope to compare overflow failure behaviour of headrest and its relation with the air permeability test results.

MATERIAL AND METHOD

2.1 Material

Within the scope of the study, 3 types of laminated automotive upholstery fabrics were produced from 100% PET (Polyethylene-terephthalate) yarns. Two of the fabrics produced are woven and one is warp knitted fabric. Three types of laminated automotive upholstery fabric were laminated with two different PU lamination foams. Six fabric variants were obtained in the study. Information of fabric variants was shown in Table 2.

Table 2. Fabric variations produced in the study

Fabric Type	Lamination Foam
woven fabric 1	laminated foam 1
woven fabric 1	laminated foam 2
woven fabric 2	laminated foam 1
woven fabric 2	laminated foam 2
warp knitted	laminated foam 1
warp knitted	laminated foam 2

2.1.1 Production of fabrics

In the study, woven fabric 1 and woven fabric 2 samples were produced on dobby weaving machines, and the warp knitted fabric sample was produced on tricot warp knitting machine. All of the yarns used in the production phase are obtained from 100% PET polymer in accordance with

automotive standards. Some construction information of woven and knitted fabrics were shown in Table 3 and Table 4.

2.1.2 Finishing processes applied to the produced fabrics

The same finishing processes were applied to all fabrics produced. A washing process was applied to remove the dust, oil and oligomers that occur during the production phase of the yarns and fabrics. Then, a process using temperature and chemical/mechanical ordering was carried out in a Stenter machine, which achieves width-length stabilization of the fabrics, followed by flame lamination. The gas pressure, machine speed, distance between the cylinders and the thicknesses at the entrance/exit of the machine were constant for all flame-lamination processes. 2 different lamination foams were used in the study. The fabrics produced were cut in the cutting machine and stitched in the sewing machine to be turned into an automotive headrest upholstery cover. As a result of these productions, finally 6 different laminated foam structures as upholstery cover were produced from six different laminated fabrics.

2.1.3 In-situ process

After the cutting and sewing processes, the final laminated headrest upholstery covers were injected with foam through the in-situ process. In the in-situ process, the polyol and isocyanate materials were fed from separate feeding units. In the meantime, previously sewn and prepared headrest upholstery covers were placed in the closed mold that will form the shape of the final product. The mouth of the mold is designed to contain an opening for foam feeding inlet. After the foam was poured into the mold in the determined weight, it expands among the mold and fills the inside of the fabric cover. Injected foam, which expands to the size allowed by the closed mold, formed as the final form of the headrests. Parameters such as foam hardness and density were determined by the ratio of polyol and isocyanate in the formulation. There are two different method for the in-situ process. The vertical method is applied for complex geometries whereas the horizontal method is used for basic geometries. In this study, the horizontal production method was applied for the in-situ process of all samples due to the basic shape of the headrest. All variables in the in-situ process were kept constant for the production of all samples. The components of headrests are shown in Figure 2.

Table 3. Woven fabrics' construction information

b	Yarn Type	Weave unit	Weft Yarn Type (denier)	Warp Yarn Type (denier)	Number of Filament	Warp Density (yarn/cm)	Weft Density (yarn/cm)
Woven fabric 1	Friction Texturised	2x2 twill	PET 450	PET 450	144	24	18
Woven fabric 2	Friction Texturised	2x2 twill	PET 300	PET 450	144	28	19

Table 4. Warp knitted fabric construction informations

Yarn Type	Number of Filament	Machine Fineness (F/inch)	Course Density (C/cm)
PET 100 denier	36	28 fein	20-22

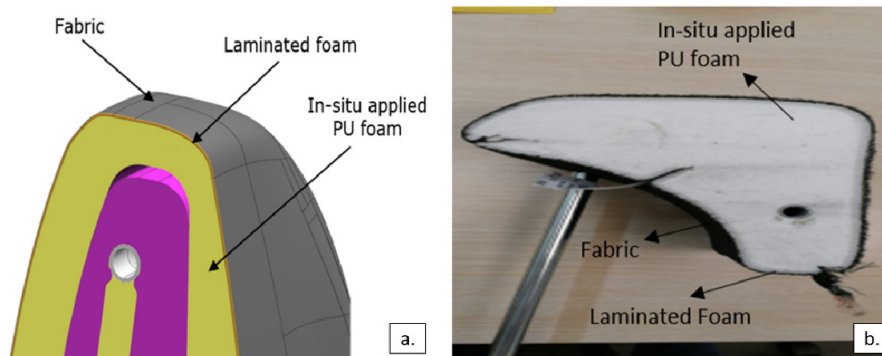


Figure 2. Headrest components a. Schematic image of headrest b. Real image of headrest

2.2 Method

2.2.1 Performed tests on laminated upholstery fabrics

Unit mass

Unit mass of face fabrics, foams and final laminated fabrics were tested according to the TS EN 12127 standard. Total weight was measured, then the laminated layers were separated and measured separately. Five samples having 100 cm² area were taken from each type of materials and their weights were measured. The mean value per square meter weight was calculated.

Peeling Strength

After the flame lamination process, the peeling strength of the upper surface fabric to the lamination materials was tested in the Zwick test machine for length and width directions of the fabric according to FIAT 50441/05 standard. According to the FIAT 9.55441 specification, the adhesion strength of the upper surface fabric and the lamination material to each other must be equal to or greater than 0.8 daN. If peeling strength between the two layers is intense, manual separation cannot be performed at the beginning of the test and the test result is stated as "no separation" (NS).

Air permeability

In this study air permeability of non-laminated face fabrics, foams, and laminated fabrics were measured. The air permeability property has been measured according to the TS 391 EN ISO 9237. This method is being used for all types of fabrics, including industrial fabrics, nonwovens, and textiles [22, 23]. The basic principle of the air permeability test is that the velocity of the airflow in the vertical direction through a given area of the fabric is measured at the pressure difference within the test area of the fabric in a given time range. The air permeability is defined as the speed of the air passing in the vertical direction through a part of the test with determined conditions such as test area, pressure drop, and time in the

vertical direction. During the test, pressure of 200 Pa was applied on to the area of 20 cm². Ten measurements were done for each group. The arithmetic means and % CV (Coefficient of variation) of the measurements taken were calculated and reported.

2.2.2 Performed tests on final products after the in-situ process

Observing samples with Stereo Microscope

The ZEISS / Stemi 508 Zoom Microscope device used in this study, which is used to observe metal, plastic, and textile materials, provides a wide range of images between 40X and 100X. In this study, the area where the driver's head touches the headrest during driving was observed.

3. RESULTS AND DISCUSSION

3.1 Unit mass results

The weights of the face fabrics (unlaminated) and foams (Sample W1-W2-WK-F1-F2) before lamination and the weights of the laminated foams and fabrics (Sample L1-L2-L3-L4-L5-L6) after the lamination process were shown in Table 5.

According to the unit mass measurements, it was seen that warp knitted fabric had the lightest weight, whereas woven fabric 2 had the heaviest weight. It was also determined that lamination foam 1 was lighter than lamination foam 2. Laminated fabric test results showed that lamination foam 2 lost some weight after lamination process while lamination foam 1 did not lose weight.

3.2 Peeling strength results

The peeling strength between the fabrics and the foams were measured. As can be seen in Figure 3, no separation was observed from any of the samples. During the adhesion test of these materials, crumbling is observed in the foams after the attraction force applied for separation. No separation means that there is good adhesion between the fabric and foam for all samples.

Table 5. Unit mass of samples

Fabric Type	Laminated Foam	Total Weight (g/m ²)	Fabric (g/m ²)	Foam (g/m ²)	Samples Codes
woven fabric 1	-	-	268	-	W1
woven fabric 2	-	-	275	-	W2
warp knitted	-	-	216	-	WK
laminated foam 1	-	-	-	177	F1
laminated foam 2	-	-	-	185	F2
woven fabric 1	laminated foam 1	444	265	179	L1
woven fabric 1	laminated foam 2	438	270	168	L2
woven fabric 2	laminated foam 1	451	272	179	L3
woven fabric 2	laminated foam 2	450	272	178	L4
warp knitted	laminated foam 1	393	210	183	L5
warp knitted	laminated foam 2	375	215	160	L6

**Figure 3.** The samples subjected to tensile force during the adhesion test

3.3 Air permeability test results

The air permeability results of fabrics were shown in Table 6.

Table 6. Air permeability test results of structures

Samples	Mean (mm/s)	% CV (mm/s)
W1	178.2	2.6
W2	129.5	2.8
WK	1353	1.6
F1	95.4	9.6
F2	63.2	16.6
L1	69.1	8.5
L2	77.6	7
L3	64.4	16
L4	74.9	16.7
L5	107.8	15.4
L6	151.6	15.2

In Table 6 the highest air permeability result belongs to WK, as warp knitted fabric have more porosity in the structure than the woven fabrics. When woven fabrics are compared, it is observed that the air permeability of W1 is higher than that of W2 due to the lower warp density of W1

than W2. Comparison of lamination foams showed that F1 is more permeable than F2. When the air permeability of laminated fabrics compared, it was observed that laminated warp knitted fabrics (L5, L6) have higher air permeability than that of laminated woven fabrics (L1, L2, L3, L4). This result showed that the porosity structure of warp knitted fabric caused to a more permeable final product. When the results of woven fabrics compared, there was not seen any difference between the results of fabrics laminated with W1 (L1, L2) and that of fabrics laminated with W2 (L3, L4). These results mean although there is a small difference between the air permeability of woven fabrics (W1, W2), it was not observed in final laminated fabrics (L1, L2, L3, L4).

3.4 Stereo Microscope Results

The 40X images taken with stereo microscope from the final product headrests injected with PU by in-situ technology was shown in Figure 4. Although it has a wide imaging range of stereo microscope, the value at which PU overflow failures can be observed was determined as 40X. Therefore this magnification was used in the measurements.

It was seen from Figure 4 that there is no PU overflow failure was observed in L1 (a.), L2 (b.), L3 (c.) and L4 (d.), whereas there are PU overflow failures at observed samples L5 (e.) and L6 (f.). The observation of overflow failures on L5 and L6 can be a result of the higher permeability and porosity of the warp knitted fabrics as both L5 and L6 samples were produced with warp knitted fabric.

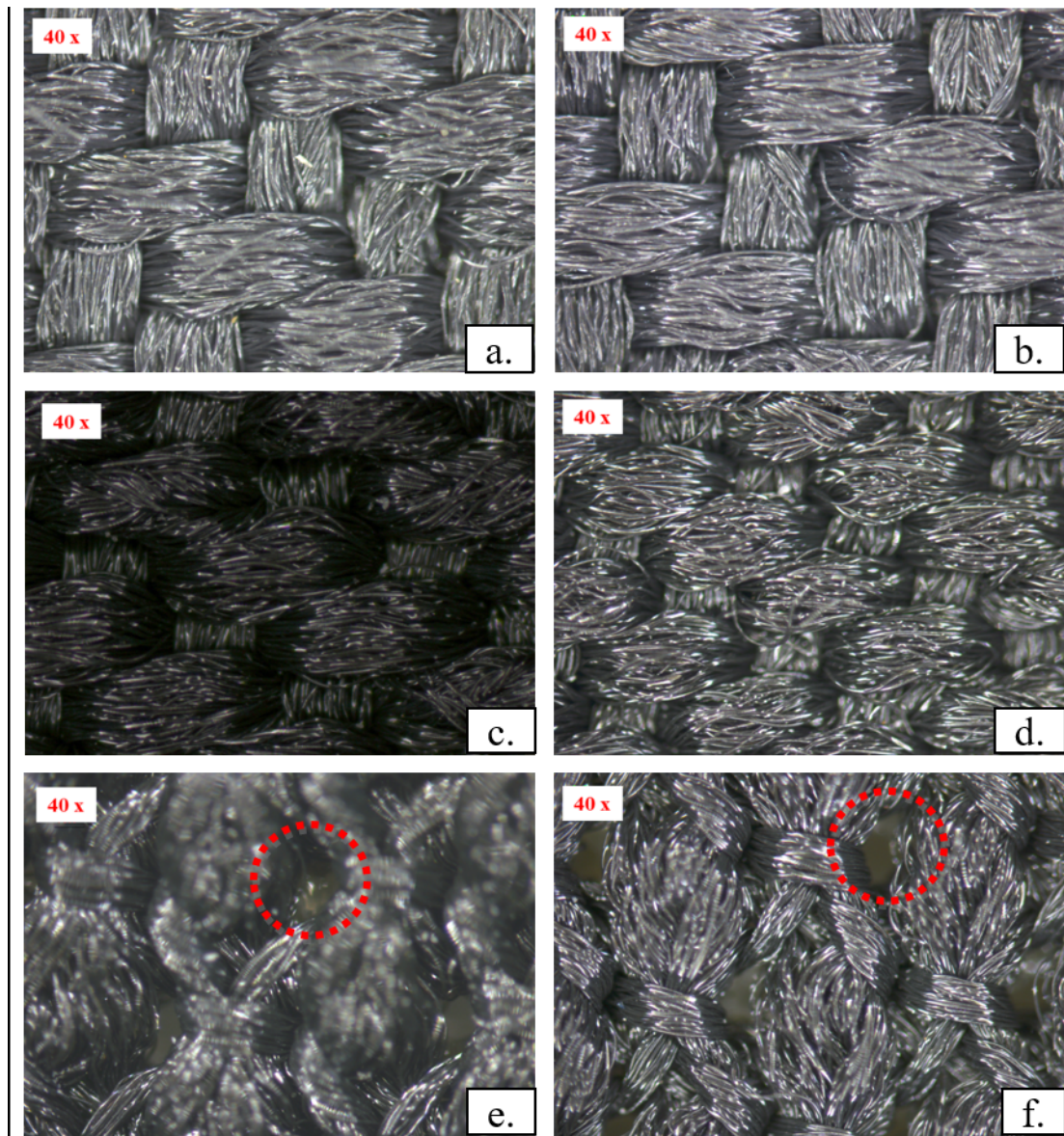


Figure 4. 40X zoom image of samples a. L1 sample b. L2 sample c. L3 sample d. L4 sample e. L5 sample f. L6 sample

4. CONCLUSION

In this study; the weight, air permeability and adhesion of laminated layers have been analyzed and evaluated in order to predict the over-flow behavior of foam during the in-stu process.

Comparison of air permeability and weight results of individual layers showed that the heavier fabric and foam has the less air permeability (see Table 5). However the comparison of air permeability and weight results after lamination showed the opposite result. The same fabrics, which were laminated with F2, showed more air permeability than that of laminated with F1, even though the F2 layer's weight was higher than the F1 layer's before lamination. The comparison of burned foam weights showed that F2 lost weight during the flame lamination process.

As a result, it can be concluded that the laminated fabrics, which have a higher weight, have lower air permeability.

No difference was observed between the peeling test results of all fabrics. Therefore any relation between peeling strength and the over-flow failure in the in-stu process was not found.

Analysis of stereo microscope images showed that over-flow failure was observed on the warp knitted fabrics, whereas none was observed on the surface of the woven fabrics. This may be a result of either fabric construction type or total fabric weight.

As a result of this study it can be concluded that air permeability and the weight of the fabric have a remarkable effect on the final quality of the in-stu process in respect of overflow existence. In conclusion, fabrics which have lower weights may cause more overflow failure due to a higher air permeability.

Air permeability of 100 mm/s should be set as a limit value for this process in order to avoid overflow failure.

REFERENCES

1. Elmogahzy YE. 2020. Performance characteristics of technical textiles: Part II: Transportation textiles. *Engineering Textiles*. Cambridge: Woodhead, 365-398. ISBN 9780081024881.
2. Kovalova N, Kulhyvy P, Vosahlo J, Havelka A. 2019. Experimental and numerical study of sewing seams of automobile seat covers under unidirectional and multiaxial loading. *Tekstil ve Konfeksiyon* 29(4), 322-335.
3. Ömeroğulları BZ. 2019. Improvement of multifunctional automotive textile. *Tekstil ve Konfeksiyon* 29(2), 113-120.
4. Jerkovic I, Pallarés JM, Ardanuy M, Capdevila X. 2013. Abrasive elements and abrasion resistance tests for car seat upholstery. *Journal of Engineered Fibers and Fabrics* 8(3), 35-41.
5. Deng R, Davies P, Bajaj AK. 2003. Flexible polyurethane foam modelling and identification of viscoelastic parameters for automotive seating application. *Journal of Sound and Vibration* 262(3), 391-417.
6. Moon J, Kwak SB, Lee JY, Kim D, Ha JU, Oh JS. 2019. Synthesis of polyurethane foam from ultrasonically decrosslinked automotive seat cushions. *Waste Management* 85(2019), 557-562.
7. Fung W. 2000. *Textiles in automotive engineering*. Cambridge: Woodhead. ISBN 1855734931.
8. Haroglu D, Powell N, Seyam AFM. 2017. A textile-based optical fiber sensor design for automotive seat occupancy sensing. *The Journal of the Textile Institute* 108(1), 49-57.
9. Oylar S, Mecit D. 2019 A study about the effect of weft yarn parameters on the physical parameters of automotive upholstery fabrics. 19th World Textile Conference Textiles at the Crossroads (AUTEX 2019), Ghent, Belgium.
10. Shim E. 2019. Coating and laminating processes and techniques for textiles In Smith WC (Ed.). *Smart Textile Coatings and Laminates*. Swastan, UK: Woodhead, 11-45.
11. Bulut Y, Sülar V. 2010. Kaplama veya laminasyon teknikleri ile üretilen kumaşların genel özellikleri ve performans testleri. *Tekstil ve Mühendis* 15(71), 5-16.
12. Singha K. 2012. A review on coating & lamination in textiles: processes and applications. *American Journal of Polymer Science* 2(3), 39-49.
13. Aksoy S, Erbil S, Dağdeviren M. 2020 August. Investigation of Lamination Thickness of Seat Upholstery Effect on Seat Heater Pad Performance. 9th International Conference on Advanced Technologies (ICAT'20), Istanbul, Turkey.
14. Batič E, Gorjanc DŠ. 2021. Characteristics of laminates for car seats. *AUTEX Research Journal*, 21(4), 4-5. 379-392
15. Chapman R. 2010. Applications of nonwovens in technical textiles. *Woodhead Publishing Limited* (Oxford), 3-16.
16. Singha K. 2012. A review on coating & lamination in textiles: processes and applications. *American Journal of Polymer Science*, 2(3): 39-49
17. Glenn GM, Orts WJ, Nobes GAR, Gray GM. 2001. In situ laminating process for baked starch-based foams. *Industrial Crops and Products* 14(2), 125-134.
18. Fatahi I, Yazdi AA. 2010. Assessment of the relationship between air permeability of woven fabrics and its mechanical properties. *Fibres and Textiles in Eastern Europe* 6(83), 68-71.
19. Cay A, Vassiliadis, S., Rangoussi, M., Tarakcioglu I. 2004. On the use of image processing techniques for the estimation of the porosity of textile fabrics. *International Journal of Signal Processing*, 1(1), 51-54.
20. Cay A, Tarakcioglu I. 2008. Relation between fabric porosity and vacuum extraction efficiency: Energy issues. *Journal of the Textile Institute*, 99(6), 499-504.
21. Ogulata, RT, Mavruz S. 2010. Investigation of porosity and air permeability values of plain knitted fabrics. *Fibres & Textiles in Eastern Europe*, 18 (5(82)), 71-75.
22. Ogulata RT, Mezarcioz S. 2012. Total porosity, theoretical analysis, and prediction of the air permeability of woven fabrics. *Journal of the Textile Institute* 103(6), 654-661.
23. Padleckiene I., Petrusis D. 2008. The change of air permeability and structure of breathable-coated textile materials after cyclic stretching. *Materials Science (Medžiagotyra)* 14(2), 162-165. ISSN 1392-1320.



Prototype Design and Manufacture of the New Generation Highly Automated Brushing Machine in Home Textile

İlker Ertuna¹  0000-0001-5388-6819

Mustafa İnalöz¹  0000-0002-0913-4617

Nazlı Yoldaşoğlu¹  0000-0003-2884-0573

Fatma İpek¹  0000-0002-4043-3172

Aslı Atar¹  0000-0003-0708-8845

Ali Küçükpetek¹  0000-0003-2728-101X

Ceren Göde²  0000-0001-6819-4620

¹Menderes Tekstil Department of R&D Center, Denizli

²Pamukkale University Department of Machinery and Metal Technologies

Corresponding Author: Fatma İpek, fatmaipek@arge.menderes.com

ABSTRACT

Brushing/Raising is one of the important physical process. Raising, which is one of the mechanical finishing processes, is based on the principle of creating a feathered surface by taking out of the fibers from the threads to the fabric surface. It is a process that changes appearance, touch and usage characteristics of the fabric. It gives volume, saturation and soft effect to the fabric. The ability of fabric to be resistant to physical effects is only possible with the high mechanical properties of the fabric. However, it is a sensitive process because it causes weight and strength reduction in the fabric. Desired raising effect can not be obtained with single pass in current brushing machines and, due to process recurrence: Loss of strength, energy and extra labor cost are experienced. Mechanical and electrical components in existing machines are frequently malfunctioning due to inadequate design and material quality and work inefficiently. The quality of the fabric produced on current machines is low and due to the lack of automation, the second quality ratio is high.

The highest quality flannel fabric of the world was produced with the newly designed machine. While the new generation of brushing machine has many innovative aspects compared to existing machines, the most important innovation is to achieve homogeneous, efficient and effective raising effect in a single pass. This superior effect was achieved with the newly constructed brushing wire design. With the new generation brushing machine, the best quality flannel fabric has been produced faster, more efficient, and more energy efficient. It has automation at the top level. It produces a fabric with higher strength in a single step, has superior mechanical design, and at the same time has long-lasting material and less tendency to failure.

1. INTRODUCTION

Raising is a mechanical finishing process based on the pulling of fibers from the yarn with the help of metal wires passed through the surface of the woven or knitted fabric.

This process is carried out via pulling out the weft fibers from the fabric with the aid of a plucking and smoothing wires of drums on a raising machine, giving volume, filled, and soft air effect to the fabric. This process can be done at every stage of the production; however, it is usually

ARTICLE HISTORY

Received: 27.01.2021

Accepted: 10.08.2021

KEYWORDS

Raising, soft touching effect, brushing machine, brushing machine providing a homogenous feather effect, raising wire

To cite this article: Ertuna İ, İnalöz M, Yoldaşoğlu N, İpek F, Atar A, Küçükpetek A, Göde C.. 2021. Prototype design and manufacture of the new generation highly automated brushing machine in home textile. *Tekstil ve Konfeksiyon*, 31(4), 242-249.

included in the final processes. The reason for this process is to give the desirable handling and appearance properties to the fabric [1-2].

The fabric strength for these forces determines the performance characteristics of the fabrics. For this purpose, performance tests (stiffness, abrasion resistance, pilling, tear strength, bursting strength, etc.) are applied on the fabric. The most important of them are the tensile strength and breaking elongation % tests. Tests are applied on the fabric for warp and weft direction [3].

The effect of drum speed on the raising process in the machine was investigated. upgrade process and number of upgrade passages their effects on various fabric properties [4].

The problems experienced during the current raising process are;

- Due to the wire design, high-strength touch effect fabrics can not be made at high speed and in one go,
- Decrease in strength due to process recurrence,
- Oil stain, insufficient touch effect, low strength, second quality due to damage / wrinkle problems,
- Excess chemical use due to repair process to solve strength problem,
- High amount of process recurrence due to insufficient brush suction system,
- High energy consumption due to double passing,
- Increased energy, maintenance and labor costs resulting from inadequacies in design,
- The high frequency of the faults occurring in the machine depending on the automation and cannot maintain detection,
- High level of ambient dust, formation of contaminant and grease fabric waste, occurrence of fire risk, problems related to environment and occupational health and safety arising from the use of repair chemicals and high waste from maintenance.

The aim of the study is to create a raising machine prototype that has the following features;

- To change the current double-pass production of raising machines to the single pass one,
- Increase the production speed, reduce the amount of second quality,
- Remove completely repairable pile/touch faults caused by conventional raising machines,
- Increasing energy efficiency via reducing electricity consumption during production,
- Reducing maintenance time and cost,

- Reducing the amount of scrap,
- reducing stop times and working area dust during production,
- Prevent contaminant wastes caused by lubrication completely,
- Providing occupational health and safety via high level automation,
- Having technical features that reduce operator-induced errors.

However, the raising process has been investigated on latest technology raising machines that are owned by our company. Since the desired technology can not be provided with the wire produced by the current technology machine producers, the wire design has been done in our own way. By designing original systems with R & D possibilities, the process of designing according to the requirements of the textile machinery sector, which is mostly dependent on imported, pioneered at the national level at the point of catching the Industrial 4.0 revolution in the textile sector.

2. MATERIAL AND METHOD

2.1 Material

The general view of the raising machine is as in figure 1.

2.1.1. Roller Unwinding

Some problems with the dock wrapping unit were affecting the fuzzing effect. It also caused balance and runout problems in the dock roller. The main problems of this section are cloth breakage and the cloth getting dirty when it touches the ground. With using Dancer scales and infinite round pots, dock release unit with automation control and brake system was built.

2.1.2. Pre-Drying Unit

The amount of moisture on the fabric affects the homogeneous fuzzing effect. Due to the fact that the exit humidity could not be kept constant, the desired hair growth effect could not be achieved. That is why, by controlling the condensate temperature in the drum with the steam drum cylinder and using less steam, the humidity in the outlet drum was controlled more precisely and a steam drying unit was installed to provide moisture control by resistance measurement method.

2.1.3. First and Second Drum Units

Manually controlling the tension on the cloth surface at the drum exit by the operator causes some errors. These errors are in the form of unwanted pilling effect, oil stain, loss of strength, belt breakage. In this section, we aimed to eliminate the problems experienced with the raising wire, the design of which belongs to us. A needle / wire system was made to provide the pilling effect with homogenous desired weight and strength. This system is configured by figure 2.

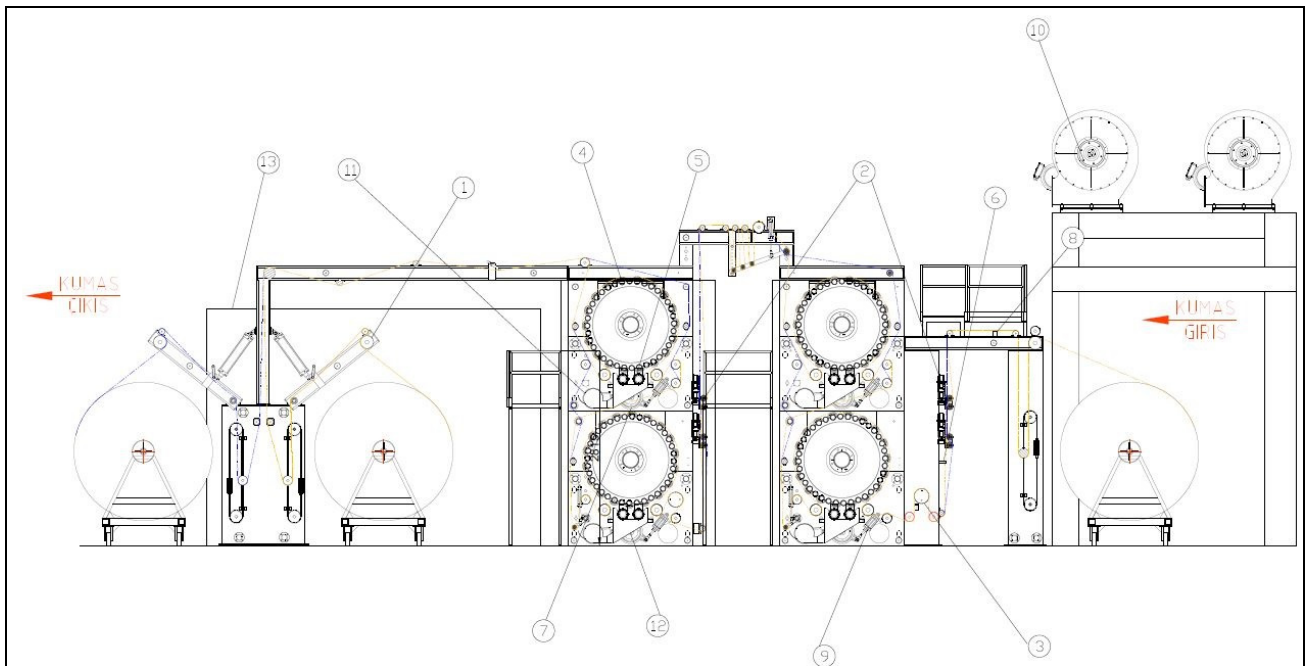


Figure 1. Brushing Machine Design

1. Draft Roller Units, 2. Vertical Scale, 3. Heating Drum, 4. First and Second Drum Wire Design, 5. First and Second Drum Reducers, 6. Sewing Sensor, 7. Drum Drive Belt, 8. Static Bar, 9. Belt Tensioner System, 10. Pressure Prostate, 11. Roller Winding Unit, 12. Closed Loop Communication System, 13. Electric Panel

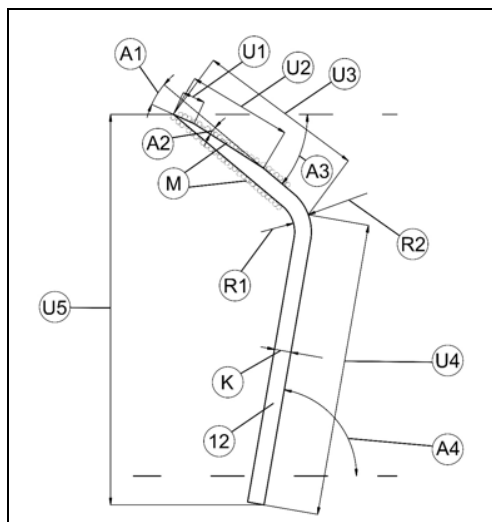


Figure 2. Raising Wire Design

Raising wire; Thickness (K), 1st angle (A1), 2nd angle (A2), 3rd angle (A3), 4th angle (A4), 1st length (U1), 2nd length (U2), 3rd length (U3), 4th length (U4), 5th length (U5), 1st diameter (R1), 2nd diameter (R2) is included.

Thickness (K) measure is between 0,35 mm and 0,5 mm, 1st angle (A1) is between 14° and 17°, 2nd angle (A2) is between 6° and 8°, 3rd angle (A3) is between 42° and 47°, 4th angle (A4) is between 75° and 82°. 1st length (U1) is between 0,51 mm and 0,58 mm, 2nd length (U2) is between 2,48 mm and 2,54 mm, 3rd length (U3) is between 3,98 mm and 4,03 mm, 4 th length (U4) is between 6,8 mm and 7,2 mm, 5th length (U5) is between 8,7 mm and 9,25 mm. 1st diameter (R1) is between 0,76 mm and 0,82 mm, 2nd

diameter (R2) is between 1,18 mm and 1,22 mm designed as in Figure 1. Thanks to the special design that this range of values reveals, the homogeneous pilling effect that can be achieved in the fabric with single pass instead of double pass.

A motor with a torque capacity that will provide the desired fuzzing effect on the fabric in a single pass of the plucker and scanner drive reducers on the drum has been selected and it has been carried out in closed loop. This engine is shown in figure 3. In addition, the sharp tip of the raising wire can be sprayed with metal dust (M) to meet different needs.

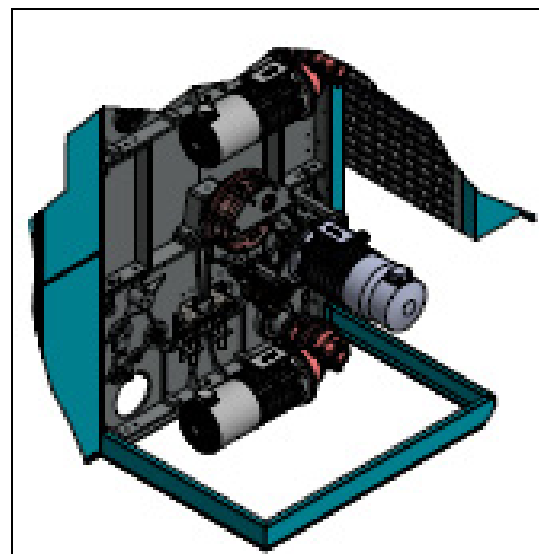


Figure 3. Technical Drawing of motor in drum unit

2.1.4. Dedusting (Dust Suction) System

The main problem in this section was the escaping of the broken cloth or machine parts into the dust suction line. In order to eliminate this problem, the appropriate design of the suction duct and fan propellers has been made. This design is shown in figure 4. Since the cleaning of the brush is more effective, the vacuum system with brush was performed as shown in figure 4.

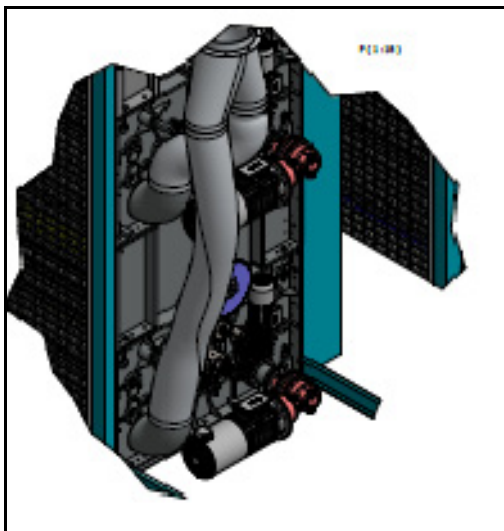


Figure 4. Dedusting System (Brush Vacuumed System)

2.1.5. Roller Winding Unit

The problem encountered in this section is the slippage of the fabric over the draft roller during the dock wrapping process. As a solution to this problem, it has been suggested that the surface of the drafting roller should be covered with suitable rubber so that the fabric does not slip, and that appropriate opening systems should be made to wrap the fabric properly in the dock. It is synchronized with the vertical scale roll to ensure optimum tension operation at high speed.

2.1.6. Automation

An innovative machine design was made in order to achieve the desired pile height in one go. In this study, the raising process can be monitored by measuring the height and density of the fibers emerging from a raised fabric (pile) [5]. In order to reach a more effective solution to the above-mentioned mechanical problems, an automated approach was required. For this reason, it was planned to make the rollers on the drum through automation with the help of belt tension air I/P regulator. For the dust extraction system, it was aimed to prevent malfunctions that may occur through the vacuum malfunction sensor. It is envisaged that a fast and convenient communication system between PLC and driver can eliminate these problems.

2.2 Method

Today, the desired fuzzing effect cannot be achieved at once in raising machines. Due to process repetitions, the

fabric shows low strength, energy and labor loss. There is an increase in the number of second quality products resulting from repetitive processes. The draft roller is covered with rubber material to prevent the fabric from slipping during production. In the dock unloading and wrapping units, a vertical scale system, which compensates the fabric more, is used instead of the dancer scale system. Fabric at the exit of the inlet heating drum with the help of automation humidity was controlled. With the specially designed raising wire, homogeneous fuzzing effect provided in double pass is provided in one pass. By choosing the most suitable geared and asynchronous closed-loop motor for the raising machine, motor burns were prevented and optimum fuzzing effect was achieved. The machine works independently from the operator with the seam sensing sensor placed at the fabric entrance. The belt tension air of the cylinders is controlled via automation with the help of I/P. With the pressure prostate attached to the dust collection pipeline, waste pieces of cloth or dust are prevented from escaping into the pipeline during production. With the special design made to the dust collection line, escaping of dust is prevented. Belt pulley resistant to rupture and deformation has been selected.

Today, failure to detect malfunctions in raising machines causes second quality production. Downtime is increasing. Owing to automations, fault detection times are shortened. The compressed air supplied to the brake system is given to the PLC control via the I/P converter. Humidity is measured with a moisture measuring device placed on the cloth heating drum. The steam is proportionally controlled according to the desired humidity. Moisture measurement is made by measuring resistance with two cylinders insulated from the body of the raising machine. The new raising machine design has the ability to save and recall recipe runs for different fabrics. This provides speed and convenience to the operator. The belt tension system air of the scanner and plucker drum cylinders is done by automation over I/P. Current and new generation PLC system is used. The information exchange between the PLC and the driver is done via the Profinet communication system. Thus, electrical noise is prevented.

3. RESULTS AND DISCUSSION

3.1. Engineering Calculations and Analysis

3.1.1. Dust Measurement

Machine dust was detected in an independent laboratory with a dust measurement device called Dustmate via providing ambient conditions of 35.2 ° C, 1.011 mbar, 47% humidity. The device measures with the scattering principle of light. The device contains a diaphragm pump. The device samples the air with a constant and controlled flow rate by means of this pump. The measuring range of the device is 0-65.00 mg/m³. The device can simultaneously measure and store TSP, PM 10, PM 2,5 and PM 1 measurements.

Dust measurements were made in 4 different regions in the working area of the Raising Machine. Dust in the determined areas was made in two different ways at the

beginning and at the end of the project. It was found that the machine-borne dust reduced by 10% with more efficient dust collection through dust extraction system made in our prototype raising machine. The measurement results are given in Table 1.

3.1.2. Estimation of Production and Productivity

After the machine was switched on, it was seen that the production with the targeted 24 m / min was made and at the same time the desired napping effect was provided at one time. It was found that the amount of second quality was reduced by providing a homogeneous napping effect in one go.

3.1.3. Energy Estimation

EFF 3 engine efficiency average 85%, IE2 engine efficiency 92% average A minimum of 8% energy saving will be achieved with the IE2 class motor to be used in the Menderes Raising machine instead of the EFF3 class low efficiency motor used in the existing machines. In our prototype raising machine, it has been observed that the annual electricity consumption is reduced by 55.95% due to the use of high-efficiency motors and feathering in a single pass, and the desired target is achieved.

Table 2 shows that, instead of the low EFF3 class motor used in the current system, 10% energy savings are achieved with the IE2 class motor, resulting in 55.92% savings in annual energy consumption.

3.1.4. Humidity Control

In the dryer section, the vapor pressure on the drums is 3 bar. The specific enthalpy of steam at 3 bar pressure is 2738 kJ / kg [5].

$$H_{fg} = H_2 - H_1$$

$$H_{fg} = 2738 - 427 = 2311 \text{ kJ/kg} = 552 \text{ kcal/kg}$$

$$Q = m \times (H_2 - H_1)$$

$$Q = 50 \text{ kg/h} \times (552 \text{ kcal/kg})$$

$$m = 27600 \text{ kcal/h}$$

$$Q = Q_1 + Q_2$$

$$Q = m \times c \times \Delta t + m \times L_b$$

$$27600 \text{ kcal/h} = m \times 1 \text{ kcal/kg}^\circ\text{C} \times (100 - 20)^\circ\text{C} + m \times 540 \text{ kcal/kg}$$

$$m = 44,51 \text{ kg/h}$$

$$m = 741,833 \text{ g/min}$$

$$\text{Machine speed} = 20 \text{ m/min}$$

$$\text{Fabric width} = 2700 \text{ mm}$$

$$\text{Amount of water to evaporate over fabric} = b \text{ (g/m}^2\text{)}$$

$$741.83 \text{ (g/min)} = 20 \text{ (m/min)} \times 2.7 \text{ (m)} \times b \text{ (g/m}^2\text{)}$$

$$b = 13.73 \text{ gr/m}^2$$

3.1.5. Steam Consumption

The inlet steam line of the steam drum is 3/4" in diameter. Accordingly, the amount of steam; There is approximately 50 kg of steam consumption per hour in the drying drum of the raising machine with 1 steam drum and 5/4 " steam feed.

a. Mechanical Analysis

3.2.1. Strength Analysis

Structural strength and fatigue analyze of the drums and cones in the drums area under the loads that were applied during the operation of the raising machine were performed.

Table 1. Dust Measurement Results

Measure Zone	PM10 (µg/m3)		PM2,5 (µg/m3)		PM1 (µg/m3)	
	First	Second	First	Second	First	Second
Brushing Mac. Zone 1	116,3	101,6	38,4	34,5	12,30	11,0
Brushing Mac. Zone 2	120,1	107,9	37,5	33,7	12,10	10,9
Brushing Mac. Zone 3	123,1	111,6	36,1	32,8	12,13	10,8
Brushing Mac. Zone 4	128,2	115,8	39,2	36,4	12,20	11,2

Table 2. Energy Measurement

Measure Number	Engine Name	Pcs	Power kW	Work Hour	Current Consumption kWh	Single Pass Consumption kWh
1	Roller Unwinding	1	3	406	1218	609
2	Draft	8	1,5	406	4872	2436
3	Intermediate Draft	2	0,75	406	609	305
4	Drum	4	18,5	406	30044	15022
5	Plucker-Smoother	8	15	406	48720	24360
6	Roller Winding	2	1,5	406	1218	609
7	Dust Suction	2	22	406	17864	8932

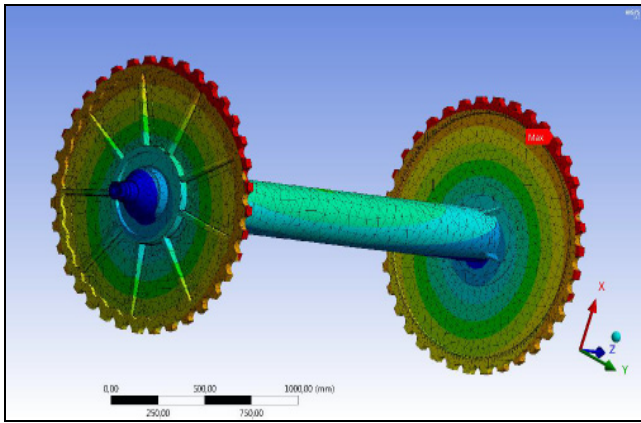


Figure 5. Modelling of ANSYS

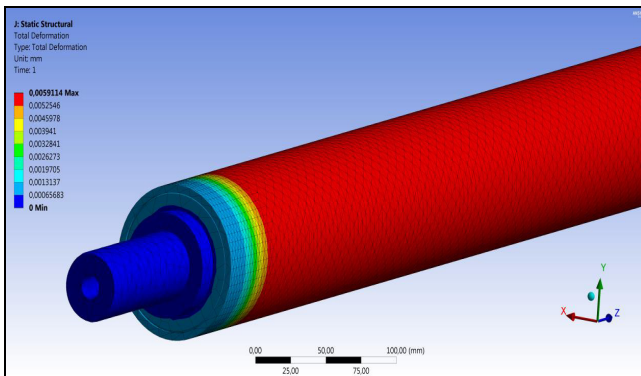


Figure 6. Modelling of ANSYS

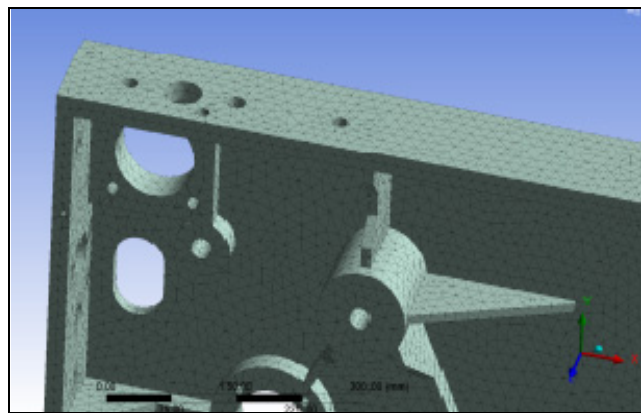


Figure 7. Modelling of ANSYS

The model CAD data was transferred to the Ansys Workbench environment. Static strength analysis of position and loading conditions was carried out by an independent firm and evaluated as equivalent stress (Von-misses stress) and deformation. The system also calculated the critical buckling load on the profiles under the pressurized load. Plates, panels and so on. a higher theoretical approach was targeted using "shell modeling" methods. Links of low significance level were modeled with "beam elements". The parts that cannot be adapted in the model are connected with "bonded contact". The plates between the bolts and the surfaces between the parts were also defined as "no-separation contact". The bolts are defined as beam elements in the ANSYS Workbench environment. The total deformation on the system was found to be a maximum of 0.67 mm. The red regions in figures 4, 5, and 6 show that where sinkage is highest [6].

3.2.2. Physical Tests for Fabric

Physical tests (strength, shrinkage, feather-touch) were applied on the surface of raised and non-raised woven fabrics. The mechanical properties of the fabric were evaluated statistically [7-8].

3.2.3. Tensile Strength Analysis

The tensile strength of raised and non-raised woven fabrics was investigated for both warp and weft directions. It is observed that the tensile strength of the raising fabric in the weft and warp direction is lower than the tensile strength of the non-raised fabric in the weft and warp direction [9-10]. However, the tensile strength of our new generation raising machine has been increased by 10-20% than the tensile strength of the existing raising machines with the help of the desired feathering with a single passage.

3.2.4. Shrinkage Analysis

The test results of the shrinkage analysis at the entrance and exit of the raised and non-raised fabrics were examined. It is seen that the shrinkage test of the raising fabric in the weft and warp direction is lower than the shrinkage test in the weft and warp direction of the non-raised fabric. Shrinkage of our new generation raising machine is higher than the shrinkage of the existing raising machines with the help of providing the desired feathering with a single passage.

Table 3. Tensile Strength Analysis

Test No	Current Raising (N)		New Designed Raising (N)		Non-raised (N)	
	Warp	Weft	Warp	Weft	Warp	Weft
1	240	270	265	290	269,8	294,8
2	245,5	269,8	265,6	289	269,7	294,7
3	243	270,4	264,8	289,5	270,5	295
4	244	268,9	264,9	290,1	270,2	295,2
Ort.	243	269,7	265	289,6	269,8	295

Table 4. Shrinkage Analysis

Test No	Current Raising (%)		New Designed Raising (%)		Non-raised (%)	
	Warp	Weft	Warp	Weft	Warp	Weft
1	-2,6	-0,65	-2,0	-0,65	-2,2	-0,7
2	-2,7	-0,63	-1,95	-0,66	-2,1	-0,69
3	-2,5	-0,66	-1,98	-0,65	-2,0	-0,71
4	-2,2	-0,61	-2,1	-0,64	-2,2	-0,68
Ort.	-2,5	-0,64	-2,0	-0,65	-2,1	-0,7

4. CONCLUSION

- It will be able to apply air comply with brake system according to the diameter of the roller and automatically increase the brake pressure when the machine is stopped while the machine is running. The automation has prevented the problems such as creasing and shrinkage in the fabric.
- The problem of creasing in the fabric was eliminated with proper material selection, design and also preventing the spin and unwinding of scale cylinders.
- At the output of the heating drum, the moisture on the fabric was controlled to achieve the desired pilling effect.
- By controlling the humidity on the fabric, energy is saved by controlling the steam entering the heating drum.
- A raising machine wire was designed to provide homogenous pilling effect.
- An automation system was built that controls the plucking-smoothing cone wire cleaning brush settings and provides operator notification.
- A suitable drive belt has been identified and production losses have been reduced with the choice of belts to work without breaking and deforming for longer.
- The new fan impeller design increases the capacity of the suction fan and avoids the risk of fire due to fan failure.
- A vacuum sensor was installed to create failure notice when the vacuum line is not sufficiently vacuumed, cylinder contamination was prevented via on time notice of insufficient vacuum.
- With proper brush and material design, dead fibers are prevented from blocking between brushes and the cleaning period is extended.
- It has been prevented that the broken piece of fabric or machine parts escapes into the dust suction line.
- The surface of the drafting cylinder is covered with a proper material so that the fabric does not slip.
- Instead of the dancer scales system, a suitable vertical scales system was made to balance the fabric more conveniently.
- A proper opening system was made to ensure that the fabric was properly wrapped around the roller.
- The infeed roller brake tension was adjusted with automation control.
- The steam was controlled via automation with the aid of proportional valve and a humidity sensor at the exit of the cloth heater.
- Belt tension air flow of plucking and smoothing cylinders was performed with I/P automation.
- Electricity and steam consumption were tracked via automation.
- Certain amounts of energy have been saved with using a new generation of proper engine reducers and drivers.
- The number of faults derived from PLC system has been reduced with current and new generation PLC system.
- While the production was done at the speed of 20 m/min in the past, now 24m / min production is realized with 20% speed, 21% production and 137% product increase in raising machines.
- The amount of second quality decreased by 80-100% thanks to single pass technology instead of double pass technology to provide desired napping and soft touch effect.
- A 20% speed increase on the machine resulted in more homogenous and more effective pilling.
- It has been observed that the shrinkage problems caused by raising the yarns, homogeneous feathering and the reduction of deformations on the yarn surface during feathering, decreased from 2.5% to 2.2% in the weft direction and from 3.5% in the warp direction to 3.0%.
- Since the repair process due to the strength problem has been abolished, 3800 kg of chemicals have not been used, in other words, 16500 TL worth of chemicals have been used less.
- A 100% reduction has been achieved in repairable napping-soft touch based defects caused by the raising machine.
- The reduction in strength was reduced by 10-20% as the desired pilling effect was achieved in a single pass.

- As the use of high-efficiency motors and obtaining desired napping in a single pass have been achieved, annual electricity consumption has decreased by 54%.
- In the case of roller changes and short stoppages, the energy consumed was reduced by 8.7% due to the fact that the dust extraction fan was not connected to automation.
- In addition to providing homogeneous napping effect with total machine humidity control, steam consumption is also reduced by 13%.
- Annual maintenance time decreased by 10% and cost by 48%.
- Because of the more efficient dust collection with the newly constructed dust extraction system, the dust originating from the machine given to environment has decreased by 8-10%.

In addition to the innovative technological developments in our work, the prototype raising machine's digitalization and digitization work was also carried out as the first step in the process of going to the dark factories during the Industrial 4.0 revolution. In addition to text, design and production of raising machine is shown in figure 7.

Acknowledgement

This study has been supported by TÜBİTAK with the project number of 3151020 and has been successfully completed. A patent application was filed with the Turkish Patent and Trademark Office on 22nd February 2018 with the number of 2018/02547. The authors would like to thank the Ministry for its financial support.

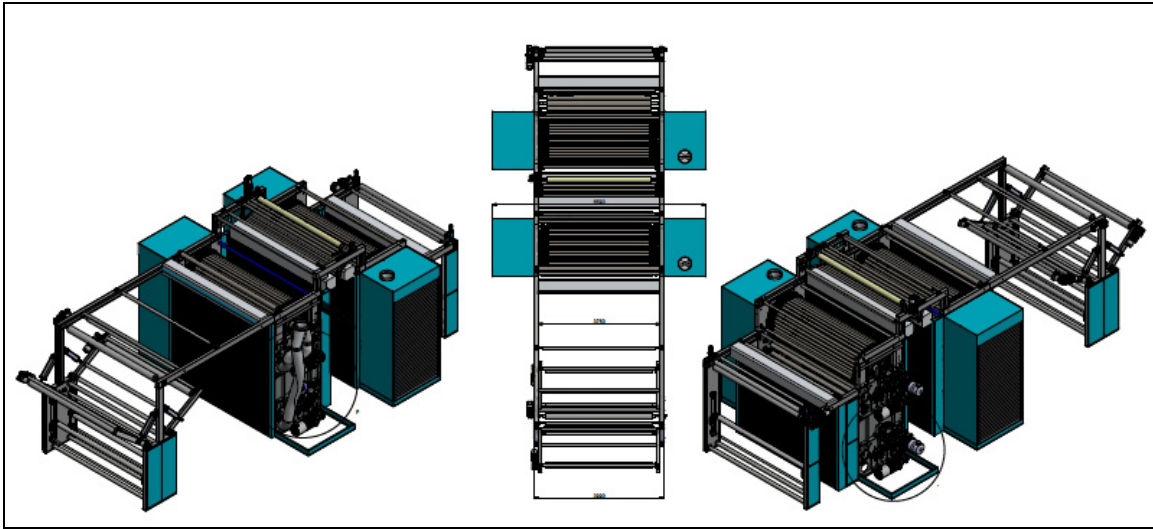


Figure 8. Design and Production of Raising Machine

REFERENCES

1. Özdemir H, Yavuzkasap D. 2012. The Effects of Raw Material, Weft Setting and Weave on the Breaking Strength, Elongation at Break and Tear Strength of Upholstery Double Fabrics. *The Journal of Textile and Apparel* 22 (2), 159-165.
2. Carfagi M, Furferi R, Governi L. 2005. A Real-Time Machine-Vision System For Monitoring The Textile Raising Process. *The Journal of Computers in Industry* 56, 831-842.
3. Sarpkaya Ç, Özgür E, Sabır E. 2015. The Optimization of Woven Fabric Tensile Strength with Taguchi Method Based on Grey Relational Analysis. *The Journal of Textile and Apparel* 25(4).
4. Sabır E C, Maralcan A. 2010. 2/1 Z Dimi PES/VIS/EA Dokuma Kumaş Özelliklerine Şardon Parametrelerinin Etkisi. *Electronic Journal of Textile Technologies* 4(2), 1-8.
5. Carfagni M, Furferi R, Governi L. 2005. A Real-Time Machine-Vision System For Monitoring The Textile Raising Process. *The Journal of Computer in Industry* 56, 8-9.
6. Kuo Y, Yang T, Huang G W. 2008. The Use of A Grey Based Taguchi Method for Optimizing Multi Response Simulation Problems. *The Journal of Engineering Optimization* 40 (6), 517-528.
7. Su T L, Chen H W, Ma C M, Lu C F. 2011. Improving the Quality of Combed Yarn Spun by OE Rotor Spinning Using The Grey-Taguchi Method. *The Journal of Fibres & Textiles in Eastern Europe* 19(2), 23-27.
8. Hasan H, Somayeh A T, Ghafour A. 2012. Grey Relational Analysis to Determine the Optimum Process Parameters for Open-End Spinning Yarns. *Journal of Engineered Fibers and Fabrics* 7 (2), 81-86.
9. Ünal P G, Taşkın C. 2007. %100 Poliester Kumaşlarda Dokunun ve Sıklıkların Kopma Mukavemetine Etkisi. *Tekstil ve Konfeksiyon Dergisi* 2, 115-118.
10. Özgür E. 2013. Master Thesis, Seçilmiş Dokuma Kumaşların Kalite Özelliklerine Boyamanın ve Şardonlamanın Etkisinin İstatistiksel Yöntemlerle Araştırılması. University of Çukurova, Turkey.



DSS-Based Process Control and FMEA Studies for Different Processes in the Field of Textile

Yeliz BURUK ŞAHİN¹  0000-0002-6215-5193

Ezgi AKTAR DEMİRTAŞ²  * 0000-0002-3762-6256

¹ Eskisehir Osmangazi University / Industrial Engineering Department / Eskisehir Osmangazi University, Meselik Campus, 26040 Eskisehir/Turkey

² Eskisehir Osmangazi University / Industrial Engineering Department / Eskisehir Osmangazi University, Meselik Campus, 26040 Eskisehir/Turkey

Corresponding Author: Ezgi Aktar Demirtas, eaktar@ogu.edu.tr

ABSTRACT

Today, in many textile firms, high defect rates and inefficiency stand out due to the intensive labor in the production processes. For this reason, to be able to detect failure modes and effects, number of defects and defect rates fast and intervene in the process just in time is vital for textile firms. Accelerating feedback by producing accurate and effective quality reports and helping senior management's decision processes will reduce appraisal costs and delivery time. In this study, Failure Mode and Effect Analysis and Statistical Process Control techniques have been integrated with a Decision Support System for different processes of textile. Thanks to the proposed integrated system in the fast fashion/textile sector, defect and/or failures will be prevented or detected on time by determining the sources of error with an effective database and monitoring system. So, process capability will increase by preventing material, operations and human-induced scraps.

ARTICLE HISTORY

Received: 16.04.2021

Accepted: 12.10.2021

KEYWORDS

Process failure mode and effect analysis, statistical process control, decision support system, demerit control charts

1. INTRODUCTION

In today's world where competition does not know any borders and similar companies proliferate, production with low cost, short delivery time and high quality is the main goal. The most important criterion for continuity in the market is customer demands. Customers no longer want to buy a different product than they request, and they avoid paying for the companies' wasted resources. In this environment where customer expectations increase, it will be possible to survive through the adoption and implementation of Total Quality Management (TQM). All activities such as determining the responsibilities and quality policies of the senior management, conducting the training activities related to quality management in every field and level, continuously improving the quality by the

help of quality teams and KAIZEN studies and ensuring the full participation of the workforce in the quality improvement activities constitute the philosophy of TQM. Within this management philosophy, the set of activities that ensure the effective performance of quality control activities is called Quality Assurance System (QAS). In other words, QAS is a group of activities that includes planning, organizing, directing and controlling quality in order to provide products suitable for the consumer [1]. These activities are classified as managerial and operational. Activities such as quality planning, analysis of quality costs, market research, customer relationship management and supplier evaluation are included in the managerial activities; various methods such as Acceptance Sampling, Process Capability Analysis (PCA), Statistical

To cite this article: Buruk Sahin Y, Aktar Demirtas E. 2021. DSS-Based process control and FMEA studies for different processes in the field of textile. *Tekstil ve Konfeksiyon*, 31(4), 250-263.

Process Control (SPC), Design of Experiment, Quality Function Deployment, Failure Mode and Effects Analysis (FMEA) are also examined under operational activities.

Failures and hazards that arise from the risk factors such as material, human, machines and equipment are the main potential risks in production systems. To reduce the risks in a system, various methods have been discussed in the literature. As a well known and widely used method, FMEA aims to define and prevent failures in design, process and systems. Process FMEA focuses on potential failure modes of the process that are caused by manufacturing or assembly process deficiencies [2]. The implementation of FMEA in textile industry includes numerous studies such as spreading and cutting [3], sewing [4], weaving [5-6], knitting [7], spinning yarn production [8] and finishing process in fabric dyeing [9].

On the other hand, SPC identifies the source of the problems in a specific process and prevents the production of nonconforming units. SPC provides decreasing in quality-related costs and increasing in productivity [10]. Basic SPC tools such as Control charts are widely used for high-quality production in many sectors, including textile production companies [11-13].

A DSS is computer-based programs used to support decisions and action plans in organizations and businesses. It analyzes the system by reviewing large amounts of data by compiling comprehensive data that can be used in decision making. Thus, DSS collects and analyzes data and generates comprehensive information reports. It increases efficiency with the advantage of timely problem solving and solution development. DSSs assist decision makers to improve quality of decision processes and tasks [14].

Database management system, model-based management system and dialog generation and management system are the main components of DSSs [15]. A decision maker gathers data from pure data sources (databases, text sources, information stores, etc.), then processes and makes it necessary for the decision. Finally, previously prepared templates, data processing methods, data mining studies, etc. are used to prepare possible scenarios that can support decision making process. The DSS concept uses a combination of human judgment and computer-provided information. Mete et al. [16] proposed a DSS based occupational risk assesment study of a gas pipeline construction. They developed a DSS based on Python package of Pythagorean fuzzy VIKOR for risk assessment. Febriani et al. [17] proposed an expert system that applies the FMEA method for developing quality control systems in brake disc production lines. The top 5 risk priority number (RPN) rankings of each quality defect play an important role in determining the recommended action in the expert system.

An integrated methodology, including DSS-based FMEA and SPC has been proposed in this study. This integrated approach includes various techniques such as Pareto charts, Cause-Effect Diagrams, Demerit Control Charts (DCC) for attributes and Process FMEA. It was carried out in a textile company that produces t-shirts, shirts, trousers, jackets, vests and coats for men and women. Handcrafting, which is common in the textile sector, is also valid for this company. Although the professional employees in the production line show great care during the production, slow feedbacks due to manual processing and reporting of defects in the quality control points cause serious quality problems. In the first application, a DSS-based Process FMEA was proposed for T-shirt production process. Critical failure modes and effects were determined and tried to be reduced by the help of DSS. In the second application, with the help of DSS, the number of defects, defect types and defect weights are recorded to the database in a fast and accurate way. Thanks to the data kept in the database, the process is dynamically monitored and it is determined whether it is under control. Pareto and DCC were used for monitoring the process in DSS.

In the proposed method, quality control personnel will log into the system with their user name and password. The defect types and numbers, which they encounter during the control are entered into the DSS interface. Defect types and numbers can be kept in a database and the results of analysis related to SPC studies will be reported on a daily basis. In this way, data entry errors and time loss at control points will also be eliminated. So, quality reports will be produced in a fast and error-free manner, helping the decision-making processes of the senior management. Process control activities supported and improved by DSS will contribute to the increase in production quality. DSS-based quality control techniques are not widely used in textile companies as in many areas. When the limited number of DSS-based studies are examined, no application of DSS-based FMEA and SPC studies including Demerit Control Charts, Pareto Charts etc. has been found in the textile industry to the best of our knowledge. Therefore, it can be said that the present study will fill an important gap in the literature within the scope of the textile industry.

2. MATERIAL AND METHOD

In this part of the study, SPC tools and Process FMEA are introduced.

2.1 Pareto and Demerit Control Charts

Pareto Chart, developed by Italian economist Wilfredo Pareto, is a bar chart used to distinguish the important causes of a problem from the less important ones. Pareto diagrams created on the basis of check sheets play an important role in determining vital fews, rather than trivial many, causing big losses (80% -20% rule).

Control charts are one of the important SPC techniques for process monitoring. They can be used to check whether the process is under control or not [18]. Out-of-control signals indicate assignable causes in the process. Assignable causes may result in process shifts and/or excess variability. The shifts and the excess variability can be reduced when the assignable causes eliminated. Univariate control charts can be used for monitoring single quality characteristic, whereas multivariate control charts monitor more than one quality characteristics in a single chart [13].

Control charts for attributes such as P, NP, C, and U charts are used to identify and eliminate the causes of various types of defects [19]. P and NP are used to monitor go/no-go type data (defective numbers and defective rates) based on the binomial distribution. On the other hand, C and U charts are used to monitor defect count data using Poisson distribution. By the help of DCC, instead of monitoring the number of non-conformities, a demerit statistic, a linear combination of the counts of defect types, is used to simultaneously monitor the counts for different defect types. As seen in Table 1, various types of defects can be classified into the following categories [20]. Additionally, relevant studies for various DCC forms using fuzzy structures in different sectors can be examined [21-25].

The most commonly used weights are assigned to classes respectively in the last column of Table 1.

The weights of classes and the defect numbers in each class are used to calculate demerit points. In the traditional approach, demerit points are plotted on a control chart with $\pm 3\sigma$ control limits. Demerit statistics are calculated using the weighted demerit points [13].

c_{iA} , c_{iB} , c_{iC} and c_{iD} represent the number of defects in Classes A, B, C, D in the i th inspection unit, respectively. Defects in classes are independent of each other.

The formulation of DCC are shown in Equations (1-6):

d_i : weighted total number of demerits in inspection unit i ,

n : the total number of inspection units,

D : the total number of demerits

u_i : the number of demerits per unit i

$$d_i = 100 \times c_{iA} + 50 \times c_{iB} + 10 \times c_{iC} + 1 \times c_{iD} \quad (1)$$

$$D = \sum_{i=1}^n d_i \quad (2)$$

Table 1. Defect types

Class	Defect	Impact	w
A	Very Serious	Failed to function, subsequent equipment damage, injuries/deaths to personnel	100
B	Serious	High degree of customer satisfaction	50
C	Moderately Serious	Degraded product performance, increased maintenance cost	10
D	Minor	The effects can be negligible	1

$$u_i = \frac{D}{n} \quad (3)$$

$$UCL = \bar{u} + 3\sigma \quad CL = \bar{u} \quad LCL = \bar{u} - 3\sigma \quad (4)$$

$$\bar{u} = 100 \times u_A + 50 \times u_B + 10 \times u_C + 1 \times u_D \quad (5)$$

$$\sigma = \sqrt{\frac{[(100)^2 \times u_A + 50^2 \times u_B + 10^2 \times u_C + u_D]}{n}} \quad (6)$$

u_A , u_B , u_C and u_D represents the average number of A, B, C and D type defects.

2.2 Process FMEA

FMEA can be defined as a methodology that enables to evaluate potential hazards/failures in a system, design, process, or equipment. Occurrence (O), Severity (S) and Detectability (D) are three main inputs in FMEA [26]. Occurrence refers to the probability of the failure mode for a defined period. Detectability is a measure of the ability to find potential failures before the system or customer is affected. Severity is an indication of the importance and emergency impact of failure on system or user.

Each of the risk factors S, O, and D, is evaluated using a 10-point scale. By the multiplication of three factors (S, O and D), the RPN is calculated. Higher RPN values have a higher risk priority and more importance than lower RPN values. The RPN values are the indication of priority level for improvement and corrective actions are developed from this comparative results.

3. RESULTS AND DISCUSSION

3.1 Application in a Textile Firm

The company, where DSS-based SPC studies are carried out, produces shirts, trousers, jackets, vests and coats for men and women. This firm which is competing with global brands in the industry, serves more than 180 stores in Turkey and abroad. The DSS was brought together with the user via Excel VBA. DSS-based integrated approach proposed by the authors is given in Figure 1. In the following subsections, DSS-based applications for the jacket and basic T-shirt processes of the textile firm are presented. Excel VBA macros are used for the design of DSS.

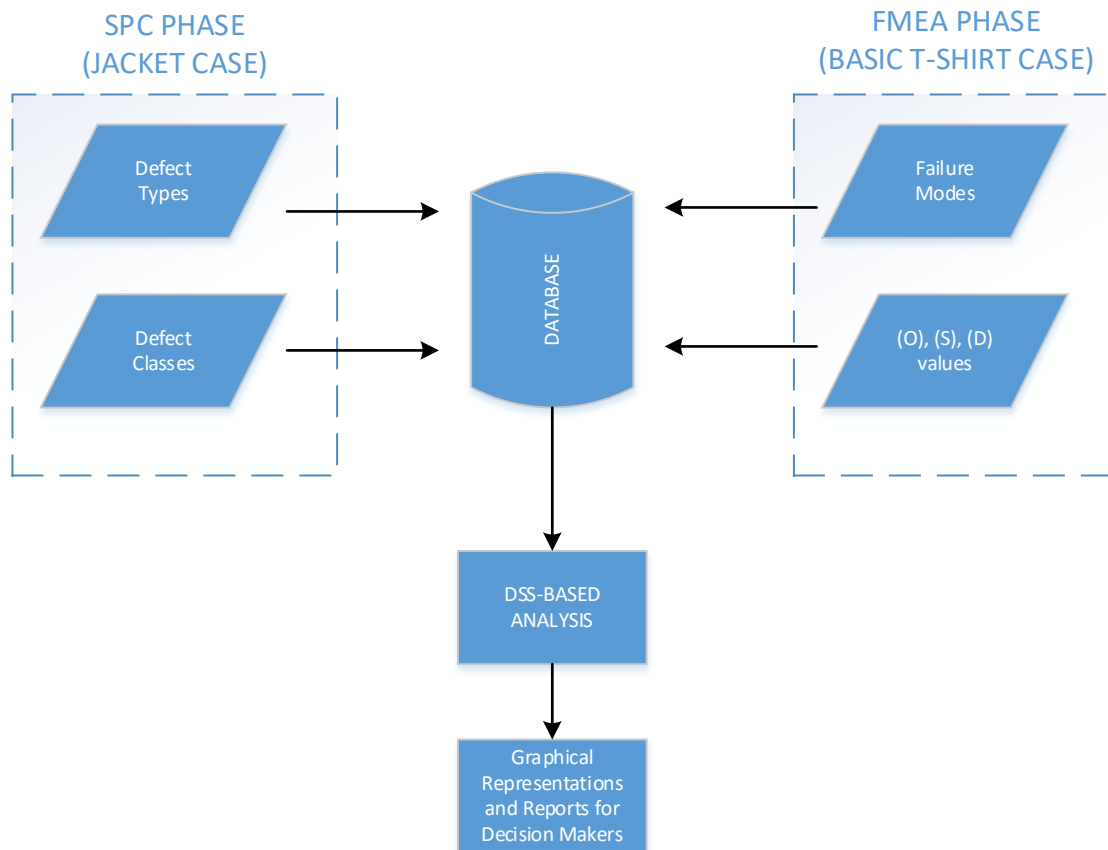


Figure 1. Flowchart of the DSS-based SPC and FMEA

3.1.1 DSS-based Statistical Process Control

When observing the production lines specific to the products, it is seen that many operations at the quality control points are manual. The controllers record the types and numbers of defects they encounter while examining the semi-finished products in a form which is designed specifically for the firm. It causes slow feedback and does not offer instant analysis and reporting. Since there is no computer-aided application or database, the reliability of the data is low. Computer aided production/control system is of great importance in terms of business objectives in textile enterprises where manual processes are intense. For this reason, the defect monitoring system at three different control points in the company's jacket production line has been integrated with a DSS. It is aimed that quality controllers and the senior manager use different interfaces in the system where they can log in with their usernames and passwords. With the proposed system; operators at control points ensure that the types and numbers of errors they encounter in their units are entered into the system on a date basis and kept in a database. The control points mentioned are sleeve preparing, primer and final product. These points are coded as CNT1, CNT2 and CNT3, respectively. At the CNT3 point; the final checks of the jacket, the production of which is completed by going through the sleeve attaching, collar fastening and side pocket preparation processes, are performed. There are a total of 21 critical defect types at the CNT1 point, 19 at the CNT2 point, and 17 at the CNT3 point. Defect types displayed in DSS interface are coded as CNTi-DFj due to company confidentiality.

The classes and weights of defects were determined by a team of production manager, industrial engineer and textile engineer by depending on the definitions on Table 1. The expert group, who assigned the defects at each control point to the classes, benefited from their experience and historical information. For all type of defects that may be encountered in the jacket production process rework rates, rework times and costs are recorded by the company. This information could not be shared with the reader due to company confidentiality. The expert group assigned the defects that could cause serious dissatisfaction to the customer after shipment and cause the rejection of the lot to be class B and weighted it with 50 points. Although it can be detected during production and corrected by rework, defects that increase cost and processing times are assigned to C class and weighted with 10 points. Even if the product is shipped, negligible defects that do not cause dissatisfaction with the customer are included in the D class and 1 weight point is assigned. The di values used to determine the limits of the control chart were also calculated using the relevant weights. In Demerit control charts, very serious defects that may cause harm to people or even death during the use of the product are evaluated in Class A. Since such defects were not encountered in the jacket production process, no assignment to Class A was made. Classes for defect types are shown in Table 2.

Table 2. Classes for defect types

Defects (CNT ₁)	Class	Defects (CNT ₂)	Class	Defects (CNT ₃)	Class
CNT1-DF1	B	CNT2-DF1	B	CNT3-DF1	D
CNT1-DF2	C	CNT2-DF2	B	CNT3-DF2	D
CNT1-DF3	C	CNT2-DF3	B	CNT3-DF3	C
CNT1-DF4	D	CNT2-DF4	C	CNT3-DF4	D
CNT1-DF5	B	CNT2-DF5	D	CNT3-DF5	B
CNT1-DF6	C	CNT2-DF6	D	CNT3-DF6	C
CNT1-DF7	C	CNT2-DF7	D	CNT3-DF7	C
CNT1-DF8	B	CNT2-DF8	B	CNT3-DF8	D
CNT1-DF9	D	CNT2-DF9	C	CNT3-DF9	D
CNT1-DF10	D	CNT2-DF10	C	CNT3-DF10	B
CNT1-DF11	D	CNT2-DF11	D	CNT3-DF11	C
CNT1-DF12	B	CNT2-DF12	B	CNT3-DF12	D
CNT1-DF13	B	CNT2-DF13	C	CNT3-DF13	C
CNT1-DF14	C	CNT2-DF14	C	CNT3-DF14	D
CNT1-DF15	B	CNT2-DF15	D	CNT3-DF15	B
CNT1-DF16	D	CNT2-DF16	D	CNT3-DF16	D
CNT1-DF17	D	CNT2-DF17	D	CNT3-DF17	D
CNT1-DF18	B	CNT2-DF18	B		
CNT1-DF19	C	CNT2-DF19	C		
CNT1-DF20	C				
CNT1-DF21	C				

The controllers at all three control points enter the number of jackets they have examined throughout the day, the defect types and numbers they encounter into the system via an interface (Figure 2). These data kept in the database are used in the forming of Pareto and DCCs. An example of a data set obtained as a result of entries made for 15 days is presented in Appendix A.

side (weighted frequencies) were obtained by multiplying the weight value of the class in which the defect took place with the frequency of defects. For example, in CNT1, approximately 80% of the problems causes from DF7, DF3 and DF6 according to the Pareto chart formed by weighted frequencies of defects.

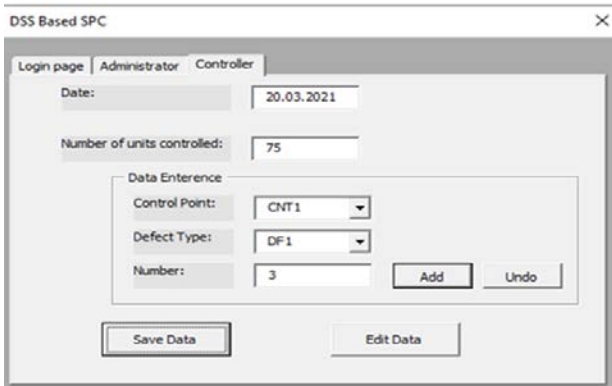


Figure 2. Interface for defect entries

With the interface used by senior managers, pareto charts can be formed for the desired date range and control points. Besides, it can be monitored whether the process is under control with the help of DCC graphics. The interface for managers is displayed in Figure 3.

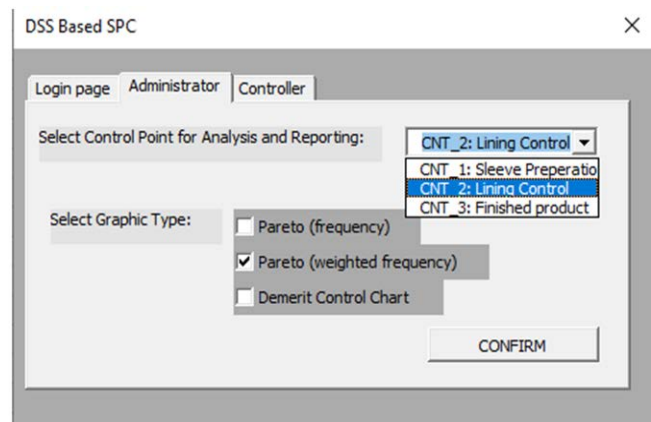


Figure 3. Interface for managers

Control limits, control charts and information messages about graphic interpretation regarding DCC can be viewed by the managers via “DCC button”.

Pareto charts can be formed for both defect frequencies and weighted defect frequencies via “Pareto Chart button”. Thus, decision makers have the chance to evaluate the defect types corresponding to 80% of the problems by taking into account the weights placed in Table 1 and/or frequencies of defects, with the help of pareto charts. Pareto charts for all control points drawn with data for the last 15 days are displayed in Figure 4. Pareto charts on the ride

When demerit control chart option is selected in Figure 3, admin is allowed to enter a date range shown in Figure 5. In this step, weight selections are made with the administrator authority. The defect types for the selected control points are displayed and the administrator is expected to choose the class corresponding to these defects. Also, in this step, the weights corresponding to the class type are displayed in parentheses. Demerit control chart is drawn based on the weight parameters entered for the selected control point.

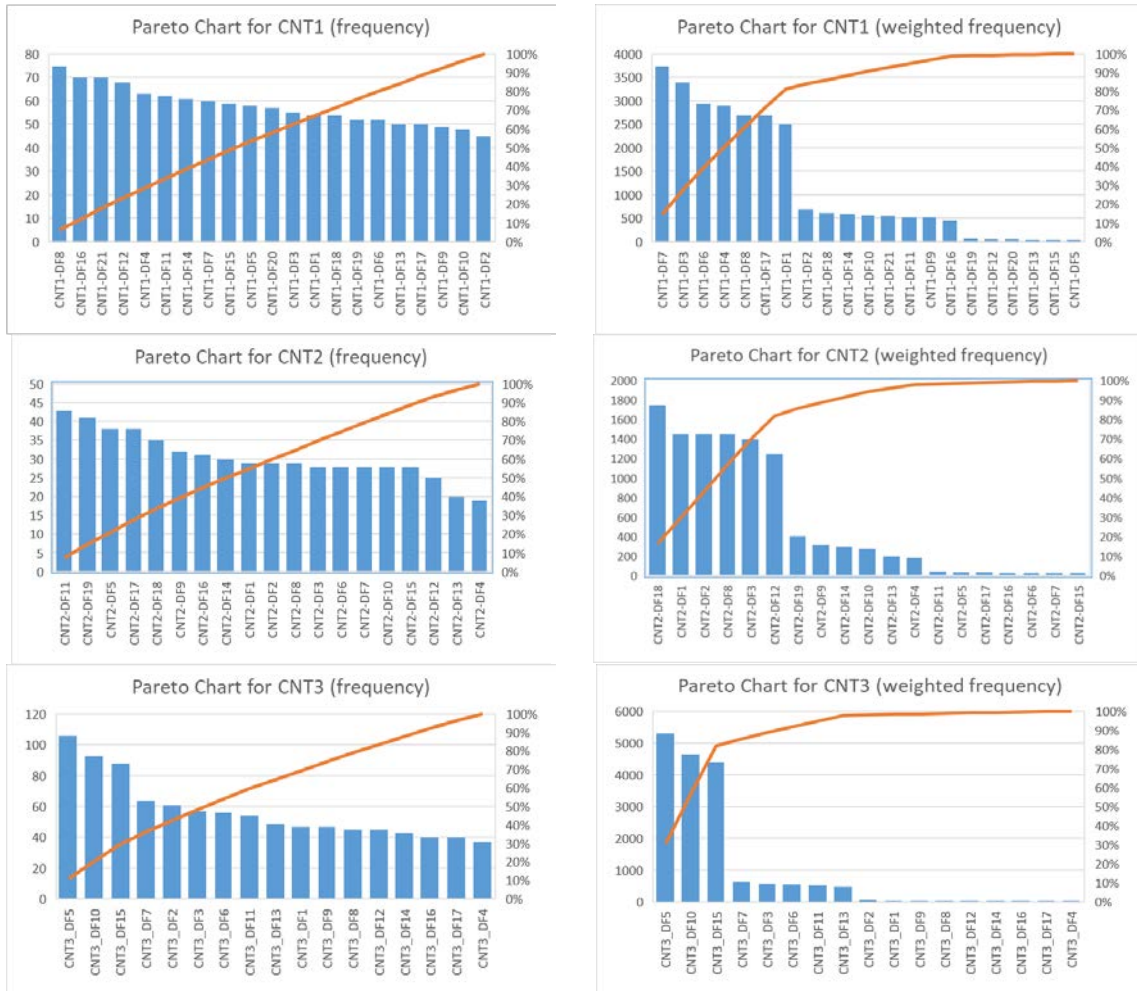


Figure 4. Pareto charts for all control points



Figure 5. Interface for demerit control chart

Table 3. Control limits for DCC

	Σ	<i>UCL</i>	<i>CL</i>	<i>LCL</i>
CNT1	3.595	33.685	22.900	12.114
CNT2	2.322	16.461	9.497	2.532
CNT3	2.082	14.733	8.485	2.238

Control charts are drawn for all control points based on the 15-day observation values and the control limits in Table 3. When the control charts in Figure 6 were examined, the process is under control for the last 15 days' data. In the next stages, with the help of DSS-based analysis and graphics, the situation of whether the process is under control or not will be dynamically monitored. In out of control situations, it will be possible to intervene in the process in a timely manner.

For three control points, the DCC control limits obtained with the last 15 days' data are shown in Table 3. Control limits were calculated by the help of DCC formulations mentioned in equations (1-6) before.

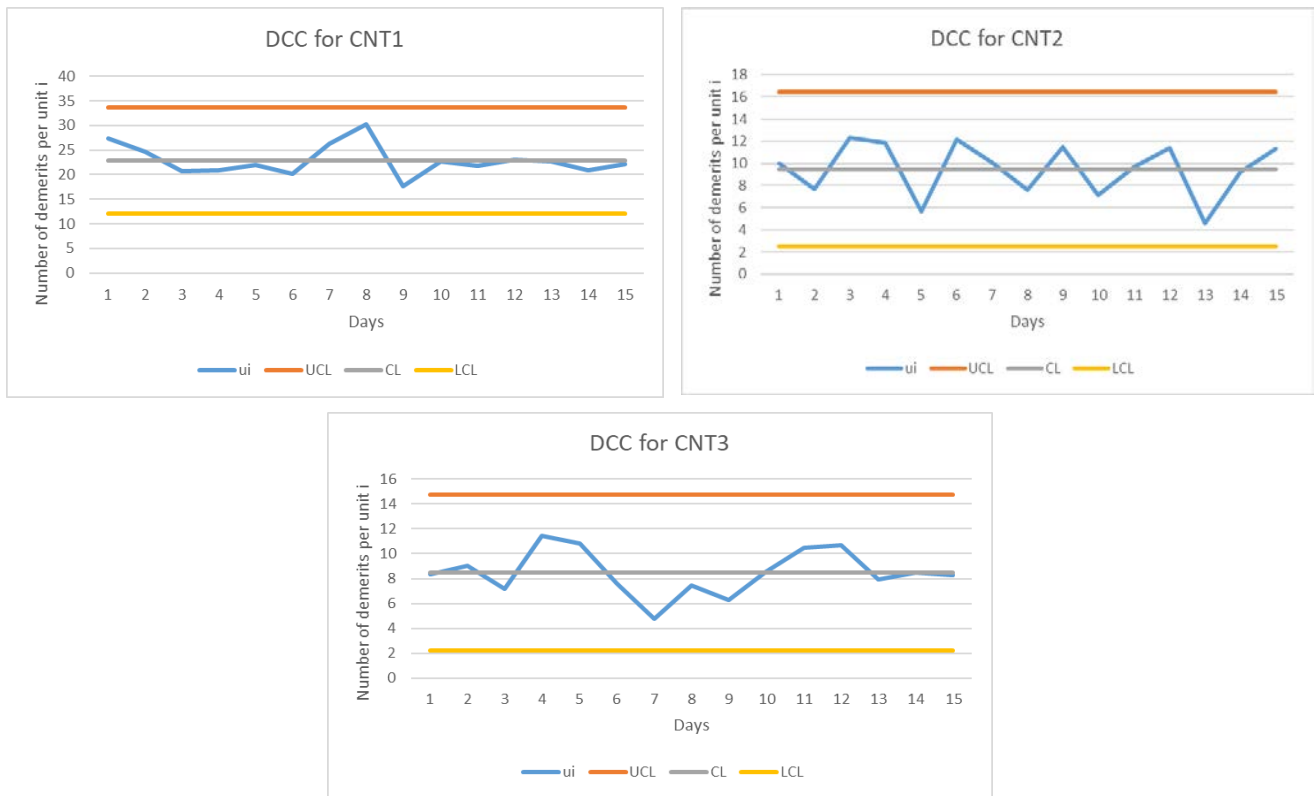


Figure 6. Demerit control charts for the last 15 days

3.1.2 DSS-based process FMEA

For FMEA application, basic T-shirt was chosen as one of the most frequently ordered and produced product types.

Production Process

The production process is managed in accordance with some orders designed by foreign customers, and the schedules can even be updated daily/hourly. A production plan is usually prepared according to planned orders. Monthly, weekly and daily goals are determined within this plan. There is a checkpoint throughout the enterprise almost after each processing step. Although the company pays great attention to controls, there are no error-preventing activities. Instead of preventing error before, cutting is done well above the number of orders by taking into account high error rates. This leads to a high percentage of resource waste, and in order to change this point of view, it is aimed to take corrective and preventive actions by descending to the root causes of errors with the help of process FMEA.

It is summarized as follows the basic process steps for the basic T-shirt product:

Fabric Control: The dimensions of fabrics are measured and recorded. Fabric cleaning, waste and defect controls are performed. In the laboratory, many properties such as fabric durability, paint quality, color and homogeneity are checked. Properties that must be checked according to the selected fabric also vary.

Steaming: All unprocessed fabrics are washed and cleaned first and then processed in a large steam machine. Thus, the shrinkage that may be encountered after washing is minimized. The steaming machine, thanks to its high steam power, allows the fabric to pull as much as possible and reach its final size, improving the quality of the fabric.

Cutting: Afterwards, the selected fabric is cut according to the pattern, and the cutting process takes approximately three hours. At the cutting stage, machines are selected according to the fabric type. If the fabric is a delicate fabric such as satin, a laser cutting machine is chosen, otherwise one of the cutter machines is chosen. The fabric of the product examined in the study is processed in cutter. According to the fabric type, laser cutting, knife cutting or manual cutting can be done. A large number of parts can be cut at the same time with the appropriate machine.

Classification: It is the stage in which the cut semi-finished products are counted and the parts are checked in detail. After the number of parts and measurement checks, the parts are distributed to the processing points on the production line. It is very important to do this application before the sewing phase. In this way, possible errors are minimized.

Sewing: This is the stage of sewing the parts according to the model. It consists of different sub-stages according to each model. The model is analyzed and the sub-work steps are determined. Operator-job matching is performed according to the job steps.

Control: The control stage after sewing requires a lot of attention. In cases of detected errors, necessary repairs are made and precautions are taken.

Logo Seam: It can be printed with a pressed machine or the logo can be sewn manually. According to customer's request; metal logo, plastic logo, printing logo or other kinds of logo can be used.

Ironing and Packaging: After appropriate ironing, quality control is carried out according to customer standards and the products are packed according to customer requirements and the labeled products are made ready for shipment.

DSS-based process FMEA for the basic T-shirt production process

The textile production process is one of the processes in which errors and wastes are observed intensively due to its

labor-intensive structure. Increasing waste rates due to high production speed cause inefficiency, and the pressure created by daily targets together with the fatigue caused by the complex structure in the processes leads to more errors. All defects that may be encountered during the production phase are shown in Figure 7 with a process type cause-effect diagram according to the process steps.

The most common types of defects are stain, bad fabric smell, looseness and shrinkage, regional defects, deviation in seam, logo seam and measurement defects. In addition, incorrectly applied work studies and incorrect determination of production times, incorrect planning and human factors also lead to high scrap rates and even bottlenecks with inefficiency and loss of speed.

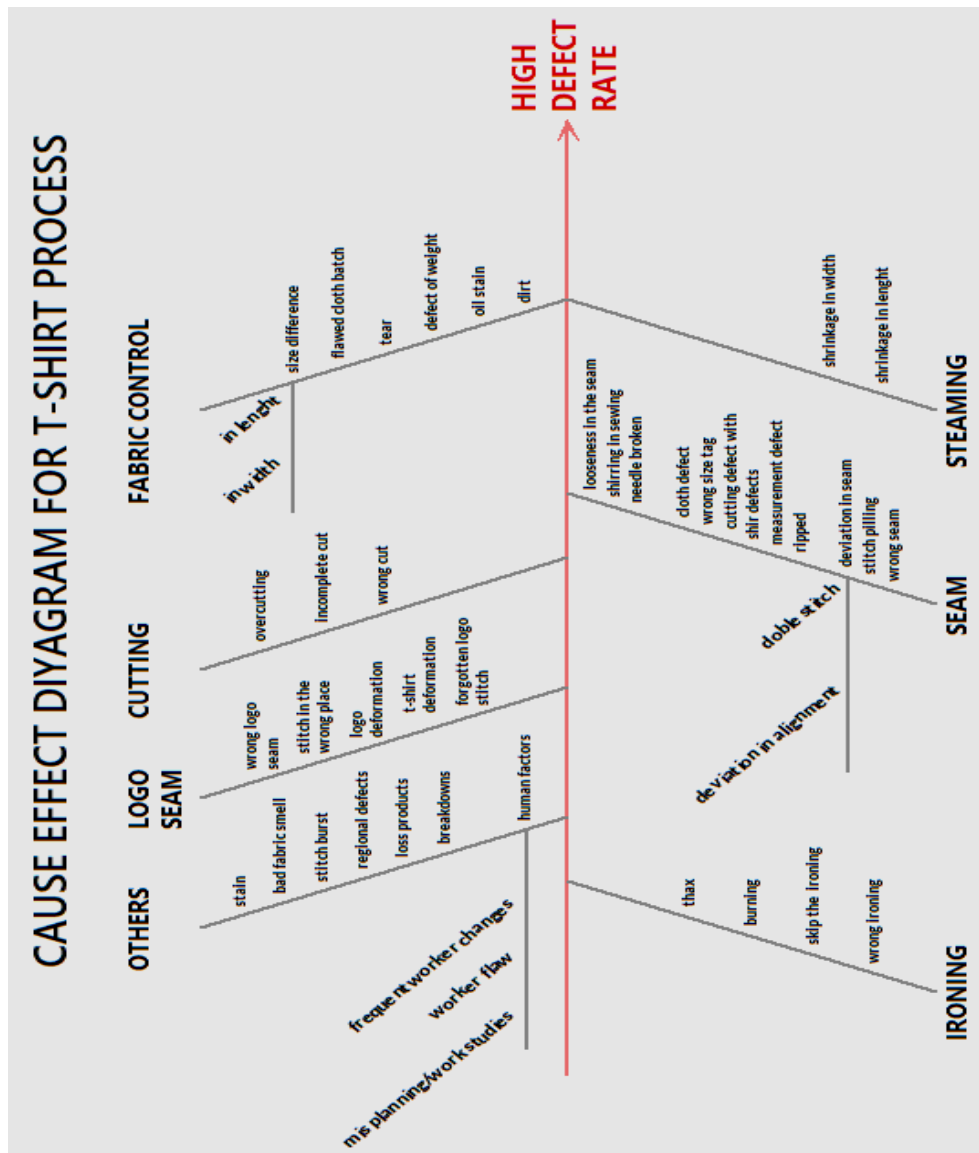


Figure 7. Cause-Effect diyagram for basic t-shirt process

At the next stage, the aim is to report DSS-based FMEA results by identifying the possible causes and effects of current and potential failures with the FMEA team. If the reasons for the failures are understood and expressed correctly, optimal results can be obtained. A large number of reliable and accurate data is required for the effective FMEA studies. With the help of the observations and collected data, the frequency of the failures, the results it caused, the probability of detecting the error and the RPN values were determined.

Between arch September 2020, about 53000 products from the basic T-shirt model produced in the enterprise were checked and the error numbers are shown in Figure 8 with pareto according to the error types.

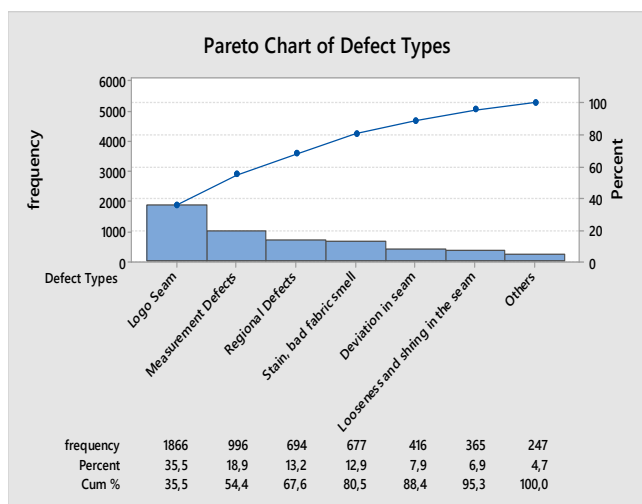


Figure 8. Pareto chart for defect types in basic t-shirt process

The most frequently observed failures in pareto constitute the scope of DSS-based FMEA. When calculating PRN, risk factors were valued between 1-10 in the DSS interface (Figure 9) by the employees in the FMEA team. Relative frequencies were used to determine the values related to the occurrence factor.

As a result of the calculations, the RPN values given in Figure 10 were obtained. The RPN represents the entire risk for the system user and serves as a decision tool for the actions. The larger the RPN is, the greater the priority that the risk is lowered with the help of design and quality assuring actions; individual values for S, O, and D that are greater than 8 should be more closely observed; the product

of O and D gives information concerning the probability that undetected parts with defects will reach the hands of the customer [27].

The screenshot shows the 'DSS based FMEA' interface. It includes a 'Data Source' section with a date range selector from 'March 2020' to 'September 2020'. The 'FMEA Process' section has a 'Potential Failure Mode' dropdown set to 'Deviation in seam'. Below this are three sections for 'Severity', 'Occurance', and 'Detectibility', each with a dropdown menu. The 'Severity' dropdown is set to '6', 'Occurance' to '8', and 'Detectibility' to '2'. At the bottom, there are buttons for 'Save Data', 'Edit Data', and 'Show RPN Graph'.

Figure 9. Interface for FMEA process

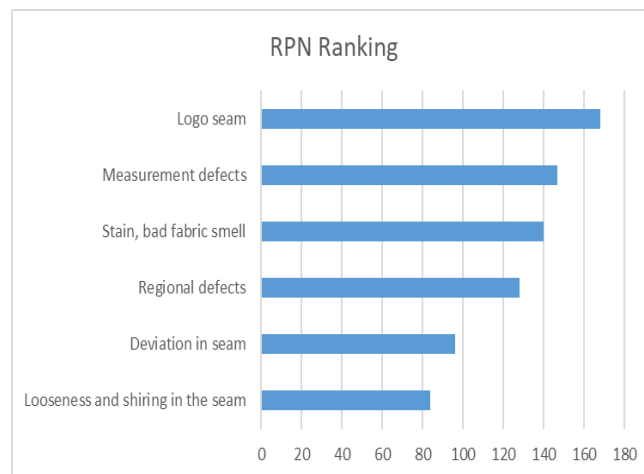


Figure 10. Ranking according to RPN values

According to RPN values in Figure 8, potential failure modes related to the failure effects and failure causes are summarized in Table 4:

Table 4. Failure modes and effects, causes of failures

Potential failure mode	Potential failure effects	Potential causes of failures	Current process control detection
Logo sewing	Mistakes in sewing metal or plastic logos indicating the brand.	<ul style="list-style-type: none"> • Logo sewing in the wrong place, • Wrong rope use, • Logo defects such as cuts and tears, • Influence of human factors 	<ul style="list-style-type: none"> • In process inspection by monitoring the appearance of logo in logo seam step
Measurement defects	The final product does not have equal dimensions with the original.	<ul style="list-style-type: none"> • Wrong seam allowance, • Hurry due to bottleneck, • Incorrect work studies 	<ul style="list-style-type: none"> • Post process inspection by checking the measure of product for every 20 samples manually
Regional defects	Tears, cuts, dents, scuff marks etc. on the product.	<ul style="list-style-type: none"> • Defect originating from logo sewing, • Transport-related defect, • Defects caused by machining, • Contract manufacturing defect, • Influence of human factors, • Incorrect work studies/standard time 	<ul style="list-style-type: none"> • In process visual inspection by monitoring defects of the product
Stain, bad fabric smell	Occurrence of undesirable events such as permanent or temporary stains, dirt, odors in the product.	<ul style="list-style-type: none"> • Negligence of periodic machine cleaning, • Transport-related contamination, • Hygiene neglect in contract manufacturing, • Influence of human factors 	<ul style="list-style-type: none"> • In process visual inspection by monitoring defects of the product
Deviation in seam	Stitch not aligned correctly, double stitching.	<ul style="list-style-type: none"> • Frequent machine downtime, • Misalignment in the machine, • Hurry due to bottleneck, • Influence of human factors, • Incorrect work studies/standard time 	<ul style="list-style-type: none"> • Post process inspection by checking the alignment of seam by a gauge
Loseness and shirring in the seam	Problems caused by the fabric being too stretched or released while sewing.	<ul style="list-style-type: none"> • Hurry due to bottleneck, • Influence of human factors, • Incorrect work studies/standard time 	<ul style="list-style-type: none"> • Post process visual inspection by checking on product appearance by a gauge

3.2 Improvement Proposals

An effective incoming quality control system should be established for the logos and fabric outsourced, and acceptance sampling techniques should be used. It has been suggested to detect and warn the subcontractors that send the faultiest products.

Standard times should be re-arranged by time studies. Employees working in the processes of fabric cutting, sewing and logo sewing should also act as controllers, and material-related defects should be prevented before errors occur. Especially experienced workers should be selected for these processes, the circulation of workers should be reduced and sustainability should be ensured with an effective performance system. In order to control the performance evaluation system fairly, color identity application can be proposed. With this implementation, it is possible to define a color code for each worker and use this small set of colored adhesive paper to easily determine which product is sewn by which worker. Thus, employees who work meticulously and do their job well can be

identified and wage incentives can be provided for error-free work.

The lack of motivation of employees due to situations such as intense pace, insufficient breaks, pressure, stress, lack of communication and unwilling work that result in a decrease in productivity are remarkable. Rearranging shifts is important for employees to be fit, motivated and focused. In addition, workers' rest and break time adjustments will contribute to minimizing fatigue and reducing errors. The processes that cause the bottleneck should be analyzed, and the disruption of production due to factors such as loss, waste, stolen should be prevented. For this, it has been proposed to integrate additional control points for more frequent counting and control effort. Intensive manual labor and reducing the amount of sub-contraction is another issue that needs to be considered.

To reduce machine-related failures and contamination, preventive maintenance, machine cleaning and replacement of old machine parts and equipments can be error-reducing solutions. During the production phase, human and machine

based factors have the potential to cause undesirable faults such as dirt, oil, odor, and permanent or temporary stains and odors. The cost of damages such as time, labor, energy loss encountered as a result of errors is enormous. If it is not noticed during production and reaches the consumer, it may cause prestige and customer loss. If a permanent stain occurs on a large amount of products, the production plan may be disrupted. With 5 S applications in the T-shirt production process, the confusion in the process can be reduced, and defects caused by contamination and odor can be greatly reduced. It is important to regularly clean the containers in which the products are transported.

Rough and non-transparent sacks used in storage cause lint in the product, and the fabric or thread getting stuck in the sack and rupture causes damage to the product. To remedy this, using smooth and transparent sacks are proposed. Thus, it will now be less likely to cause damage to the product, as it is more reliable and easier to visual control.

In addition, it can be a good precaution to warn employees about cleanliness and order, and to hang noteworthy announcements on the entrance panels of sewing sections where problems are common.

With regular start-up trainings and DSS-based error tracking system similar to the previous application, the negative impact of human factors can be largely eliminated by determining the sources of errors. For example, with the recruitment of new workers, production disruption occurred frequently, and a questionnaire was recommended to prevent this. Until a decrease was achieved in the number of resignations, it was considered to conduct an "Employee Satisfaction Survey". With this questionnaire, it was aimed to determine the reasons for leaving the job and to get suggestions to improve the general working conditions. Among the recommendations are giving incentives or awards to employees with few mistakes, providing training on the use of simple quality tools by creating quality circles, encouraging the suggestion system working with applications such as before-after kaizen and 5 S. Thus, reducing the workforce circulation as much as possible, and ensuring that each employee specializes in two jobs are intended.

Human-induced errors such as inexperience workers, contract labor and labor circulation were noticed in almost every process. In particular, it has been observed that measurement errors occurring during sewing operations are caused by reasons such as being hasty to meet daily targets, keeping the seam allowance more or less, taking wrongly measured pieces to the production line, distraction of the worker, lack of motivation, adjustment problems in the machine. The reason for the measurement defects during cutting is that the number of fabrics put on top of each other is above the machine cutting capacity. Other reasons can be stated as the negligence of the process follow-up during

cutting and the insufficiency of the controls performed during the classification.

Preventive actions have been proposed to reduce these identified causes. It is not possible to apply a different preventive action for faults that occur during cutting because the only action is to stack the fabrics and put them in the machine. The fact that the fabrics are not damaged during cutting generally depends on the fabric structure. However, in some cases, when the required number of pieces is high, the workers keep the number of fabrics too much in order for the process to be completed quickly, and this situation causes the cutting capacity of the machine to be exceeded and the related cutting errors lead to measurement distortion. For this reason, it was recommended to warn and inform the machine supervisor about the cutting numbers before the operation. One of the precautions taken to reduce the size defects that occur during sewing may be to leave one sample model in the working area of each operator. It is important to note that the measurements are exactly accurate according to the main model. The observations made showed that the production lines were created arbitrarily. Instead, the same work step can be given to each operator, enabling workers to specialize in their work.

4. CONCLUSION

This study consists of two different DSS-based applications in jacket and basic T-shirt production processes of the firms in the textile field.

In the first application, manual control and data entry operations at control points in the jacket production process were integrated with a DSS. Thus, correct data usage has become possible in SPC and a dynamic structure has been given to SPC studies. In addition, an interactive bridge has been created between the worker, controller and manager. With the new system, it is predicted that the communication between the employee and the manager will be faster and more secure.

Based on the data recorded in the database, the decision maker can draw Pareto charts by taking into account both frequencies and weighted frequencies for the desired date range, and can determine the defect types that cause 80% of the problems. It can test whether the process is under control or not by means of DCC graphs whose limits are calculated using defect weights and numbers. If an out-of-control situation is observed, it has the chance to intervene on time.

In the second application, a DSS has been designed where FMEA analysis can be performed during the basic T-shirt production process. In this way, it will be possible to make the necessary improvements by analysing failure modes and effects on the customer before shipment. With the

developed DSS, first of all, potential failure modes, which were obtained from the records of the previous period and were inscribed as priority errors in the pareto diagram, were obtained. RPN values obtained based on probability, severity and detectability values are presented to the user with graphical visualization. For failure modes with high RPN values, preventive actions regarding failures have been developed by the FMEA team. The proposed DSS analyzed the previous period data, directed them to areas where precautions could be taken primarily, and the existence of such a system created FMEA awareness among employees. The proposed DSS facilitates the calculation of RPN scores in FMEA process. This study is also useful in terms of easily calculating post-improvement RPN scores in future studies and seeing the effects and benefits of the measures taken for improvement

Thanks to the DSS-based FMEA and SPC applications designed to be used in different textile processes, it has become easier for senior managers to interpret, analyze and make certain decisions. With the proposed system, an increase in the production quality and income of the company is expected in the long term.

Jacket is a product with a high share in turnover. Therefore, serious defects can lead to high costs. The people in the

position of decision maker in the company, want to monitor the process variability with the help of an appropriate tool after the defects in the jacket production process are classified. Demerit control charts are SPC tools developed specifically for this reason. Despite the developing automation systems, the textile industry maintains its labor-intensive structure. For this reason, many human-induced errors occur. Especially in the T-shirt production process, errors vary according to the model. The more details, fabric sensitivity and processing there are in the ordered product, the more various types of errors occur for the product. FMEA is a useful analytical tool that aims to identify and eliminate known or potential losses/errors in the system during the design or process phase. In further studies, both SPC and FMEA studies can be maintained for many processes in the enterprise. In this article, only one of the DSS-based methods (FMEA/SPC) is exemplified for each process. At the same time, an effective failure tracking system should be established for production processes in textile enterprises with intensive human factors. With a DSS that works in integration with other rapidly developing artificial intelligence techniques, an effective error prevention, error diagnosis and debugging system can be developed, and systems can be created to reduce losses and prevent inefficiency.

REFERENCES

1. Burnak N, Demirtaş EA. 2019. *Toplam Kalite Yönetiminde İstatistiksel Süreç Kontrol*. Eskişehir: ESOGÜ yayınları.
2. Sharma KD, Srivastava S. 2018. Failure mode and effect analysis (FMEA) implementation: A literature review *Journal of Advanced Research in Aeronautics and Space Science* 5, 2454-8669.
3. Küçük M, İşler M, Güner M. 2016. An application of the FMEA method to the cutting department of a clothing company *Textile and Apparel* 26(2), 205-212.
4. Paired E, Swadeshi AH, Shokohyar S. 2017. Analyzing the enhancement of production efficiency using FMEA through simulation-based optimization technique: A case study in apparel manufacturing *Cogent Engineering* 4(1), 1284373
5. Beyene TD, Gebeyehu SG, Mengistu AT. 2018. Application of Failure Mode Effect Analysis (FMEA) to Reduce Downtime in a Textile Share Company *Journal of Engineering, Project, and Production Management*, 8(1), 40.
6. Beyene TD, Gebeyehu SG. 2019. Application of failure mode effect analysis (FMEA) for efficient and cost-effective manufacturing: A case study at Bahir Dar textile share company, Ethiopia *Journal of Optimization in Industrial Engineering* 12(1), 23-29.
7. Tekez EK. 2018. Failure modes and effects analysis using fuzzy topsis in knitting process *Textile and Apparel* 28(1), 21-26.
8. Mutlu NG, Altuntas S. 2019a. Hazard and risk analysis for ring spinning yarn production process by integrated FTA-FMEA approach *Textile and Apparel* 29(3), 208-218.
9. Mutlu NG, Altuntas S. 2019b. Risk analysis for occupational safety and health in the textile industry: Integration of FMEA, FTA, and BIFPET methods *International Journal of Industrial Ergonomics* 72, 222-240.
10. Montgomery DC. 2009. *Introduction to Statistical Quality Control*, United States of America, New York: John Wiley and Sons.
11. Ertuğrul İ, Özçil A. 2014. The application of 'p' and 'p-CUSUM' charts into textile sector in the statistical quality control process *Textile and Apparel* 24(1), 9-14.
12. Yıldız TÖ, Vahaplar SŞ. 2015. An application on fancy shirting fabric production through distribution-free quality control charts *Textile and Apparel* 25(2), 97-103.
13. Yılmaz H, Yanık S. 2020. Design of demerit control charts with fuzzy c-means clustering and an application in textile sector *Textile and Apparel* 30(2), 117-125.
14. Zarate P. 2013. *Tools for collaborative decision-making*. United States of America, New York: John Wiley & Sons.
15. Guo Z, Ngai E, Yang C, Liang X. 2015. An RFID-based intelligent decision support system architecture for production monitoring and scheduling in a distributed manufacturing environment *International journal of production economics* 159, 16-28.
16. Mete S., Serin F., Oz NE, Gul M. 2019. A decision-support system based on Pythagorean fuzzy VIKOR for occupational risk assessment of a natural gas pipeline construction *Journal of Natural Gas Science and Engineering* 71, 102979.
17. Febriani RA., Park HS, Lee CM. 2020. A Rule-Based System for Quality Control in Brake Disc Production Lines *Applied Sciences* 10(18), 6565.
18. Senturk S, Erginel N, Kaya I, Kahraman C. 2014. Fuzzy exponentially weighted moving average control chart for univariate data with a real case application *Applied Soft Computing* 22, 1-10.
19. Li CI, Pan JN, Huang MH. 2019. A New Demerit Control Chart for Monitoring the Quality of Multivariate Poisson Processes *Journal of Applied Statistics* 46(4), 680-699.
20. Dodge HF. (1928) A method of rating manufactured product *The Bell System Technical Journal* 7, 350-368.
21. Rasouli O, Zarei MH. 2016. Monitoring and reducing patient dissatisfaction: A case study of an Iranian public hospital *Total Quality Management & Business Excellence* 27(5-6), 531-559.
22. Niazmand K., Mirzazadeh A, Rezaie K. 2014. A fuzzy SQFE approach in supplier's performance monitoring *International Journal of Production Research* 52(22), 6841-6862.

23. Nembhard DA, Nembhard HB. 2000. A demerits control chart for autocorrelated data *Quality Engineering* 13(2), 179-190.
24. Shu MH, Chiu CC, Nguyen TL, Hsu BM. 2014. A demerit-fuzzy rating system, monitoring scheme and classification for manufacturing processes *Expert Systems with Applications* 41(17), 7878-7888.
25. Ho SL, Xie M, Goh TN. 2003. Process Monitoring Strategies for Surface Mount Manufacturing Processes *International Journal of Flexible Manufacturing Systems* 15(2), 95-112.
26. Yazıcı K, Gökler SH, Boran S. 2020. An integrated SMED-fuzzy FMEA model for reducing setup time *Journal of Intelligent Manufacturing* 32, 1547-1561.
27. Bertsche B. 2008. *Reliability in automotive and mechanical engineering: determination of component and system reliability*. Berlin Heidelberg: Springer-Verlag.

Appendix.A Defect types and numbers (data for the last 15 days)

DEFECT TYPE	w	1	2	3	4	5	6	7	8	9	10	11	12	13	14	15
CNT1-DF1	50	3	5	1	6	3	5	6	8	3	2	3	2	3	2	2
CNT1-DF2	10	1	4	2	7	2	2	3	0	4	2	5	4	1	3	5
CNT1-DF3	10	4	3	1	3	1	5	2	3	5	2	6	9	6	3	2
CNT1-DF4	1	4	8	5	1	4	2	5	3	3	3	4	5	6	4	6
CNT1-DF5	50	7	3	2	1	2	5	6	7	0	4	5	4	4	2	6
CNT1-DF6	10	6	4	6	3	4	1	2	1	2	8	2	3	4	4	2
CNT1-DF7	10	6	2	3	4	2	3	7	1	4	5	3	6	0	6	8
CNT1-DF8	50	6	9	4	5	4	4	6	7	0	4	6	3	5	7	5
CNT1-DF9	1	6	1	3	4	5	4	3	4	2	5	1	2	3	2	4
CNT1-DF10	1	8	4	5	2	3	4	3	4	5	0	1	3	2	1	3
CNT1-DF11	1	5	6	5	5	4	5	3	4	3	5	3	4	4	3	3
CNT1-DF12	50	3	6	5	2	5	8	6	4	6	2	3	5	7	1	5
CNT1-DF13	50	5	3	3	3	3	0	3	4	4	3	3	5	4	5	2
CNT1-DF14	10	6	4	3	7	1	3	5	2	3	7	4	3	2	2	9
CNT1-DF15	50	7	3	4	4	5	4	2	7	6	4	1	4	2	4	2
CNT1-DF16	1	1	2	8	5	9	7	1	4	5	2	6	5	0	6	9
CNT1-DF17	1	3	2	2	4	2	3	2	4	5	7	3	4	3	4	2
CNT1-DF18	50	3	2	6	3	5	0	4	5	1	7	4	3	3	4	4
CNT1-DF19	10	2	2	5	5	5	1	4	1	7	2	5	2	5	4	2
CNT1-DF20	10	4	7	2	3	5	3	2	5	1	4	6	4	5	4	2
CNT1-DF21	10	3	2	6	3	7	1	6	2	4	8	6	9	6	4	3
CNT2-DF1	50	1	1	1	4	0	3	2	2	4	1	2	3	1	1	3
CNT2-DF2	50	1	2	2	2	0	5	3	0	2	1	3	1	2	2	3
CNT2-DF3	50	3	0	2	1	2	3	2	1	3	4	1	2	0	1	3
CNT2-DF4	10	1	3	1	3	1	2	1	0	2	0	0	0	0	1	4
CNT2-DF5	1	5	1	4	3	2	2	0	3	2	0	5	2	5	3	1
CNT2-DF6	1	1	3	1	3	1	2	2	1	2	1	4	2	3	1	1
CNT2-DF7	1	2	2	1	2	5	2	1	0	1	4	0	1	1	3	3
CNT2-DF8	50	1	3	3	2	1	2	2	2	1	0	3	3	1	3	2
CNT2-DF9	10	1	1	1	5	3	4	4	0	2	0	2	4	2	2	1
CNT2-DF10	10	2	3	1	5	2	2	1	1	2	0	3	4	0	1	1
CNT2-DF11	1	2	4	5	6	2	2	6	2	2	3	1	2	1	2	3
CNT2-DF12	50	1	1	4	2	1	2	0	2	0	1	1	3	0	3	4
CNT2-DF13	10	2	0	2	1	1	1	0	3	0	4	1	0	2	2	1
CNT2-DF14	10	1	1	2	4	3	0	0	0	5	1	4	1	2	4	2
CNT2-DF15	1	3	3	2	1	3	2	0	2	2	3	3	3	1	0	0

CNT2-DF16	1	3	2	2	1	3	3	3	1	0	4	4	1	0	1	3
CNT2-DF17	1	5	3	0	6	0	3	2	1	2	3	2	3	6	2	0
CNT2-DF18	50	6	2	4	2	2	1	4	3	3	2	2	2	1	1	0
CNT2-DF19	10	1	3	4	4	1	1	3	2	9	2	1	5	2	3	0
CNT3_DF1	1	4	1	4	6	3	0	4	5	1	3	2	3	5	3	2
CNT3_DF2	1	4	4	3	5	3	4	4	3	5	6	2	5	4	6	2
CNT3_DF3	10	1	3	7	5	5	3	0	2	3	4	1	2	5	2	4
CNT3_DF4	1	3	2	1	3	0	4	5	2	1	4	1	1	7	1	1
CNT3_DF5	50	4	7	1	5	6	3	2	3	1	3	5	8	3	4	1
CNT3_DF6	10	3	8	0	4	3	4	2	4	3	4	1	3	2	2	3
CNT3_DF7	10	4	1	5	3	3	5	8	4	2	2	4	5	4	2	2
CNT3_DF8	1	5	1	3	5	1	6	2	5	4	2	3	2	1	1	3
CNT3_DF9	1	3	3	5	2	6	1	1	2	1	5	6	2	4	4	1
CNT3_DF10	50	3	2	2	6	2	4	1	0	3	2	4	3	5	3	3
CNT3_DF11	10	4	2	6	5	2	2	2	6	2	3	2	2	2	3	1
CNT3_DF12	1	1	1	4	0	1	1	4	3	0	4	2	3	8	3	9
CNT3_DF13	10	3	2	3	1	6	5	1	2	0	3	3	1	3	2	4
CNT3_DF14	1	1	2	4	2	4	2	2	4	3	2	3	3	4	2	4
CNT3_DF15	50	2	1	3	2	4	0	1	4	3	4	4	2	0	3	5
CNT3_DF16	1	0	0	1	5	1	4	2	3	3	4	4	3	2	3	4
CNT3_DF17	1	7	2	1	1	3	5	5	2	4	1	2	1	1	1	3



Development of Multifunctional Bio-based Cotton Composite

Emine Altinkaya[†]  0000-0002-5652-3156

[†] Manisa Celal Bayar University / Department of Bioengineering / Faculty of Engineering, Muradiye, Manisa, Turkey

Corresponding Author: Emine Altinkaya, emine.altinkaya@cbu.edu.tr

ABSTRACT

In this study, the production and characterization studies of clay-chitosan based composites were investigated. The composite products were characterized by Scanning Electron Microscopy, Thermo Gravimetric Analysis, and Fourier Transform Infrared Spectroscopy. Besides antibacterial effect of the composites against *S. Aureus* and *K. Pneumonia* and dye adsorption properties were investigated. The effects of contact time, ionic strength, pH, and temperature on removal of remazol blue were investigated for the adsorption studies. The comparison was performed based on the characterization results of treated and untreated cottons. It was revealed that the one-step process of clay-chitosan-based fabrics gave significantly good properties to fabrics. These improved properties expressed the dyeing free-salt, antibacterial activity, and enhanced dyeability (dye adsorption capacity) of cotton. Consequently dyeability of the cottons was increased with the treatments. These treatments can be used in textile industry for the free salt dyeing which is a desirable property for the cotton in addition to the gained antibacterial activity. As a result, clay-chitosan composites can be considered as a hopeful composite for the multifunctional finishing textiles.

1. INTRODUCTION

Textile finishing is an important stage in making textile products suitable for use. The processes involved in textile finishing are the steps where the most water and energy consumption is made. Wastewater produced by textile processing plants leads to serious water and air pollution. With increasing environmental awareness, environmentally friendly and sustainable products and methods are preferred in textile goods production. Modern consumers' demand for both aesthetic and multi-functional products is increasing day by day. UV protection, antibacterial, water-oil repellency, self-cleaning properties can be gained to the fabric by using finishing agents. Organic, inorganic, and composite materials can be used in the finishing process. In the textile sector, environmentally friendly processes are needed that can meet the demands of consumers and save

water and energy. In recent years, traditional methods have been replaced by nanotechnology, biopolymers, enzyme, chemical products obtained from natural sources, plasma applications [1, 2].

Dyes are utilized in various fields such as textiles, cosmetics, plastic, leather, etc., for coloring the products [3]. Factories discharge large amounts of environmentally hazardous toxic waste, mostly of textile dye and finishing salts. The hydroxyl group in cellulose is negatively charged upon contact with water. The dyes used for cotton are generally anionic. The negative charges of cotton repulse the dye. And so the repulsion of negative charges decreases the dyeing of cotton. A great quantity of electrolyte is used to recovery the affinity between anionic dye and negative charged cotton [4]. But the release of these electrolytes into nature causes great damage to the environment. Textile

ARTICLE HISTORY

Received: 08.01.2021

Accepted: 07.09.2021

KEYWORDS

Cotton, antibacterial, chitosan, montmorillonite, remazol blue, adsorption, dyeing free salt

To cite this article: Altinkaya E. 2021. Development of multifunctional bio-based cotton composite *Tekstil ve Konfeksiyon* 31(4), 264-273.

dyes and finishing salts used in fabric dyeing account for 17-20 percent of water pollution [5]. The pollutions (finishing salts, textile dyes) are ecotoxic, and give a huge hazardous to environment, human, animals, etc. The pollution should remove from waste water. [6]. Salt-free dyeing is important for the textile industry due to being an ecofriendly method [4]. The dyeability of fabric can be enhanced by modification or cationization of the fabric surface. The fabric surface can be cationized with chitosan and enhanced the dyeability of fabric. These processes applied to the fabric are classified as salt free dyeing [7].

Various techniques such as chemical adsorption, oxidation, ozonation, coagulation are utilized for the elimination of organic and inorganics impurities from drain water [8]. Adsorption is the most using method due to get rid of dye contamination from drain water. Adsorbent materials can be classified into five category based on their ability: plant waste, fruit waste, natural inorganic materials, waste of industry, and bioadsorbents [8]. Clays as a natural inorganic material are widely used in adsorption studies [9].

Clays are natural materials with high surface area. Clays have many usage areas due to their mechanical, thermal, and unique properties. KSF is a natural clay mineral. KSF has no adverse effects on humans and animals [10]. Montmorillonite (KSF) has a large adsorption capacity thanks to smectite group in structure [11]. The use of additives such as KSF can be considered a universal method to increase adsorption capacity [12]. Coating the cotton with KSF can help to dye with a small amount of paint thanks to the adsorption capacity of KSF. KSF is an effective reinforcement material in enhancing the antimicrobial effect [12].

Chitosan, deacetylated chitin, is inexpensive, abundant, non-toxic, biocompatible, and eco-friendly material [13]. Chitosan is an abundant biopolymer in the world that makes chitosan economic [14]. And also chitosan is attractive biopolymer due to having antibacterial and adsorption properties. It is used for dye removal from wastewater [15]. The polycationic structure enhances the dye adsorption capacity of chitosan [6, 11, 16]. Chitosan-inorganic composite have wide application areas (drug release, packaging material, biodegradable materials, dye removal, electrochemical sensor) [17]. Chitosan-inorganic composites can be used to obtain multifunctional properties [18].

In this study, it was aimed to fabricate the bio-based multifunctional composites material via using invaluable properties of chitosan and KSF. It was aimed to gain the fabric dye adsorption capacity, antibacterial properties, free salt dyeability and effective dyeing with a small amount of paint. For these purpose cotton was treated with chitosan, KSF and dihydroxy ethylene urea (MDEU) in one step process.

Novelties of this study are “gain antibacterial properties to the cotton thanks to the natural properties of chitosan and KSF”, “enhance the affinity between cotton and dye thanks

to the properties of clay and chitosan,” and “obtain eco-friendly, economic, and effective fabric dyeing without using “finishing salts” by improving the affinity between fabric and dyestuff”.

The dye [Remazol Blue (RB)] adsorption and antibacterial feature of cotton samples were studied. Then the samples were characterized via Scanning Electron Microscopy (SEM), Thermo Gravimetric Analysis (TGA) and Fourier Transform Infrared Spectroscopy (FTIR) instruments.

2. MATERIALS AND METHODS

2.1. Materials

100 % cotton fabric (153 g/m²) was utilized in this study. The cotton was bleached and scoured woven. Chitosan (highly viscous, average MW: 500000-700000 gm⁻¹, degree of deacetylation: 75-85 %), MDEU, and glacial acetic acid (CAS Number: 64-19-7) were supplied from Fluka, Huntsman, and Sigma- Aldrich, respectively. KSF MMT (surface area of 20-40 m²/g) was supplied from Fluka. Chemical composition of KSF is 3.0% MgO, 18.0% Al₂O₃, 55.0% SiO₂, %3.0 CaO, 1.5% K₂O, 4.0% Fe₂O₃, 5.0% Sulphate, <0.5% Na₂O, and 10.0% loss on ignition.

2.2. Fabrication of Sample

2.2.1 Fabrication of Cot-KSF

KSF mixture was prepared for cotton padding. For this purpose 2% KSF mixture was prepared overnight to swell the clay. The cotton was padded in swelled 2% KSF mixture and squeezed. The wet cotton was dried for 5 min and cured for 3 min at 80 °C and 120 °C, respectively.

2.2.2 Fabrication of Cot-KSF-chi

The 2% KSF mixture was prepared overnight to swell the clay. Chitosan solution (2%) was prepared with 2% acetic acid solution. The chitosan solution was added in swelled KSF mixture and mixed for 6h at 60 °C. Cotton was padded in the mixture (KSF-chi) and wringed. The wet cotton was dried for 5 min and cured for 3 min at 80 °C and 120 °C, respectively.

2.2.3 Fabrication of Cot-KSF-chi-MDEU

The 2% KSF mixture was prepared overnight to swell the clay. MDEU (150 kg m⁻³) was added to the swelled KSF mixture. Chitosan solution (2%) was prepared with 2% acetic acid solution. The chitosan solution was added in the KSF-MDEU mixture and mixed for 6h at 60 °C. Cotton was padded in the mixture (KSF-chi-MDEU) and squeezed. The wet cotton was dried for 5 min and cured for 3 min at 80 °C and 120 °C, respectively.

2.3. Characterization of Samples

2.3.1. FTIR analysis

The describing of functional groups in sample structure was investigated by Fourier Transform Infrared (FTIR) analysis.

ATR-Perkin Elmer Spectrum BX-II model FTIR was used for investigation [19].

2.3.2. Scanning electron microscopy (SEM)

The samples morphologies were investigated by scanning electron microscope (FEI Quanta FEG 250 SEM). The accelerating voltage was 5-12 kV. The fabricated samples were prepared for SEM analysis by coating the surface with gold [19].

2.3.3 Thermo gravimetric analysis (TGA)

The Thermo Gravimetric Analysis of samples was performed with Perkin Elmer Diamond TG/DTA. Samples were analyzed by heating (30 to 600 °C) under nitrogen flow (10 °C min⁻¹) [19].

2.4. Adsorption Study

For this study, 25 mL Remazol Blue solution was prepared in different initial concentrations. 0.1 g of treated and untreated cotton fabrics (1 cm x 1 cm) were used due to adsorption studies. The cotton fabric was removed from Remazol Blue solution when the equilibrium was achieved. The latest concentration of Remazol Blue solution was investigated by UV- visible spectrophotometer (Shimadzu, model UV 1601) at 604 nm. The adsorbed (at equilibrium) dye amount q_e (mg/g) was calculated according to the equation:

$$q_e = \frac{C_0 - C_e}{m} V \quad (1)$$

where C_0 (mg/L) is the beginning concentration of Remazol blue, V indicates the solution volume (L), m (g) indicates the cotton fabric mass, and C_e (mg/L) is the equilibrium concentration of Remazol Blue solution. The adsorption studies were performed in a thermostat shaking water bath (150 rpm) at different temperatures of 298, 308, 318 and 338 K [20].

2.5. Kinetic Study

Kinetic studies were performed by using 25 mL RB solution and 0.1 g untreated and treated cotton fabric. The cotton was put into the RB solution and mechanically agitated at various temperatures. The adsorbed dye at certain interval of time was determined with UV- visible spectrophotometer [20].

2.6. Effect of pH

The impact of beginning pH on adsorption of RB on treated and untreated cotton fabric was investigated at various pH values (4–10).

The initial pH values were adjusted by 0.1 M NaOH and 0.1 M HCl. 0,1g cotton was used in this study. The study

conditions; RB concentration was 15 ppm, shaking time was 90 min, temperature was 298 K [20].

2.7. Effect of Ionic Strength

Effect of ionic strength on RB adsorptions of cotton was performed using various concentrations of NaCl (12–50g/L). 0,1g cotton was used in this study. The study conditions; RB concentration was 18 ppm, shaking time was 90 min, temperature was 298 K [20].

2.8. Antibacterial Activity

The antibacterial activity of fabricated samples was investigated against Gram-negative bacteria (*Klebsiella pneumonia*-ATCC 4352) and Gram-positive bacterium (*Staphylococcus aureus* - ATCC 6538) according to AATCC Test Method 100-2007. The reduction of bacteria was evaluated in “0” and “24” h. 1 mL diluted bacteria (1–2 × 10⁵ CFU mL⁻¹) was added on fabric samples (diameter: 4,8cm). The fabric samples were incubated at 37 °C for “0” and “24” h. The incubated fabric was put in 100 mL distilled water and shook for 1 min. 1μL from this solution was put on agar and incubated at 37 °C for 24 h [19].

The following equation gives the percentage reduction of bacteria (R) by the cotton samples:

$$R = 100 * \frac{B - A}{B} \quad (2)$$

where A is the number of bacteria of “24”h treated, B is the number of bacteria of “0”h treated samples [13]. Antimicrobial activity of Cot-KSF, Cot-KSF-chi, and Cot-KSF-chi-MDEU was investigated.

3. RESULTS AND DISCUSSION

3.1. Characterization of Samples

3.1.1. FTIR analysis

Figure 1 shows the FTIR analysis of untreated cotton, cot-KSF, cot-KSF-chi, and cot-KSF-chi-MDEU. The samples exhibited similar spectra as exhibited in Figure 1. The broad band at around 3350 cm⁻¹ indicated the OH stretching that overlapped the N-H stretching vibration. The broad band at around 3350 cm⁻¹ was OH stretching for untreated cotton and cot-KSF while N-H stretching vibration for cot-KSF-chi, and cot-KSF-chi-MDEU. The peaks around 2920-2925 cm⁻¹ indicate the C-H stretching vibrations and also indicate the C-H stretching vibration in –CH₂ and –CH₃ of chitosan. The small peak at around 1320, 1570, and 1670cm⁻¹ was indicated the C-N (amide III) stretching, N-H (amide II), and carbonyl group (amide I) vibrations, respectively. The peak at around 1058 cm⁻¹ the peak was shown in all samples but the intensity of the peak was decreased for cot-KSF-chi, and cot-KSF-chi-MDEU. The decrease in intensity of peak can be explained with the interaction Si-O-Chitosan bonding [21-24].

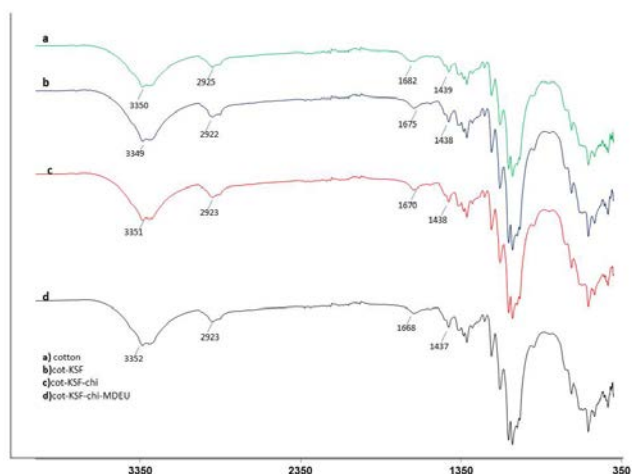


Figure 1. FTIR Analysis of untreated cotton, cot-KSF, cot-KSF-chi, and cot-KSF-chi-MDEU.

3.1.2. Scanning electron microscopy (SEM)

The SEM analysis of untreated cotton, cot-KSF, cot-KSF-chi, and cot-KSF-chi-MDEU was indicated in Figure 2 at 5000x magnifications. Figure 2a shows the untreated cotton surface. The fiber of untreated cotton can be seen clearly. The KSF particles are seen on the cot-KSF sample indicated in Fig.2b. The coated chitosan and KSF on cotton can be seen in Fig.2c. as can be seen in Fig 2c and 2d chitosan filled the gap between the fibers. MDEU was used as crosslinker agent for cot-KSF-chi-MDEU and so the chitosan and KSF hang on to the cotton surface.

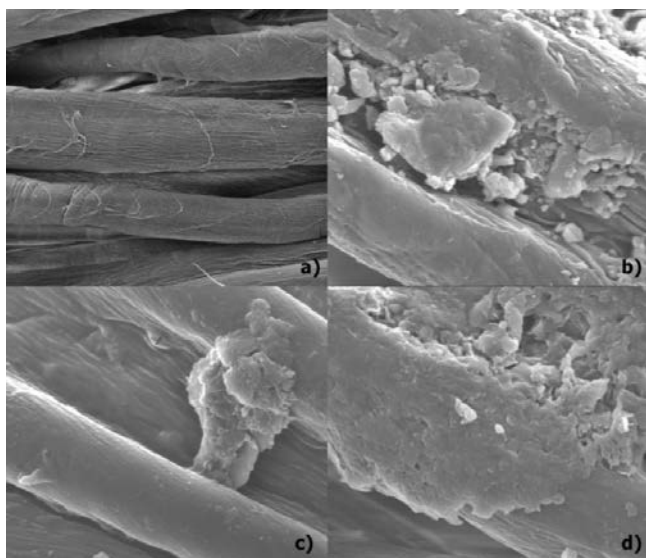


Figure 2. SEM figure of a) untreated cotton, b) cot-KSF, c) cot-KSF-chi, and d) cot-KSF-chi-MDEU.

3.1.3 Thermo gravimetric analysis (TGA)

The TGA curves of samples were given in Figure 3. The decomposition temperature of untreated cotton, Cot-KSF, Cot-KSF-chi, and Cot- KSF -chi-MDEU was investigated as 369, 362, 351, and 351 °C, respectively. The decomposition temperature of untreated cotton was investigated at around 369°C as reported in Gaan and Sun study [25]. The max. decomposition temperature was

decreased from 369 to 351°C for untreated cotton, Cot-KSF, Cot- KSF -chi, and Cot- KSF -chi-MDEU. The max degradation temperature of cellulose was decreased after treatments. The decrease in max decomposition temperature can be due to damage of strong H bonds in cellulose. The materials in the structure of samples can be lead to damage of H bonds in cellulose. Shanks and Ouajai reported that cellulose which has greater crystalline structure decompose at higher temperature [26]. And also Altınışık et al. reported that the CI (crystallinity index) of cellulose was decreased after treatments and the lower CI led to the decrease in decomposition temperature [19].

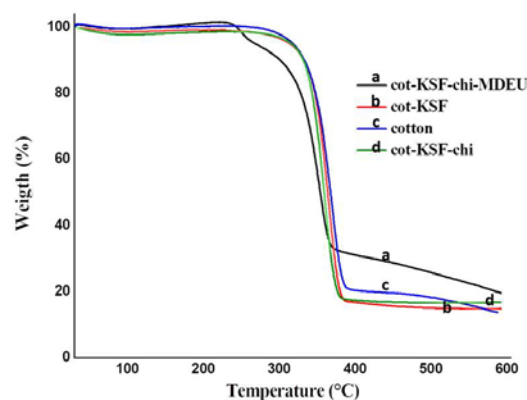


Figure 3. TG curves of samples untreated cotton (c), cot-KSF (b), cot-KSF-chi (d), and cot-KSF-chi-MDEU (a).

Table 1. Results of thermogravimetric analysis.

Sample	T (°C)	Mass loss %
Cotton	369	80
Cot- KSF	362	85
Cot- KSF -chi	351	83
Cot- KSF -chi-MDEU	351	69

3.2. Effect of pH

Investigation of the impact of pH on RB adsorption on the treated and untreated cotton fabric was investigated at beginning dye concentration of 15mg/L with an amount of treated and untreated cotton fabric of 0.1 g/25 mL for equilibrium time of 90 min at 25 °C.

The results of RB dye adsorption in the pH range 4–10 were given in Fig. 4. The adsorption of RB on the treated and untreated cotton fabric, q_e (mg/g), decreased as the acidity decreased. The increase in acidity makes the adsorbent surface positively charged, thereby leading to an increase in adsorption of RB on adsorbent. Generally the removal of anionic dyes increase as the pH value increased while for cationic dyes decreased [3, 27].

Clay has hydrated sodium, silanol groups (SiOH) on the surface, and R-NH₃⁺ groups (chitosan) in the interlayer area [4, 28]. The decrease in pH level gave rise to protonation of -NH₂ group (-NH₃⁺) on the surface and ionization of SiOH. At low pH values, protonation of clay surface enhanced the electrostatic interaction. On the other hand, as the pH

values increased (more basic) the surface of clay was deprotonated. Deprotonation of the surface made difficult the access of negatively charged dye molecules to surface adsorption sites. The results exhibited the interaction between the adsorbent and dye molecules. The interactions were hydrogen bonding and the van der Waals interactions [29].

Figure 4 shows that the max adsorption capacity was evaluated at pH 4 for treated and untreated cotton. At pH 4 the optimal adsorption capacity (removal of RB dye) was reached due to an electrostatic interaction between anionic RB dye and the protonated sample surface. At higher pH levels dye adsorption capacity was decreased result of the competition between OH⁻ ions and anionic RB dye molecules [29].

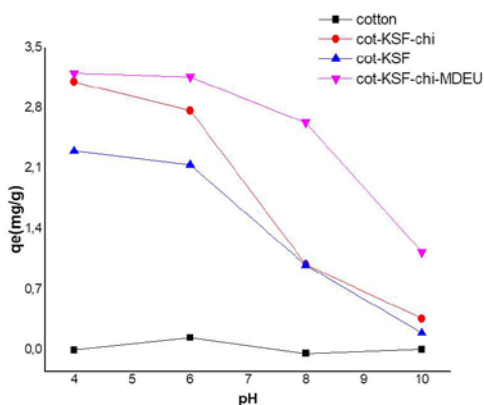


Figure 4. Impact of pH on dye adsorption of cotton, Cot- KSF, Cot- KSF -chi, and Cot- KSF -chi-MDEU.

3.3. Effect of Ionic Strength

The impact of salt concentration on dye removal was investigated. The dye solution was adjusted pH 4 where is the max adsorption observed. The attraction between adsorbate ions and adsorbent surface decreased from 0 (g/L) to 50 (g/L) salt concentration. So that q_e (mg/g) of adsorbent (treated cotton samples) decreased [30-32]. As indicated in Fig. 5, the adsorption capacities of treated samples were decreased while untreated cotton's was increased. The increase in ionic strength enhanced the electrostatic attraction between untreated cotton and RB.

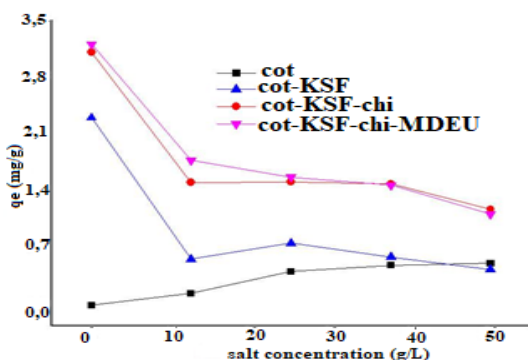


Figure 5. The impact of ionic strength on adsorption capacity of cotton, Cot- KSF, Cot- KSF -chi, and Cot- KSF -chi-MDEU.

3.4. Adsorption Isotherm

Dubinin-Radushkevich, Langmuir, Brunauer-Emmett-Teller, and Freundlich isotherm equations were used to investigate the equilibrium character of adsorption.

Langmuir adsorption supposes that adsorption takes place at homogeneous active sites on the adsorbent and adsorbed molecules. Langmuir isotherm is proper for monolayer adsorption on a homogeneous surface. The Langmuir isotherm equation with linearized form is indicated below [20, 33]:

$$\frac{C_e}{q_e} = \frac{1}{q_m L} + \frac{C_e}{q_m} \quad (3)$$

where C_e indicates the equilibrium concentration (mgL^{-1}) of dye in solution, q_e (mgg^{-1}) is the adsorbed dye per unit weight at equilibrium, q_m indicates the monolayer adsorption capacity (mgg^{-1}), L is the constant of Langmuir related to adsorption energy.

The fundamental properties of Langmuir isotherm may be explained in terms of dimensionless constant separation factor R_L [34]:

$$R_L = \frac{1}{1 + b \cdot C_0} \quad (4)$$

where b indicates Langmuir constant, C_0 indicates beginning dye concentration (mgL^{-1}). The R_L explains the type of isotherm to be linear ($R_L = 1$), irreversible ($R_L = 0$), favorable ($0 < R_L < 1$), and unfavorable ($R_L > 1$). The values related to Langmuir isotherms are given in Table 2. The given R_L values are between 0 and 1. According to R_L values indicated in Table 2, the adsorption is favorable.

The Freundlich isotherm is an experimental equation to describe the adsorption on the heterogeneous surfaces as well as multilayer sorption. The Freundlich isotherm equation is given below with linearized form [35]:

$$\log q_e = \log K_f + \frac{1}{nf} \cdot \log C_e \quad (5)$$

where the K_f (mgg^{-1}) and nf are the constant of Freundlich isotherm. K_f indicates adsorption capacity and nf represent adsorption intensity. C_e is the remnant dye concentration in solution; q_e is the adsorbed dye on adsorbent at equilibrium. The calculated values of

Freundlich isotherms are given in Table 2. Given correlation coefficient (R^2) values depict that Freundlich isotherm is unfavorable.

Dubinin-Radushkevich (DR) isotherm is presented as [27, 34]:

$$\ln q_e = \ln X_m - \beta \cdot \epsilon^2 \quad (6)$$

where X_m is the DR monolayer adsorption capacity ($molg^{-1}$), q_e (mgg^{-1}) indicates the adsorbed dye per unit weight of adsorbent, β (mol^2J^{-2}) is the constant related with sorption energy and ϵ is Polanyi potential which is given below as:

$$\epsilon = R \cdot T \cdot \ln \left(1 + \frac{1}{C_e} \right) \quad (7)$$

where T indicates temperature (K), R indicates gas constant (8.314 Jmol⁻¹K⁻¹) and C_e indicates the equilibrium concentration of dye (mol L⁻¹). The mean free energy E (kJmol⁻¹) was calculated using the following equation:

$$E = \frac{1}{\sqrt{2\beta}} \quad (8)$$

The calculated parameters were indicated in Table 2.

Brunauer–Emmett–Teller isotherm equation is given as below:

$$\frac{C_e}{(C_i - C_e)q_e} = \frac{1}{Bq_{\max}} + \frac{B-1}{(Bq_{\max})} \left(\frac{C_e}{C_i}\right) \quad (9)$$

The calculated values, given in Table 2 indicated the Langmuir isotherm is favorable than Freundlich, Brunauer–Emmett–Teller isotherms, and Dubinin–Radushkevich (DR) [34–35]. It is confirmed by high values of R² for all samples. It can be also confirmed with RL values. The adsorption is favorable since RL values are between 0 and 1. Langmuir adsorption depicted that the adsorption took place at homogeneous active sites on the adsorbent and adsorbed molecules. And also the results show that the adsorption is monolayer adsorption.

3.5 Thermodynamic

Thermodynamic parameters give information about the feasibility and nature of the adsorption process. Thermodynamic parameters were obtained by given equations to analyze the impact of temperature on the adsorption [36].

$$\Delta G^\circ = -RT \ln 1000K_d \quad (10)$$

$$K_d = \frac{q_e}{C_e} \quad (11)$$

where q_e indicates the amount of adsorbed dye (mg) per L at equilibrium, C_e indicates the equilibrium concentration (mgL⁻¹) of dye in solution, K_d indicates the distribution coefficient for the adsorption.

The enthalpy (ΔH°) change is calculated by the equation:

$$\ln 1000K_d = -\frac{\Delta H^\circ}{RT} + \frac{\Delta S^\circ}{R} \quad (12)$$

where R(8.314 J mol⁻¹K⁻¹) indicates gas constant, T(K) indicates the solution temperature. The calculated thermodynamic parameters were presented in Table 3.

The calculated enthalpy (ΔH°) values of cotton, Cot- KSF, Cot- KSF -chi, and Cot- KSF -chi-MDEU are 7.371, 25.992, 36.091, and 44.860 kJ/mol, respectively. The positive (+) values depict the possibility of physical adsorption and the endothermic reaction [34].

As seen in Table 3 standard free energy ΔG° values are negatives (-) at all the experimental temperatures. The (-) value of ΔG° depicts that the RB adsorption is spontaneous for all samples in other words the system doesn't need energy from an external source. As the temperature increase, the ΔG° values become more negative. On other words, the higher temperature makes the adsorption more spontaneous for all samples [28]. The (+) values ΔS° of samples suggest the increase in randomness at solution (dye solution) –solid interface (adsorbent) [30, 37, 38].

Table 2. Result of adsorption isotherms at 298 K.

	q _{exp} (mg/g)	q _{max} (mg/g)	R _L	R ²	
Langmuir					
$\frac{C_e}{q_e} = \frac{1}{q_m L} + \frac{C_e}{q_m}$	Cotton	0.17	0.16	n.d	0.997
	Cot- KSF	1.2	1.45	0.16	0.993
	Cot- KSF -chi	2.1	2.22	0.87	0.996
	Cot- KSF -chi -MDEU	3.4	6.38	0.034	0.993
Freundlich	q _{exp} (mg/g)	K _f (mg/g)	n _f	R ²	
$\ln q_e = \ln K_f + \frac{1}{n_f} \ln C_e$	Cotton	0.17	0.28	-7.62	0.744
	Cot- KSF	1.2	0.63	5.52	0.931
	Cot- KSF -chi	2.1	1.90	29.59	0.2035
	Cot- KSF -chi -MDEU	3.4	0.48	0.42	0.9917
Dubinin–Radushkevich (DR) isotherm	q _{exp} (mg/g)	X _m (mg/g)	E (kJ/mg)	R ²	
$\ln q_e = \ln X_m - \beta \varepsilon^2$	Cotton	0.17	0.17	n.d	0.8372
	Cot- KSF	1.2	1.26	158.11	0.7641
	Cot- KSF -chi	2.1	2.14	707.11	0.0679
	Cot- KSF -chi -MDEU	3.4	3.75	111.80	0.951
Brunauer–Emmett–Teller (BET)	q _{exp} (mg/g)	q _{max} (mg/g)	B (J)	R ²	
$\frac{C_e}{(C_i - C_e)q_e} = \frac{1}{Bq_{\max}} + \frac{B-1}{(Bq_{\max})} \left(\frac{C_e}{C_i}\right)$	Cotton	0.17	1.9x10 ⁻³	-0.05	0.9182
	Cot-KSF	1.2	0.10	0.47	0.9742
	Cot-KSF -chi	2.1	3.06	0.24	0.571
	Cot-KSF -chi -MDEU	3.4	1.83	0.52	0.7872

Table 3. Thermodynamic parameters of cotton, Cot- KSF, Cot- KSF -chi, and Cot- KSF -chi-MDEU.

T (K)	ΔG (kJ/mol)	ΔH (kJ/mol)	ΔS (kJ/mol)
Cotton			
298	-2.84		
308	-3.18	7.371	0.034
318	-3.53		
338	-4.21		
Cot-KSF			
298	-8.28		
308	-9.43	25.992	0.115
318	-10.58		
338	-12.88		
Cot- KSF-chi			
298	-9.66		
308	-11.34	36.091	0.154
318	-12.88		
338	-15.961		
Cot- KSF-chi-MDEU			
298	-12.06		
308	-13.97	44.860	0.191
318	-15.88		
338	-19.70		

3.6. Adsorption Kinetics

The impact of contact time on RB adsorption on samples is given in Fig. 6. The adsorptions of RB were studied for 180 min. As can be seen in Fig. 6, 90 min is enough to reach adsorption equilibrium for all samples.

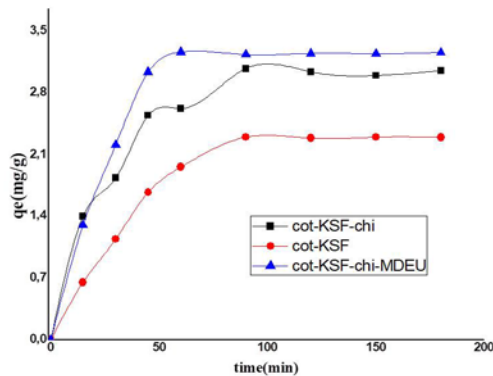


Figure 6. The impact of contact time on adsorption.

The adsorption kinetics gives information about adsorbant-adsorbate interaction. Adsorption capacity and adsorption rate are an essential factors for the selection of the best material to be used in adsorption. The pseudo-first-order and pseudo-second-order are widely used models for adsorption kinetics [3].

Pseudo-first-order kinetic equation is given below:

$$\ln(q_e - q_t) = \ln q_e - k_1 \cdot t \quad (13)$$

where q_e (mgg^{-1}) indicates the adsorbed RB at equilibrium, q_t (mgg^{-1}) indicates the adsorbed RB at any time. Pseudo-second-order kinetic model equation is:

$$\frac{t}{q_t} = \frac{1}{k_2 \cdot q_e^2} + \frac{t}{q_e} \quad (14)$$

where k_2 ($\text{gmg}^{-1}\text{min}^{-1}$) is the pseudo-second-order rate constant.

The initial rate of adsorption was calculated from the given equation:

$$h_{0.2} = k_2 \cdot q_e^2 \quad (15)$$

The half-adsorption time $t_{1/2}$ (min), indicates the required time for the adsorption to take up half equilibrium value.

$$t_{\frac{1}{2}} = \frac{1}{k_2 q_e} \quad (16)$$

Calculated $t_{1/2}$ (min) values are given in Table 4.

Elovich equation is defined as:

$$q_t = \frac{1}{\beta} \cdot \ln(\alpha\beta) + \frac{1}{\beta} \ln t \quad (17)$$

where α ($\text{mgg}^{-1}\text{min}^{-1}$) is the initial sorption rate, β (gmg^{-1}) is associated with extending of surface coverage.

Intraparticle diffusion was studied in this project. If the intraparticle diffusion (k_i) ($\text{mg}/(\text{gmin}^{1/2})$) is the rate

controlling factor, adsorption of RB varies with the square root of time. And so the adsorption rate can measure by determining the adsorption capacity of adsorbent (q_t) (mg/g) as a function of square root of time ($t^{1/2}$). If the q_t vs $t^{1/2}$ plots go through the origin, intraparticle diffusion is the one rate limiting step. On the other side when the q_t vs $t^{1/2}$ plots don't pass through the origin, it is indicated the boundary layer control (c). And also depict that intraparticle diffusion is not the only rate limiting step [39-42].

Intraparticles diffusion kinetics model is defined with the equation:

$$q_t = k_i \cdot t^{1/2} + C \quad (18)$$

The experimental and computed q_e values are close to each other for Elovich equation, Intraparticles diffusion, Pseudo-first-order, and pseudo-second-order kinetic models. And also the correlation coefficients support that RB adsorption system fit for Intraparticles diffusion, Elovich equation, Pseudo-first-order, and pseudo-second-order kinetic models. Based on the correlation coefficients pseudo-second-order kinetic model exhibits a better fit than Pseudo-first-order, Intraparticles diffusion, and Elovich equation kinetic models [20, 29].

Table 4. The results of kinetic studies at 298 K.

		q_{exp} (mg/g)	k (g mg ⁻¹ min ⁻¹)	$t_{1/2}$ (min)	h (mg/g.min)	q_e (mg/g)	R^2
The pseudo-second-order $\frac{t}{q_t} = \frac{1}{k_2 q_e^2} + \frac{t}{q_e}$	Cot- KSF	2.3	8.41x10 ⁻³	29.58	0.136	4.02	0.999
	Cot- KSF -chi	3.1	2.30 x10 ⁻³	90.91	0.05	4.68	0.996
	Cot- KSF -chi-MDEU	3.2	2.58 x10 ⁻³	58.82	0.109	6.52	0.998
The pseudo-first-order $\ln(q_e - q_t) = \ln q_e - k_1 t$	Cot- KSF	2.3	0.0282	2.54			0.9984
	Cot- KSF -chi	3.1	0.0283	2.63			0.988
	Cot- KSF -chi-MDEU	3.2	0.0463	4.12			0.995
Elovich equation $q_t = \frac{1}{\beta} \ln \beta \alpha + \frac{1}{\beta} \ln t$	Cot-KSF	2.3	0.278	1.086			0.9979
	Cot-KSF-chi	3.1	0.115	1.089			0.9855
	Cot-KSF-chi-MDEU	3.2	0.234	0.734			0.9994
Intra-particle diffusion $q_t = k_i t^{0.5} + C$	Cot-KSF	2.3	0.2931	0.3546			0.986
	Cot-KSF-chi	3.1	0.2960	-0.4801			0.999
	Cot-KSF-chi-MDEU	3.2	0.5319	-0.7419			0.998

3.7. Antimicrobial Activity Test

The antibacterial activity of Cot-KSF, Cot-KSF-chi, and Cot-KSF-chi-MDEU was investigated against the *S. Aureus* (*S.A*) and *K. Pneumonia* (*K.P*). The antibacterial activity results were given in Table 5 and shown by the reduction of bacterial counts. Cot-KSF, Cot-KSF-chi, and Cot-KSF-chi-MDEU show antibacterial activity against the *S.A* and *K.P*. KSF and chitosan have antibacterial activity [43-45]. KSF was used in antibacterial studies. The cationic nature of chitosan inhibits the growth of fungi, yeast, Gram - positive and Gram - negative bacteria [43, 45].

In this study KSF and chitosan coated cotton exhibited antibacterial activity against the *S.A* and *K.P*. The best antibacterial activity against *S.A* and *K.P* was investigated for Cot-KSF-chi-MDEU.

Table 5. Antimicrobial activity of Cot-KSF, Cot-KSF-chi, and Cot-KSF-chi-MDEU.

Samples	% Reduction of <i>S.A</i>	% Reduction of <i>K.P</i>
Cot-KSF	99.99025	99.61429
Cot-KSF-chi	99.775	99.99671
Cot-KSF-chi-MDEU	99.9625	99.99994

4. CONCLUSION

Treated (cot-KSF, Cot-KSF-chi, and Cot-KSF-chi-MDEU) and untreated cotton were fabricated. Results of the characterization were assessed. One-step process of clay-chitosan-based fabrics gained to fabric significantly good properties.

- The treated cotton samples were effectively dyed (free salt) with small quantities of dye. It is economically important for the textile industry. And also, free salt

REFERENCES

1. Periyasamy AP, Venkatesan H. 2018. Eco-materials in textile finishing. Handbook of Ecomaterials. Springer International Publishing, Cham, 1-22.
2. Montaser AS, Mahmoud FA. 2019. Preparation of chitosan-grafted-polyvinyl acetate metal nanocomposite for producing multifunctional textile cotton fabrics. *International Journal of Biological Macromolecules* 124, 659-666.
3. Bharathi KS, Ramesh ST. 2013. Removal of dyes using agricultural waste as low-cost adsorbents: A review. *Applied Water Science* 3(4), 773-790.
4. Montazer M, Malek RMA, Rahimi A. 2007. Salt free reactive dyeing of cationized cotton. *Fibers and Polymers* 8(6), 608-612.
5. Kant R. 2011. Textile dyeing industry an environmental hazard. *Natural Science* 4(1), 22-26.
6. Kadam AA, Lee DS. 2015. Glutaraldehyde cross-linked magnetic chitosan nanocomposites: Reduction precipitation synthesis, characterization, and application for removal of hazardous textile dyes. *Bioresource technology* 193, 563-567.
7. Singha K, Maity S, Singha M. 2012. The salt-free dyeing on cotton: An approach to effluent free mechanism; can chitosan be a potential option. *International Journal of Textile Science* 1(6), 69-77.
8. Sharma P, Kaur H, Sharma M, Sahore V. 2011. A review on applicability of naturally available adsorbents for the removal of hazardous dyes from aqueous waste. *Environmental Monitoring and Assessment* 183(1-4), 151-195.
9. Kausar A, Iqbal M, Javed A, Aftab K, Bhatti H N, Nouren S. 2018. Dyes adsorption using clay and modified clay: A review. *Journal of Molecular Liquids* 256, 395-407.
10. Rehan M, El-Naggar ME, Mashaly HM, Wilken R. 2018. Nanocomposites based on chitosan/silver/clay for durable multifunctional properties of cotton fabrics. *Carbohydrate Polymers* 182, 29-41.
11. Reddy DHK, Lee SM. 2013. Application of magnetic chitosan composites for the removal of toxic metal and dyes from aqueous solutions. *Advances in Colloid and Interface Science* 201, 68-93.
12. Wang Q, Chen W, Zhang Q, Ghiladi RA, Wei Q. 2018. Preparation of photodynamic P (MMA-co-MAA) composite nanofibers doped with MMT: A facile method for increasing antimicrobial efficiency. *Applied Surface Science* 457, 247-255.

dyeing is an environmentally friendly form of textile dyeing.

- Treated cottons were exhibited antibacterial properties.
- The decomposition temperature of the cotton sample decreased from 369 to 351°C after treatment
- Dye adsorption capacities of cotton samples were investigated. The adsorption of RB on the samples, q_e (mg/g), decreased with the increasing pH value. As the ionic strength increased the dye adsorption capacity of treated cotton samples decreased while untreated samples increased.
- Brunauer–Emmett–Teller, Freundlich, Dubinin–Radushkevich, and Langmuir isotherm equations were studied to investigate the equilibrium character of adsorption. Langmuir isotherm is favorable than Brunauer–Emmett–Teller, Dubinin–Radushkevich (DR), and Freundlich isotherms. The negative value of ΔG° shows that the RB dye adsorption is spontaneous for all samples. As the temperature increase the ΔG° values became more negative that showed the adsorption was more spontaneous at higher temperatures for all samples. The positive values ΔS° of samples suggest the increase in randomness at the solution (dye solution) –solid interface (adsorbent). 90 min is enough to reach adsorption equilibrium for all samples. Related to correlation coefficients, pseudo-second-order kinetic model exhibits a better fit than Elovich equation, Pseudo-first-order, and Intraparticles diffusion kinetic models.

Consequently, clay-chitosan composites can be considered as a hopeful composite for multifunctional finishing textiles. The treatment gained cotton antibacterial properties and easy & salt-free dyeing ability. The ecofriendly treatment can be used in the textile industry. And also treated antibacterial cotton can be used in medical applications.

13. Arık B, Seventekin N. 2011. Evaluation of antibacterial and structural properties of cotton fabric coated by chitosan/titania and chitosan/silica hybrid sol-gel coatings. *Tekstil ve Konfeksiyon* 21(2), 107-115.
14. Tursucular O, Cerkez İ, Orhan M, Aykut Y. 2018. Preparation and antibacterial investigation of polycaprolactone/chitosan nano/micro fibers by using different solvent systems. *Tekstil ve Konfeksiyon* 28(3), 221-228.
15. Chung YC, Wang HL, Chen YM, Li SL. 2003. Effect of abiotic factors on the antibacterial activity of chitosan against waterborne pathogens. *Bioresource Technology* 88(3), 179-184.
16. Cao C, Xiao L, Chen C, Shi X, Cao Q, Gao L. 2014. In situ preparation of magnetic Fe₃O₄/chitosan nanoparticles via a novel reduction-precipitation method and their application in adsorption of reactive azo dye. *Powder Technology* 260, 90-97.
17. Yu C. 2016. Preparation and Application of the Composite from Chitosan. *Handbook of Composites from Renewable Materials, Structure and Chemistry* 1, 371.
18. Lavorgna M, Attianese I, Buonocore GG, Conte A, Del Nobile MA, Tescione F, Amendola E. 2014. MMT-supported Ag nanoparticles for chitosan nanocomposites: structural properties and antibacterial activity. *Carbohydrate Polymers* 102, 385-392.
19. Altınışık A, Bozacı E, Akar E, Seki Y, Yurdakoc K, Demir A, Özdoğan E. 2013. Development of antimicrobial cotton fabric using bionanocomposites. *Cellulose* 20(6), 3111-3121.
20. Akar E, Altınışık A, Seki Y. 2013. Using of activated carbon produced from spent tea leaves for the removal of malachite green from aqueous solution. *Ecological Engineering* 52, 19-27.
21. Li R, Liu C, Ma J, Yang Y, Wu H. 2011. Effect of org-titanium phosphonate on the properties of chitosan films. *Polymer Bulletin* 67(1), 77-89.
22. Kang S, Qin L, Zhao Y, Wang W, Zhang T, Yang L, Song S. 2020. Enhanced removal of methyl orange on exfoliated montmorillonite/chitosan gel in presence of methylene blue. *Chemosphere* 238, 124693.
23. Kaur K, Jindal R. 2019. Self-assembled GO incorporated CMC and Chitosan-based nanocomposites in the removal of cationic dyes. *Carbohydrate Polymers* 225, 115245.
24. Abdurrahim I. 2019. Water sorption, antimicrobial activity, and thermal and mechanical properties of chitosan/clay/glycerol nanocomposite films. *Heliyon* 5(8), e02342.
25. Gaan S, Sun G. 2009. Effect of nitrogen additives on thermal decomposition of cotton. *Journal of Analytical and Applied Pyrolysis* 84(1), 108-115.
26. Ouajai S, Shanks RA. 2005. Composition, structure and thermal degradation of hemp cellulose after chemical treatments. *Polymer Degradation and Stability* 89(2), 327-335.
27. Çelebi M, Özdemir Z. 2017. Dyestuffs removal from synthetic wastewater with chitosan, cross-linked chitosan and chitosan-poly (acrylic acid) conjugate. *Tekstil ve Konfeksiyon* 27(3), 283-288.
28. Hwang SY, Yoo ES, Im SS. 2009. Effect of the urethane group on treated clay surfaces for high-performance poly (butylene succinate)/montmorillonite nanocomposites. *Polymer Degradation and Stability* 94(12), 2163-2169.
29. Chen D, Chen J, Luan X, Ji H, Xia Z. 2011. Characterization of anion-cationic surfactants modified montmorillonite and its application for the removal of methyl orange. *Chemical Engineering Journal* 171(3), 1150-1158.
30. Newcombe G, Drikas M. 1997. Adsorption of NOM onto activated carbon: electrostatic and non-electrostatic effects. *Carbon* 35(9), 1239-1250.
31. Alberghina G, Bianchini R, Fichera M, Fisichella S. 2000. Dimerization of Cibacron Blue F3GA and other dyes: influence of salts and temperature. *Dyes and Pigments* 46(3), 129-137.
32. Germán-Heins J, Flury M. 2000. Sorption of Brilliant Blue FCF in soils as affected by pH and ionic strength. *Geoderma* 97(1-2), 87-101.
33. Ali I, Alothman Z A, Alwarthan A. 2017. Uptake of propranolol on ionic liquid iron nanocomposite adsorbent: kinetic, thermodynamics and mechanism of adsorption. *Journal of Molecular Liquids* 236, 205-213.
34. Konicki W, Aleksandrak M, Moszyński D, Mijowska E. 2017. Adsorption of anionic azo-dyes from aqueous solutions onto graphene oxide: equilibrium, kinetic and thermodynamic studies. *Journal of Colloid and Interface Science* 496, 188-200.
35. Akram M, Bhatti HN, Iqbal M, Noreen S, Sadaf S. 2017. Biocomposite efficiency for Cr (VI) adsorption: Kinetic, equilibrium and thermodynamics studies. *Journal of Environmental Chemical Engineering* 5(1), 400-411.
36. Milonjić SK. 2007. A consideration of the correct calculation of thermodynamic parameters of adsorption. *Journal of the Serbian Chemical Society* 72(12), 1363-1367.
37. Bedin KC, Martins AC, Cazetta AL, Pezoti O, Almeida VC. 2016. KOH-activated carbon prepared from sucrose spherical carbon: Adsorption equilibrium, kinetic and thermodynamic studies for Methylene Blue removal. *Chemical Engineering Journal* 286, 476-484.
38. Tran HN, You SJ, Chao HP. 2016. Thermodynamic parameters of cadmium adsorption onto orange peel calculated from various methods: A comparison study. *Journal of Environmental Chemical Engineering* 4(3), 2671-2682.
39. Belaroussi A, Labeled F, Khenifi A, Akbour RA, Boubberka Z, Kameche M, Derriche Z. 2018. A novel approach for removing an industrial dye 4GL by an Algerian Bentonite. *Acta Ecologica Sinica* 38(2), 148-156.
40. Weber WJ, Morris JC. 1963. Kinetics of adsorption on carbon from solution. *Journal of the Sanitary Engineering Division* 89(2), 31-60.
41. Juang RS, Wu FC, Tseng RL. 2000. Mechanism of adsorption of dyes and phenols from water using activated carbons prepared from plum kernels. *Journal of Colloid and Interface Science* 227(2), 437-444.
42. Ho YS, McKay G. 1999. Pseudo-second order model for sorption processes. *Process Biochemistry* 34(5), 451-465.
43. Ignatova M, Manolova N, Rashkov I. 2013. Electrospun Antibacterial Chitosan-B ased Fibers. *Macromolecular Bioscience* 13(7), 860-872.
44. Maryan AS, Montazer M, Rashidi A, Rahimi MK. 2013. Antibacterial properties of clay layers silicate: a special study of montmorillonite on cotton fiber. *Asian Journal of Chemistry* 25(5), 2889.
45. Demir A, Öktem T, Seventekin N. 2008. Investigation of the usage of chitosan as an antimicrobial agent in textile industry. *Tekstil ve Konfeksiyon* 18(2), 94-102.



Synthesis and Characterization of Polyvinylimidazole and Investigation of its Antipilling Effect on Different Fabrics

Burcu Büyükkoru^{1,2}  0000-0002-3399-9899

Ali Kara¹  0000-0003-2457-6314

¹Bursa Uludağ University, Faculty of Art & Science, Department of Chemistry, Bursa, Turkey

²Rudolf-Duraner Kimyevi Maddeler San. ve Tic. A.Ş. , R&D Department, Bursa, Turkey

Corresponding Author: Ali Kara, akara@uludag.edu.tr

ABSTRACT

Pilling is one of the major concerns in textile industry. To improve pilling values of the fabrics, some methods have been reported. One of which is chemical finishing. In this study, these chemical finishing methods have been used. A key differentiator of this study is that the polymer employed as an anti-pilling agent was synthesized by the researchers of this study and does not negatively affect the hydrophilicity and brightness of fabrics. As most anti-pilling chemicals, polyvinylimidazole (PVIM) was synthesized and applied to fabrics to reduce the pilling tendency. 1.5-2 degrees improvement was observed in the pilling values ranged 4.5-5.0, which means there were no pills on the fabric surface. It has also been proven that PVIM can be used as an anti-pilling agent without negative effects on fabrics in terms of hydrophilicity, brightness and hand. The PVIM was named RUCO-PLAST EPG 18042 to be included in Rudolf-Duraner's product list.

1. INTRODUCTION

Pilling is an undesired defect of textile fabrics, consisting of a surface characterized by a number of roughly spherical masses made of entangled fibers [1]. Pilling occurs as a result of the abrasion of fabric surface occurring during washing and wearing of fabrics. Mainly, rubbing is seen in garment areas near pockets and collars, so pills are mostly found in these areas [2]. Anchor fibers that have longer fibers on the fabric surface fracture easily and the pills wear off from the fabric surface [3]. By this reason, cotton (CO), wool, and nylon 6 fibers that have anchor fibers do not have pilling problems. Stronger anchor fibers do not fracture easily, thus their pills do not easily wear off. Pilling occurs on the fabric surface for polyester (PES) or nylon 66 because polyester or nylon 66 staple fibers consist of these stronger anchor fibers areas [4].

As a result of literature review, the most important factors increasing pilling tendency are determined. The type of fibre used in a fabric is a vital factor [5]. Gintis and Mead have worked at this topic and have ranked different synthetic fibres according to their pilling tendency [6, 7]. When the polyester content increases in a polyester/cotton blended fabric, the pilling increases [8]. It has been determined that the pilling tendency of fabrics produced from viscose fibers is higher than raw fabrics produced from lyocel and modal fibers due to their fiber structural properties. Therefore, among the selected fabrics, there are also blended fabrics containing viscose [9]. One of the crucial factors effecting pilling tendencies is the type of yarn used in the fabric. Candan et al. has reported that a fabric knitted with cotton ring-spun yarns has more pilling performance than fabric with open-ended rotor-spun yarns [10]. The other important factor that affects the pilling

ARTICLE HISTORY

Received: 28.08.2020

Accepted: 30.09.2021

KEYWORDS

Pilling, anti-pilling, hydrophilicity, brightness, polyvinylimidazole

To cite this article: Büyükkoru B, Kara A. 2021. Synthesis and characterization of polyvinylimidazole and Investigation of its antipilling effect on different fabrics. *Tekstil ve Konfeksiyon* 31(4), 274-283.

tendency is the fabric type. Over the last few years, there has been growing interest in treated fabrics due to its simple production technique, low cost, high levels of clothing comfort and wide product range [11, 12].

Yarn sequence modifies the pilling tendency of the fabrics. Because of its loose structure knitted fabrics have more pilling tendency compared to woven fabrics. So, improving anti-pilling values of knitted fabrics is more difficult [13].

Pilling formation is more common in blended fabrics and it is more difficult to improve their pilling values. The most common example is fabrics made of polyester/cotton blends. In these fabrics, weaker cotton fibers are pulled out and separated from the surface as a result of abrasion. Meanwhile, the stronger polyester fibers are only broken and still seized with the other end in the fabric. Both types of fibers form pills that remain strongly associated with the fabric surface as a result of entanglement caused by abrasion [14].

To improve pilling values, some methods have been reported [14-16]. One of which is chemical finishing [17-19] Enzymes are often used as anti-pilling chemicals in this method [20-22]. They can provide sufficient pilling improvement in blended fabrics such as PES/CV, PES/CO, CO/CV. On the other hand, they are not effective enough for all viscose (CV) fabrics. Körlü et al. investigated the effect of cellulase waste on the cellulosic fabrics. The results showed that cellulose enzymes are more effective for cotton fabrics than viscose fabrics [23, 24]. Apart from enzymes, different anti-pilling chemicals have also been used. The negative effects of all these current anti-pilling agents are that they are expensive or give hard hand to the fabrics. In spite of the fact that many different chemicals have been reported to be anti-pilling chemicals [25], having only anti-pilling property is not enough for textile industry. The fabric that has been treated with anti-pilling chemicals should also exhibit other desired properties [26]. It should maintain its hydrophilicity, have a good hand and be non-yellowing. For these reasons, an alternative anti-pilling chemical is required to solve the pilling problem. The difference of the anti-pilling polymer synthesized by the researchers of this study is that it reduces the tendency of pilling without creating negative effect on fabrics in terms of hydrophilicity, hand, and brightness. The name of the synthesized and characterized anti-pilling polymer is polyvinylimidazole. To determine the effect of PVIM as an anti-pilling chemical, applications and tests had been made on many different fabrics. It was also investigated whether PVIM negatively affects the hydrophilicity and brightness of the fabrics or not. In short, PVIM is a functional polymer and has been proven to be used as an anti-pilling agent for different types of fabrics without adverse effects. Thus, the

pilling problem of fabrics is eliminated, making it possible to produce better quality products and indirectly reducing energy, production and operating costs [27].

2. MATERIAL AND METHOD

2.1. Material

2.1.1 Chemicals

Vinylimidazole (VIM), benzene, 2M AIBN in toluene were used for synthesis of polyvinylimidazole (PVIM). These chemicals were supplied from Merck.

2.1.2 Fabrics

Fabrics used in the study are determined: woven fabric-1 (W-1), woven fabric-2 (W-2), woven fabric-3 (W-3) and knitted fabric (K-1). These fabrics have different fiber composition and colour. Microscopic method was used to determine which fibers are present in fabrics by qualitatively. The brand of the microscope is Olympus and the model is BX51. After the determination of the fibers in the fabrics by microscopic method, their percentages in the fabrics were identified by chemical method according to the ISO-1833-11. The fibers in the fabrics and their percentages are provided in the Table 1. Images of fabric surfaces were taken with the digital surface microscope (LEICA brand, DVM6 model) at x44 magnification. Images are shown in Table 1.

As can be seen from the Table 1, W-1 consists of CV and PES fibers. The percentages of these fibers were determined as 78% CV and 22% PES. For W-2, PES and EL fibers were seen under the light microscope. The percentages of these fibers were determined as 66% PES, 32% CV and 2% EA by chemical method. CV, PES and EL fibers were found for W-3. The percentages of these fibers were determined as 64% PES, 32% CV and 4% EA. Only CO fibers were seen for K-1, it appears that K-1 entirely composed of CO fabrics.

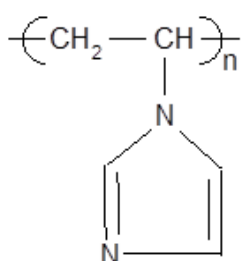
2.2 Method

2.2.1 Synthesis of PVIM

To obtain sufficient polymer and to understand the correctness of the method, reactions were repeated for 7 times. For all experiments polymer can be synthesized in success. Lots of methods were investigated and then polymer was synthesized with a method close to reported in the literature [28-34]. 15 ml of VIM (0.166 mmol) was dissolved in 30 ml of benzene (0.34 mmol). 3 g of 2 M AIBN in toluene (0.016 mmol) was added as a catalyst. Reaction was carried out at 65°C under nitrogen atmosphere. After 4 hours PVIM (Figure 1) was obtained as white solid. Using vacuum distillation benzene was removed at pressures of 500–600 mmHg and temperatures of 50°C-55°C.

Table 1. Properties of fabrics used in the study

Article	Colour	Yarn sequence	Fiber composition	Surface image of fabric under digital surface microscope
W-1 (woven fabric-1)	dark pink	woven	78% CV 22 % PES	
W-2 (woven fabric-2)	green plaid pattern	woven	66% PES 32% CV 2% EA	
W-3 (woven fabric-3)	black	woven	64% PES 32% CV 4% EA	
K-1 (knitted fabric-1)	orange	knitted	100% CO	

**Figure 1.** Structure of PVIM

2.2.2 Characterization of polymer

To characterize polymers FT-IR (Shimadzu, IR-Prestige-21), NMR (JEOL-ECZ500R), UV-Visible Spectrophotometer

(Shimadzu, UV-1700, PharmaSpec), DSC (Differential scanning calorimetry) (Perkin-Elmer DSC 4000 equipment) and elemental analysis (Perkin Elmer 2400 Series II) were used.

2.2.3 Finishing process

PVIM solutions were prepared at concentrations of 10, 20, 30, 40, 50 g/l and applied to fabrics by padding method. The brand of the foulard machine used in the applications is Ataç and the model is F-350. In this machine, the treated fabrics were passed through 3 bar pressure to obtain the pick up value of nearly 70%. After this process, the fabrics were dried at 130 °C on the Mathis-stenter frame (Mathis

brand, PTC 96 model). Dried fabrics were kept in the condition room for one day. These fabrics were reserved for hand and hydrophilicity testing. For the pilling test, all the above mentioned processes were repeated and a further batch was prepared.

To observe yellowing effect, PVIM, was applied to white treated fabric. After application process, fabric was exposed to 170 °C. Then, whiteness of the fabric was tested by using Datacolor 600™ method.

2.2.4 Measuring pilling values of fabrics treated with PVIM

To determine pilling values of the fabrics lots of methods can be used [24, 35-41]. Martindale pilling tester device which is one of the mostly preferred was used for this study. All fabrics were tested according to the ISO-12945-2 method and the pilling performance was evaluated after 2000 cycles by using Martindale pilling tester device.

2.2.5 Determination of pilling values of fabrics treated with PVIM

Subjective method was used to predict fabric's pilling tendency. Fabrics treated with PVIM received the score of 5 out of 5. This means no piling in the fabric. For reference, a score of 4 would translate to very little pilling, 3 is reserved for moderate pilling. In a fabric with a pilling score of 2, pilling is clearly visible. The score of fabrics with very intense pilling is 1.

2.2.6 Determination of hydrophilicity values of fabrics treated with PVIM

While determining the hydrophilicity values of the fabrics, the water absorption capacity of the fabrics is evaluated. For this purpose, standard method: AATC 79 is used. In this method, time is measured by using a stopwatch. Stopwatch starts immediately after the water is dropped on the fabric with a pipette and stops when the fabric absorbs the water drop. Elapsed time is recorded and noted as the hydrophilicity value of the fabric. Hydrophilicity measurements were carried out in this way on all applied fabrics. Thus, the effect of anti-pilling chemicals on the water absorbency values of the fabric was investigated.

2.2.7 Evaluation of whiteness values of fabrics treated with PVIM

Datacolor 600™ device was used to perform the whiteness test. To investigate the yellowing effect of PVIM on treated fabrics, white fabric was treated with 50 g/l PVIM. After application, the fabric was exposed to 170 °C for 1 minute in a Mathis-stenter frame. The whiteness value of this fabric was measured in Berger unit using Datacolor device. The whiteness value of the untreated fabric in Berger unit was also measured. The obtained whiteness values of untreated fabric and fabric treated with 50 g/l PVIM were compared.

2.2.8 Evaluation of hand of fabrics treated with PVIM

The hand of treated fabrics with PVIM were compared with their untreated ones. Thus, the effect of anti-pilling polymer on the hand of fabrics was investigated. The hand is evaluated according to the feeling it gives to the person at the moment of taking the fabric between the fingertips. As a result of this feeling, the fabric can be expressed as soft, slippery, bulky or thin. Although the hand is relative and varies from person to person from time to time, the favorite hand is usually the same. When the hand of the treated fabrics were compared according to their untreated ones, in consultation with many people, the hand effect of PVIM was evaluated in similar.

3. RESULTS AND DISCUSSION

3.1 FT-IR Studies

The desired peaks and adsorbents were obtained in the samples in the literature [42] and it was proved that the polymers were successfully synthesized. The FT-IR spectra of the PVIM polymers and the VIM monomer are illustrated in Figure 2.

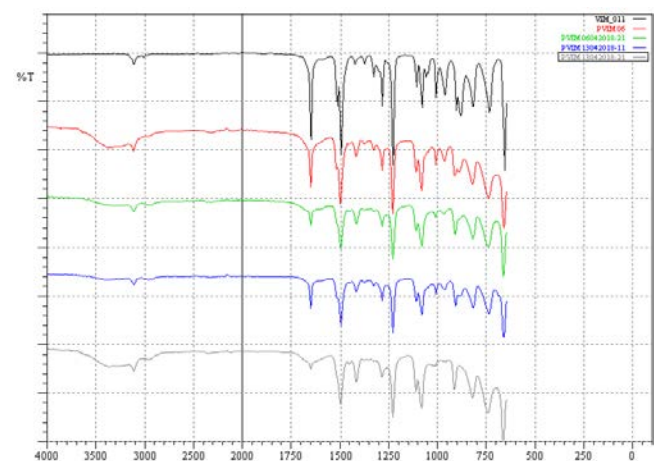


Figure 2. FT-IR spectrum for VIM and PVIM samples

In the FT-IR spectrum of the VIM homopolymer, the following peaks were detected;

- C-H (ring) stretch, 3113 cm⁻¹;
- C-H and CH₂ (main chain) stretch, 3008 cm⁻¹;
- C-C ve C-N stretch, 1494 cm⁻¹;
- (Ring) stretch, 1416 cm⁻¹;
- C-H (ring) vibration in plane and C-N (ring) stretch, 1281 ve 1226 cm⁻¹
- C-H (ring) vibration in plane, 1107 cm⁻¹;
- C-H (ring) vibration in plane and (ring) stretch, 1080 cm⁻¹;
- C-H (main chain) vibration in plane and C-C stretch 1045 cm⁻¹;
- (Ring) stretch and vibration in plane, 912 cm⁻¹;

- C-H vibration out of plane and (ring) vibration in plane, 818 cm^{-1} ;
- C-N stretch and (ring) vibration out of plane, 737 cm^{-1}
- (Ring) vibration out of plane 656 cm^{-1}

Peaks shown in the figure prove that PVIM is synthesized successfully.

3.2 NMR Studies

H atoms in PVIM structure are numbered and illustrated in Figure 3.

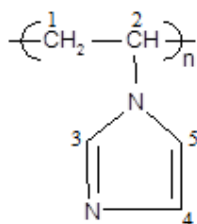


Figure 3. Numbered representation of H atoms in PVIM structure

The ^1H NMR spectra of the polymer is provided in Figure 4. Peaks prove that PVIM was synthesized successfully. When ^1H NMR spectrum of PVIM taken in deuterated dimethyl sulfoxide (DMSO- d_6) is examined, peaks are obtained as below. Methylene ($-\text{CH}_2$) protons in the main chain are multiplet between 2.49-2.50 ppm and 2H (1), ($-\text{CH}$) proton in the main chain is between 3.24-3.39 ppm as a triplet and 1H (2), ($-\text{CH}$) protons of the imidazole ring are doublet between 4.85-4.87 ppm and 1H (5), ($-\text{CH}$) protons of the imidazole ring are doublet between 5.45-5.48 ppm and 1H (4).

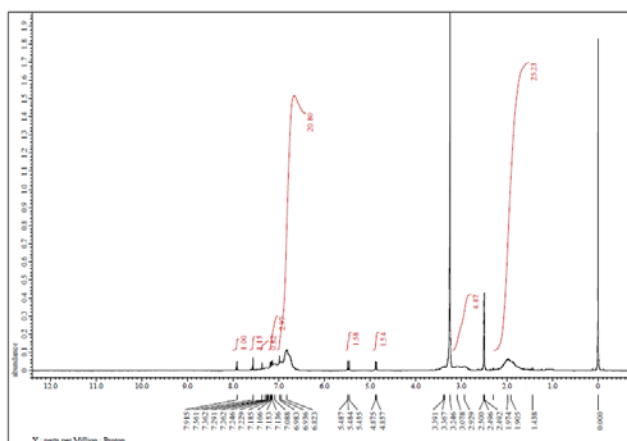


Figure 4. NMR spectrum for PVIM

These characteristic peaks seen in figure indicate that homopolymerization has taken place and PVIM synthesis is conducted successfully.

3.3 UV-Visible Spectrum

Solutions of PVIM, which was synthesized in toluene medium, were prepared in deionized H_2O to obtain

UV-visible region spectra and the electronic transitions of polymers were examined. The UV-Visible region of the polymers was observed with a sharp band. λ_{max} value of the polymer is determined as 216.8 nm (Figure 5). In the literature, some researchers which are synthesized and characterized PVIM are reported λ_{max} value of the polymer in deionized water is approximately 216 nm. By the way, only one peak (216.8 nm) is observed for the UV-VIS spectrum and it corresponds to the $\pi \rightarrow \pi^*$ transitions of $\text{C} = \text{C}$ and $\text{C} = \text{N}$ groups in the imidazole rings in the polymer structure.

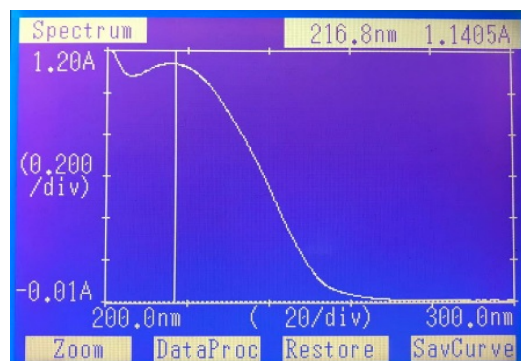


Figure 5. UV-visible spectrum of PVIM in H_2O solution

Considering that λ_{max} matches the results recorded in the literature, it is clear that the polymer was successfully synthesized.

3.4 Differential scanning calorimetry (DSC)

By using Perkin-Elmer DSC 4000 equipment, differential scanning calorimetry was performed. Measurements were taken by using 5 mg PVIM sample. Results are shown in Figure 6.

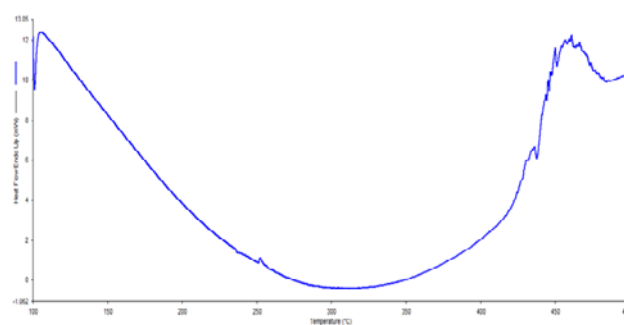


Figure 6. DSC results for PVIM

According to the DSC result, the T_m value was found to be around 440°C . In the literature, the T_m value for PVIM is reported as 440°C [43, 44]. Hence, it is proved that PVIM was synthesized successfully.

3.5 Elemental Analysis

Elemental analysis results of PVIM are shown in Table 2.

Table 2. Elemental analysis results of PVIM

Composition of the initial reaction mixture (mol%)			Elemental analysis (%)		
VIM	Benzene	2 M AIBN in toluene	Carbon	Hydrogen	Nitrogen
31.80	65.13	3.07	58.32	7.50	21.15

3.6 Effect of Polymer on Pilling Performance

Martindale pilling device was used to understand pilling tendency of treated fabrics. After that, these treated fabrics were evaluated by subjective method to determine pilling values. Concentrations of PVIM solutions were determined according to type and improvement of fabrics. PVIM applications on different fabrics has been done. The results of pilling values in these fabrics are provided in the tables below.

Table 3. Pilling results of fabric W-1 treated with different concentrations of PVIM

Artical	PVIM amount (gram/liter)	W-1 Pilling degree*
A1	0	2-3
A2	10	3
A3	20	3
A4	30	3
A5	40	4
A6	50	4-5

*Degree of pilling 5: means no pilling; 1 means very severe pilling

As can be seen from Table 3, untreated W-1 fabric has a pilling value of: 2-3. This value is significantly low and needs improvement. Because of its fiber composition made from PES and CV fiber, low pilling value is expected. PVIM treated fabrics has better pilling value. 40 g/l PVIM application is enough for W-1 fabric in order to achieve acceptable pilling degree.

Table 4. Pilling results of fabric W-2 treated with different concentrations of PVIM

Artical	PVIM amount (gram/liter)	W-2 Pilling degree
A1	0	3
A2	10	3.5
A3	20	3.5
A4	30	4-5
A5	40	5
A6	50	5

It is clearly demonstrated from Table 4, that PVIM contributes anti-pilling properties of W-2 fabric. When untreated W-2 fabric has a pilling value of: 3, 10 g/l and 20 g/l PVIM solutions improve pilling values and 30 g/l, 40 g/l and 50 g/l PVIM solutions have very positive effect on treated fabrics. 30 g/l PVIM application is sufficient for W-2 fabric to achieve acceptable pilling degree. On the other hand, with increasing amount of PVIM concentration, better values were obtained. And for fabrics treated with 40

g/l and 50 g/l PVIM solutions, the best pilling degree of 5 was achieved.

Table 5. Pilling results of fabric W-3 treated with different concentrations of PVIM

Artical	PVIM amount (gram/liter)	W-3 Pilling degree
A1	0	2-3
A2	10	3
A3	20	3
A4	30	4
A5	40	4-5
A6	50	4.5-5

Like W-1 and W-2 fabrics, W-3 untreated fabric has a pilling degree of 2-3. This low value is expected, but needs to be improved. All woven fabrics (W1, W2 and W3) used in this study, are composed of PES and CV fiber. These fiber blends cause pilling problem and it is difficult to increase their pilling values. Even so, with functional polymer PVIM, desired pilling results were achieved. As can be seen in the Table 4, 30 g/l PVIM application is enough to be obtain a good pilling value. However with increasing amount of PVIM application, values are better and nearly no pill was seen on the fabric surface.

Table 6. Pilling results of fabric K-1 treated with different concentrations of PVIM

Article	PVIM amount (gram/liter)	K-1 Pilling degree
A1	0	2-3
A2	10	3
A3	20	3-3.5
A4	30	3-3.5
A5	40	4
A6	50	4-5

For K-1 fabric, high concentrations of polymer solution had to be used. Because of the structure and low pilling grade of the knitted fabric, 50 g/l PVIM was applied to obtain a good pilling value. As can be seen, after treatments nearly 1.5-2 pilling grades of improvement were achieved. Also, for all fabrics, tendency of pilling decreased with the increasing application quantity of the polymer solution. In addition, surface images of PVIM treated and untreated fabrics after the pilling test were compared to prove that PVIM improves pilling values. Photographs showing the surface images of the fabrics are provided in Figure: 7-10. Lots of pills are observed on the surface of untreated fabrics while there are almost no pills on the surface of PVIM treated fabrics.

3.7 Effect of Polymer on Hydrophilicity of the Fabrics

Fabrics treated with PVIM were compared to untreated ones in terms of hydrophilicity. It is clear that PVIM has a

positive contribution to hydrophilicity of the fabrics. Results are provided in the tables below.



Figure 7. Surface images of W-1 A) Untreated B) 50 g/l PVIM treated

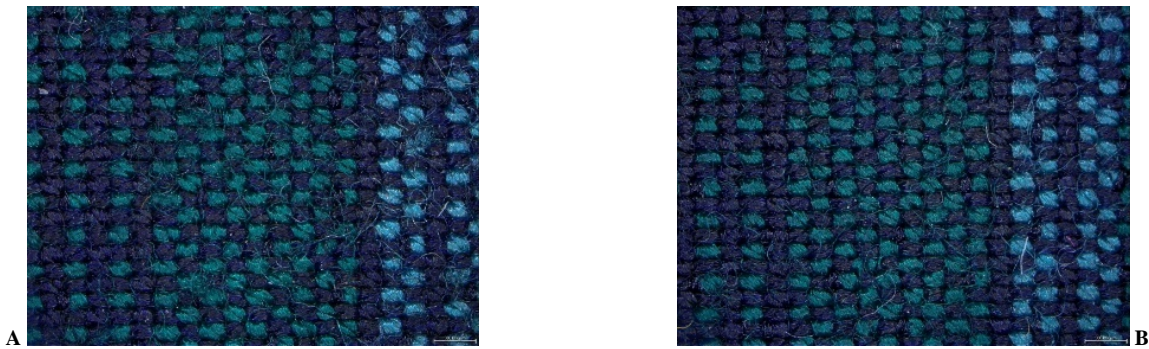


Figure 8. Surface images of W-2 A) Untreated B) 50 g/l PVIM treated



Figure 9. Surface images of W-3 A) Untreated B) 50 g/l PVIM treated

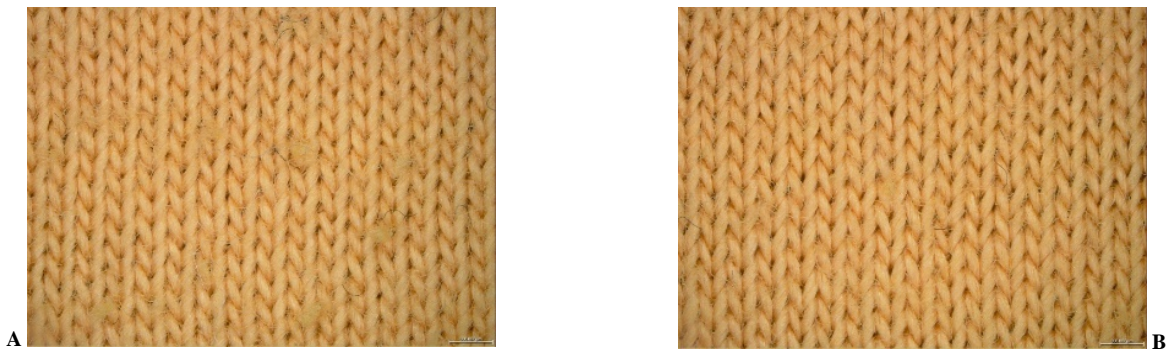


Figure 10. Surface images of W-4 A) Untreated B) 50 g/l PVIM treated

As can be seen from Table 7, hydrophilicity value of untreated W-1 fabric is 1 second. Hence, it absorbs water

immediately. When PVIM applies to the fabrics, it is clearly shown that PVIM does not effect the hydrophilicity

values negatively. For all treated fabrics with different concentrations of PVIM, hydrophilicity values are recorded as a 1 second like untreated fabric.

Table 7. Hydrophilicity results of fabric W-1 treated with different concentrations of PVIM

Article	PVIM amount (gram/liter)	W-1 Hydrophilicity value
A1	0	1 s
A2	10	1 s
A3	20	1 s
A4	30	1 s
A5	40	1 s
A6	50	1 s

It is clearly demonstrated from Table 8 that PVIM contributes hydrophilicity of the W-2 fabric. When hydrophilicity value of untreated fabric is 4 minute; hydrophilicity value of fabric treated with 10 g/l PVIM: 2 minute.

Table 8. Hydrophilicity results of fabric W-2 treated with different concentrations of PVIM

Article	PVIM amount (gram/liter)	W-2 Hydrophilicity value
A1	0	4 min
A2	10	2 min
A3	20	1,5 min
A4	30	1 min
A5	40	45 s
A6	50	8 s

Hydrophilicity of W-3 untreated fabric was not good enough and was measured as 65 s (Table 9). PVIM contributes hydrophilicity of these fabrics like W-2 fabrics 10 g/l PVIM application increased hydrophilicity to 45 s. With increasing amount of PVIM application, values were better and hydrophilicity value of fabric treated with 50 g/l PVIM was measured as 12 s.

Table 9. Hydrophilicity results of fabric W-3 treated with different concentrations of PVIM

Article	PVIM amount (gram/liter)	W-3 Hydrophilicity value
A1	0	65 s
A2	10	45 s
A3	20	40 s
A4	30	35 s
A5	40	25 s
A6	50	12 s

Like W-1 fabric, untreated K-1 fabric can absorb water immediately. Its hydrophilicity value was measured as a 1 s. When different amounts of PVIM was applied to the fabric, hydrophilicity did not affected and remained same. To conclude, PVIM helps increasing the hydrophilicity of the fabrics.

Table 10. Hydrophilicity results of fabric K-1 treated with different concentrations of PVIM

Article	PVIM amount (gram/liter)	K-1 Hydrophilicity value
A1	0	1 s
A2	10	1 s
A3	20	1 s
A4	30	1 s
A5	40	1 s
A6	50	1 s

3.8 Effect of Polymer on the Whiteness Values of the Fabrics

To investigate the yellowing effect of PVIM, white fabric was treated with 50 g/l PVIM and was exposed to 170°C for 1 minute in a Mathis-stenter frame. The whiteness value of this fabric was measured using the Datacolor 600™ device. The value obtained was 155 Berger. The whiteness value of the untreated fabric was also measured and recorded as 154 Berger. When the results obtained were compared, it was clearly seen that there was no significant difference, so PVIM does not effect the whiteness of the fabrics.

3.9 Hand of the Fabrics

A hand value of 5 out of 5 means very soft hand, a value of 1 means very hard hand. While the hand of untreated fabrics can be defined as 2-3.5, the hand of fabrics treated with PVIM can be defined as 3-4. This is the proof that PVIM does not adversely affect the hand. For some treated fabrics, hand is better than untreated ones. On the other hand, some treated fabrics are not good enough in terms of softness and slippery. For this case, softener can be added in the solution. Polymer and softener combinations were prepared and applied to the fabrics. As a result, hand value of these fabrics were 4-5 and softener did not adversely affect the pilling values of the fabrics. It can be stated that there is no drawback in adding suitable softeners as additives to improve the hand of the applied fabrics.

4. CONCLUSION

- For the aim of decreasing pilling tendency, polyvinylimidazole (PVIM) was synthesized and characterized successfully.
- Pilling values of fabrics treated with functional polymer increased by around 1,5-2 pilling grade. With the increased application amount of PVIM, pilling grades further improve. At 50 g/l PVIM treatment, for all fabrics, pilling grade of 4-5 was obtained, means there is almost no pills on the fabric surface. In fact, improvements at 40 g/l PVIM treatment could be sufficient for all fabrics.
- According to study results, PVIM didn't decrease the hydrophilicity of the fabrics similar to other chemicals

which are used in pilling improvement. On contrary, PVIM improves hydrophilicity of the fabrics.

- It was found that treated PVIM fabrics had same optical brightness value in berger unit as untreated fabrics when they are both exposed to high temperatures during drying process.
- To be included in the product list of Rudolf-Duraner, PVIM is defined as “RUCO-PLAST EPG 18042”. It is proved that RUCO-PLAST EPG 18042 can be used as an anti-pilling agent for treated fabrics.

REFERENCES

1. Furferi R, Governi L, Volpe Y. 2015. Machine vision-based pilling assessment. *Journal of Engineered Fibers and Fabrics* 15(10), 3.
2. Tomasino C. 1992. *Chemistry & Technology of Fabric Preparation & Finishing*. North Carolina: Department of Textile Engineering, Chemistry & Science College of Textiles North Carolina State University.
3. Man L, Raymand W. 2009. *Mechanisms of pilling formation and reduction by attrition methods*. Hong Kong: The Hong Kong Polytechnic University, Institute of Textiles & Clothing.
4. Li L, Jia G, Zhou W. 2009. Effect of yarn properties on the pilling of cashmere treated fabric. *Fibres & Textiles in Eastern Europe* 17, 76-79.
5. Candan C. 2000. Factors affecting the pilling performance of knitted wool fabrics. *Turkish Journal of Engineering and Environmental Sciences* 24, 35-44.
6. Gintis D, Mead E. 1959. The mechanism of pilling. *Textile Research Journal* 29, 578-585.
7. Beltran R, Wang L, Wang X. 2006. Measuring the influence of fibre-to-fabric properties on the pilling of wool fabrics, *Journal of the Textile Institute* 97(3), 197-204.
8. Sivakumar VR, Pillay KPR. 1981. Study of pilling in polyester/cotton blended fabrics. *Indian Journal of Fibre & Textile Research* 6, 22.
9. Kayseri GO, Bozdoğan F, Hes L. 2010. Performance properties of regenerated cellulose fibers. *Tekstil ve Konfeksiyon* 20(3), 208-212.
10. Candan C, Nergis UB, Iridag Y. 2000. Performance of open-end and ring spun yarns in weft knitted fabrics. *Textile Research Journal* 70(2), 177-181.
11. Oğlakçioğlu N, Marmaralı A. 2007. Thermal comfort properties of some knitted structures. *Fibres & Textiles in Eastern Europe* 15(5-6), 94-96.
12. Kahraman B. 2006. Örne kumaşlarda boncuklanma nedenlerinin incelenmesi (Master's thesis). Retrieved from YOK database. (Accession number. 185188)
13. Ukponmwan JO, Mukhopadhyay A, Chatterjee KN. 1998. Pilling. *Textile Progress* 28, 40.
14. Kowalczyk D, Brzezinski S, Kaminska I. 2015. Multifunctional bioactive and improving the performance durability nanocoatings for finishing PET/CO woven fabrics by the solgel method. *Journal of Alloys and Compounds* 649, 387-393.
15. Hashemikia S, Montazer M. 2012. Sodium hypophosphite and nano TiO₂ inorganic catalysts along with citric acid on textile producing multi-functional properties. *Applied Catalysis A: General* 417-418, 200-208.
16. Kulyk I, Scapinello M, Stefan M. 2012, June. 12th High-Tech Plasma Processes Conference (HTPP-12). *Journal of Physics* Bologna, Italy.
17. Montazer M, Mazaheri F, Khosravian SH, Azimi M, Bameni M, Sadeghi AH. 2011. Application of resins and crosslinking agents on fiber blend fabric to reduce pilling performance. Optimized by response surface methodology. *Journal of Vinyl & Additive Technology* 17(3), 213-221.
18. Tusief MQ, Mahmood N, Amin N, Saleem M. 2012. Fabric tensile strength as affected by different anti-pilling agents at various concentration and pH levels. *Journal of the Chemical Society of Pakistan* 34(1), 53-57.
19. Özgüney AT. 2016. Investigating the effects of different softeners on pilling properties and durability to washing of bamboo knitted fabrics. *Tekstil ve Konfeksiyon* 26(3), 307-313.
20. Bahtiyari MI, Duran K, Körlü AE. 2010. Usage of commercial cellulases in biopolishing of viscose fabrics. *Tekstil ve Konfeksiyon* 20(1), 57-54.
21. Ala DM, Bakıcı GG, Abdulvahitoglu A. 2017. Investigation of thickness, air permeability and pilling properties of single jersey fabrics. *Çukurova University Journal of the Faculty of Engineering* 32, 3.
22. Mavruz S, Oğulata R. 2009. Investigation of effects of repeated laundering on the knitted fabrics with biopolishing treatment. *Tekstil ve Konfeksiyon* 3, 224-230.
23. Körlü AE, Duran K, Bahtiyari Mİ, Perinçek S. 2008. The effects of cellulase enzymes on cellulosic fabrics. *Tekstil ve Konfeksiyon* 18(1), 35-41.
24. Dalbaşı ES, Kayseri GÖ. 2015. Research about the effect of the anti-pilling treatments on different structured cotton knitted fabrics. *Tekstil ve Konfeksiyon* 25, 54-60.
25. Ming Yu M, Wang Z, Lv M, Hao R, Zhao R, Qi L, Liu S, Yu C, Zhang B, Fan C, Li J. 2016. Antisuperbug cotton fabric with excellent laundering durability. *ACS Applied Materials & Interfaces* 8, 19866-19871.
26. Bui HM, Enhrhardt A, Bechtold T. 2008. Pilling in cellulosic fabrics, part 2: A study on kinetics of pilling in alkali-treated lyocell fabrics. *Journal of Applied Polymer Science* 109, 3696-3703.
27. Kertmen M, Marmaralı A. 2019, November. 17th International The Recent Progress Symposium on Textile Technology and Chemistry, Bursa, Turkey.
28. Chlistunoff J, Sansinena JM. 2014. Effects of axial coordination of the metal center on the activity of iron tetraphenylporphyrin as a nonprecious catalyst for oxygen reduction. *The Journal of Physical Chemistry C* 118, 19139-19149.
29. Lia X, Goha SH, Laia YH, Weeb ATS. 2001. Miscibility and interactions in blends of carboxyl-containing polysiloxane with poly(1-vinylimidazole). *Polymer* 42, 5463-5469.

Acknowledgement

This work was supported by the [TUBITAK-TEYDEB] under Grant [number 3170840] and by the [Bursa Uludağ University under Grant [number OUAP (F) 2019/9] It was carried out in cooperation with Uludağ University-Rudolf Duraner. The authors wish to thank the Rudolf-Duraner company, which provides the necessary fabrics and materials within the scope of the project, and provides all kinds of possibilities and devices for the textile applications of the synthesized polymers. A patent application has been filed for this study. The study has gone through a process of preevaluation successfully (with the patent number: PT2019-00086).

-
30. Guo S, Wan W, Chen C, Chen WH. 2013. Thermal decomposition kinetic evaluation and its thermal hazards prediction of AIBN. *Journal of Thermal Analysis and Calorimetry* 113, 1169-76.
 31. Tekin N, Kadıncı E, Demirbaş Ö, Alkan M, Kara A, Doğan M. 2006. Surface properties of poly(vinylimidazole)-adsorbed expanded perlite. *Microporous and Mesoporous Materials* 93, 125-133.
 32. Böhmer M, Heesterbeek WHA, Deratani A, Renard E. 1995. Adsorption of partially quarternied poly(vinylimidazoles) onto SiO₂ and Y₂O₃. *Colloids and Surfaces A: Physicochemical and Engineering Aspects* 99, 53-64.
 33. Pekel N, Güven O. 1999. Investigation of complex formation between poly(N-vinyl imidazole) and various metal ions using the molar ratio method. *Colloid and Polymer Science* 277, 570-573.
 34. Pekel N, Şahiner N, Güven O, Rzaev ZMO. 2001. Synthesis and characterization of N-vinylimidazole-ethyl methacrylate copolymers and determination of monomer reactivity ratios. *European Polymer Journal* 37(12), 2443-2451.
 35. Zhang J, Wang X. 2008. Objective pilling evaluation of wool fabrics. *Textile Research Journal* 77(12), 929-936.
 36. Furferi R, Carfagni M, Governi L, Volpe Y, Bogani P. 2014. Towards automated and objective assessment of fabric pilling. *International Journal of Advanced Robotic Systems* 11, 171.
 37. Wang XY, Gong RH, Dong Z, Porat I. 2007. Abrasion resistance of thermally bonded 3D nonwoven fabrics. *Science Direct Wear* 262, 424-431.
 38. Nihat C, Değirmenci Z, Kaynak HK. 2010. Effect of nano-silicone softener on abrasion and pilling resistance and color fastness of knitted fabrics. *Tekstil ve Konfeksiyon* 20(1), 41-47.
 39. Tusief MQ, Mahmood N, Saleem M. 2012. Effect of different anti-pilling agents to reduce pilling on polyester/cotton fabric. *Journal of the Chemical Society of Pakistan* 34(1), 53-57.
 40. Kertmen M. 2019. Örne kumaşlarda ilmeklenme sorunu ve çözüm yollarının araştırılması (Master's thesis). Retrieved from YOK database. (Accession number. 561536)
 41. Telli A. 2019. An image processing research consistent with standard photographs to determine pilling grade of woven fabrics. *Tekstil ve Konfeksiyon* 29(1), 268-276.
 42. Ghaffarlou M. 2012. Formation and characterization of interpolymer complexes of poly(n-vinylimidazole)/poly(acrylic acid) and poly(n-vinylimidazole)/poly(methacrylic acid) in aqueous medium (Master's thesis). Retrieved from YOK database. (Accession number. 321378)
 43. Uzluk E. 2008. (Master's thesis). Synthesis and characterization of some polymers and investigation of properties. Retrieved from YOK database. (Accession number. 233907)
 44. Araki M, Kato K, Koyanagi T, Machida S. 1977. Spontaneous polymerization of maleic anhydride by imidazole derivatives. *Journal of Macromolecular Science: Part A - Chemistry* 11(5), 1039-1052.



Investigation of Stretch Properties of Different Stitch Types in Garments Made of Elastane Woven Fabrics

Kıvanç GELERİ¹  0000-0003-4425-7396

Ayça GÜRARDA²  0000-0002-7317-8163

Erhan Kenan ÇEVEN²  0000-0003-3283-4117

¹Bursa Uludağ University, Graduate School of Natural and Applied Sciences, Department of Textile Engineering, Bursa, Turkey

²Bursa Uludağ University, Engineering Faculty, Department of Textile Engineering, Bursa, Turkey

Corresponding Author: Ayça Gürarda, aycagur@uludag.edu.tr

ABSTRACT

In recent years, garments made of fabrics with elastane are highly preferred. A garment made of fabric with elastane is able to stretch by about 10-30% and recovery immediately after release. In the apparel industry, sewing should not prevent the fabric from stretching in the garments made from woven fabrics with elastane. The elasticity of the seams of the garments consisting of elastic fabrics is very important. In this study, it is aimed to examine the stretch and permanent elongation properties of different stitch types of garments made of elastane woven fabrics. For this purpose, 5 different stitch types were selected as lockstitch, zig zag stitch, two thread chain stitch, three thread overlock stitch and five thread overlock stitch, and these stitches were sewn at different stitch densities (3 - 4 and 5 stitches / cm), with different sewing threads (spun polyester, core spun (poly / poly), nylon and elastic sewing thread) with different ticket numbers (80 and 120). The stretch and permanent elongation values of the sewn fabric samples were examined.

ARTICLE HISTORY

Received: 04.04.2021

Accepted: 21.08.2021

KEYWORDS

Elastane, stretch, stitch type, sewing thread, stitch density

1. INTRODUCTION

In recent years, the most of the garments are sewn with elastane fabrics. A garment made of elastane fabric can stretch approximately 10-30% and recover immediately after release. Elastane fibers can be used with all other natural and synthetic fibers today. It is sufficient to use a very small amount (2-5%) of this fiber in order to provide the desired comfort in clothes [1]. In the apparel industry, sewing should not prevent the fabric from stretching in the garments made of elastane woven fabrics. The seam appearance and performance affect the aesthetics and performance of the garment and determine its life time. For this reason, the elasticity of the seams of the garments consisting of elastic fabrics is very important.

In men's trousers sewn from elastane woven fabric, while the fabric shows a certain stretch during sitting and standing, the stitches of the trousers should also show enough flexibility. Otherwise, problems such as seam opening or stitch breakage may be encountered. In the women's blouse sewn from elastane woven fabric, while the fabric shows enough elasticity during the movement, the stitches of the blouse should also show enough elasticity. In the studies conducted in this field, the effect of silicon finish applied to cotton/elastane woven fabrics and the fixation temperature on the stretch properties of the fabric and seam performance of polyester/nylon-elastane woven fabrics were investigated [2, 3]. However, stretch and permanent elongation values of the stitched samples were not calculated.

To cite this article: Geleri K, Gürarda A, Çeven EK. 2021. Investigation of stretch properties of different stitch types in garments made of elastane woven fabrics. *Tekstil ve Konfeksiyon* 31(4), 284-294.

Parameters such as stitch type, stitch density, sewing thread type and ticket number and sewing needle number are very important in sewing elastane fabrics. Studies in this field show that not selecting one or more of these sewing parameters appropriately causes sewing problems such as seam grinning, seam opening, seam puckering or seam breakage [1, 4, 5]. It is also very important to determine the most suitable sewing parameters to be applied to these garments, since the majority of both men's and women's garments are sewn from elastane fabrics in the apparel industry.

Sewing threads, seam and stitch types are among the most important parameters affecting the appearance and quality of the garments. Stitches join the pieces of clothing to form the garment suitable for the body. Quality seams increase the performance of the garment. Poor quality stitches spoil the appearance of the garment, even if the fabric of the garment is of good quality. The most important properties of seams in a garment are its strength, elasticity, durability and appearance. These properties must be balanced with the properties of the garment's fabric to create the optimum stitch. Factors such as the weight of the fabric, stitch type, needle type, and stitch density affect the seam performance and quality properly. Quality sewing threads should be selected for the longevity of the seams of the garments. Stitch strength is the most important factor that determines the durability of the seams of the garment. As can be seen in the studies conducted in this field, the structure, ticket number and finishing processes of the sewing threads used in seams affect the seam strength of the garment [1, 6]. Choosing the best stitch type, sewing thread ticket number and sewing thread type suitable for the garment depends on variables such as fabric structure, weight and type of fabric. The wrong selection of one of these causes the formation of faulty stitch lines and leads to undesirable defects on the finished product. Therefore, optimization of seam properties is very important.

As can be seen from the studies conducted in this field, the biggest problem seen in elastane fabrics is the problem of elastane breakage caused by mechanical damage and rupture of the elastane thread during sewing [1]. In order to prevent this problem during sewing the fabric, sewing needle tip shape should be selected with round ball point. In addition, the sewing needle and sewing thread ticket number should also be selected according to the weight of the elastane fabric [7].

In the selection of a sewing thread, the elongation properties of the sewing thread play a major role in obtaining a good stitch flexibility. Sewing threads with high breaking elongation are also preferred in the stitches of clothes made of elastane fabrics. Cotton sewing threads are not flexible enough and show 6-8% elongation. Polyester and nylon sewing threads are generally preferred for flexible stitches used at the fabrics. Medium thickness synthetic sewing threads show 15-20% elongation. In recent years, flexible sewing threads with very high elasticity rates at 40-50% elongation have also been

produced and started to be used in sewing elastane fabrics [8, 12].

The corespun sewing threads are produced by taking into account all the properties required for sewing. Corespun yarns are produced by coating staple fiber polyester on endless fiber polyester (poly / poly) or by coating cotton on continuous fiber polyester (poly / cotton). Corespun threads gain high strength from the continuous fiber polyester in the middle and a natural structure and seam attitude from the staple fiber on the outside. Therefore, they have high strength and appropriate fineness. In addition, the aerodynamic feature of the hairy structure on the outer surface ensures needle cooling and less abrasion of machine parts. It is used for the sewing of blouses and t-shirts, jackets, swimsuits, uniforms and work clothes. Nylon 6.6 sewing thread is 30% stronger than nylon 6 sewing thread. Due to its high strength even in fine counts, it allows the making of fine and strong stitches. Compared to polyester sewing thread, it also has high strength and slightly greater elongation. Its stretching feature is balanced [12,13]. In recent years, flexible sewing threads with high elongation have also been produced for sewing elastic garments containing elastane. Stretch sewing thread is an ideal thread for sportswear and body-fitting garments. These sewing threads have high elongation and seam strength and provides straight seams that can stretch by preventing damages caused by seam stretch in flexible fabrics. It has a variety of fineness and color suitable for all elastic fabric types [12].

Besides sewing thread elongation, other important factors that support stitch elasticity are the correct choice of stitch type and stitch density. Although lockstitch (301), which is the most frequently used, is a stitch type with the least elasticity, sewing elasticity values can be increased with the appropriate stitch density. However, this elasticity is not enough. The elasticity of two thread chain stitch is better compared to lockstitch. The best results can be achieved with 500 group overlock stitch types with high sewing elasticity [1].

Elastic fabrics stretch a certain amount when a load is applied. When this load is removed, the fabric returns to its original state and rotates due to the recovery feature of elastane. However, it cannot be completely restored and permanent elongation occurs. In order to calculate the permanent elongation value, the fabric shrinkage value is calculated after the fabric sample is stretched at the specified elongation and held for a certain period of time. Permanent elongation is tolerable at a maximum of 2% for trousers and dresses. Garments made of elastane woven fabrics with high permanent elongation values have a high tendency against bagging in the elbow and knee areas. As can be seen from the studies conducted, bagging on the garment impairs the quality of the garment [9]. As stated in the standard of TS 6071 "Method of Determining the Strength of Woven Fabrics Against Bagging or Elongation Due to Clothing", it is revealed that as the permanent elongation value increases, the stretched fabric has difficulties in recovery. Permanent elongation of the fabrics

should not be more than 3% after the application of stretching force and 2 hours recovery time. ASTM D 3107-07 "Test Method for Stretch Properties of Woven Fabrics Made of Elastane Yarns" standard also provides a method for evaluating stretching properties of fabrics. [15, 16].

The structure of sewing threads has an important influence on mechanical, especially viscoelastic properties and elastic recovery of a sewing thread after cyclical stretching [17]. It is very important to choose the appropriate stitch and seam type for stitch elasticity. Both lockstitch and chain stitch, if adjusted carefully, will give adequate stretch for elastic fabrics. Chain stitch has higher stretch than lockstitch [18]. Due to flexibility, the sewing thread made from spun yarns has good sewing performance, good dimensional stability, and good stitch forming properties. The core spun yarns also have excellent loop forming characteristics for the high flexibility [19].

In this study, it is aimed to obtain more flexible stitches by optimizing the sewing properties of the garments made of elastane woven fabrics. Thus, the elasticity of the garments will increase even more, and the stitches will contribute to the comfort and fit of the garment and reduce sewing problems. With this study, stretch and permanent elongation values of garments made of elastane woven fabrics with different stitch types were examined and an important gap in the scientific literature was tried to be eliminated. At the same time, with this study, it is expected to provide an economical solution for the apparel industry by optimizing sewing parameters such as stitch type, stitch density, sewing thread type and sewing thread ticket number in the production of garments made of elastane fabrics, and the application of stitches to the garment.

2. MATERIAL AND METHOD

2.1 Material

In this study, woven fabric with elastane for women's dresses was selected and different stitch types were applied to this fabric sample. The structural properties of the fabric used in the experimental study are listed in Table 1.

This fabric sample was sewn with 4 different sewing threads. Each of the sewing thread has two different ticket numbers. The structural properties of the sewing threads used in the study are included in Table 2.

2.2 Method

In this study, the stretch and permanent elongation properties of the stitches applied to the elastane woven fabric were evaluated with the Flexi-Frame (James Heal) "Fabric Stretch and Permanent Elongation Test Device" shown in Figure 1. Five different stitch types as lockstitch (301) (Figure 2), zig zag stitch (304) (Figure 3), two thread chain stitch (401) (Figure 4), three thread overlock stitch (504) (Figure 5) and five thread overlock stitch (516) (Figure 6) were selected, and these stitches were sewn with different densities (3 - 4 and 5 stitches / cm) and different ticket numbers (80 and 120) and different sewing threads (spun polyester, core spun (poly / poly), nylon and elastic sewing thread). These stitches were sewn perpendicular to the weft direction of the fabric. 120 different fabric samples were obtained and their elongation and permanent elongation values were investigated.

Table 1. Structural properties of the fabric used in the experimental study

Fabric Type	Density (thread/cm)		Weight (g/m ²)	Width (cm)	Construction
	Weft	Warp			
Stretch Twill	36	40	260	137	% 93 PES - % 7 EA

Table 2. Structural properties of sewing threads used in experimental study

Sewing Thread	Thread Count (Tex)	Ticket Number	Type	Elongation (%)		Tenacity (cN/tex)
				Min	Max	
1	40	80	Spun Polyester	13	20	35.35
	27	120		13	20	36.66
2	40	80	Corespun (Poly/Poly)	18	24	49.00
	24	120		17	22	49.58
3	35	80	Nylon	15	26	61.71
	24	120		12	25	65.83
4	40	80	Elastic (Eloflex)	55	85	23.00
	27	120		50	70	33.33

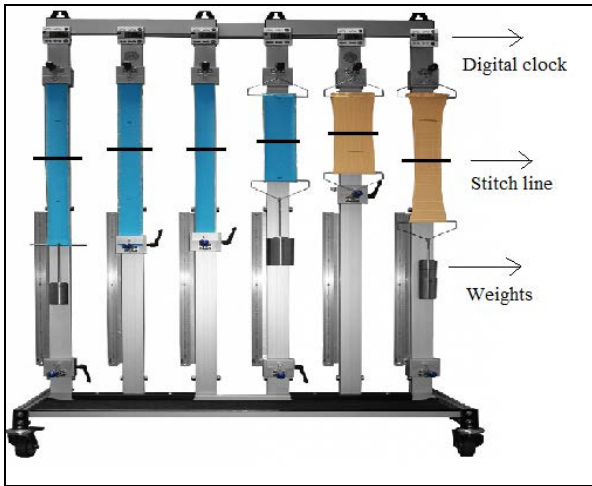


Figure 1. Stretch and recovery instrument (James Heal) [21]

order to test the elastic properties of elastane woven fabrics, TS 6071 "Method of Determination of Strength of Woven Fabrics Against Bagging or Elongation Due to Clothing" standard was used [15]. Stitch types applied to fabric samples were selected from ASTM D 6193 "Standard Practices for Seams and Sewing" standard [14]. For the test, samples those in the direction of the elastane thread were prepared in accordance with the standard TS 6071 (5 cm x 38 cm in size, long edge in the direction of the elastane thread) and cut right into the middle. The stitch types specified in the experiment plan were sewn with superimposed seam type (Figures 2-6) from the place where it was cut. Each fabric sample was conditioned according to ASTM D 1776 for experiments [20].

The 2250 g weight, determined in accordance with the standards, was hung on the samples as seen in the "Fabric Stretch and Permanent Elongation Test Device" shown in Figure 1, and was stretched for the specified periods with the help of the digital clock on the device. Elongation (%) and permanent elongation (%) of the samples were calculated by using Equations (1-2) [15].

Stitch types applied to test samples;

Lockstitch and zig zag stitches were sewn with Singer Scarlet model lockstitch sewing machine, chain stitch was sewn with Siruba model chain sewing machine and overlock stitches were sewn with Juki model overlock sewing machine. In

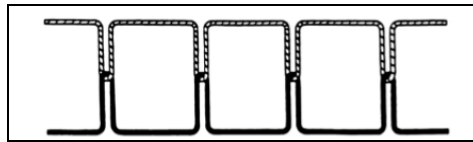


Figure 2. Stitch type 301 (Lockstitch) [14]

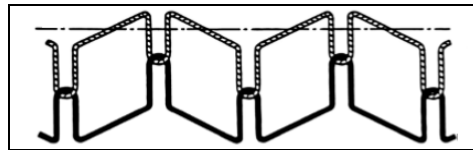


Figure 3. Stitch type 304 (Zig zag stitch) [14]

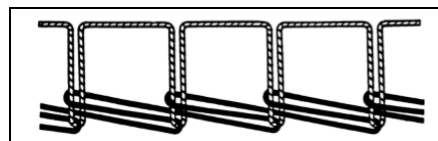


Figure 4. Stitch type 401 (Two thread chain stitch) [14]

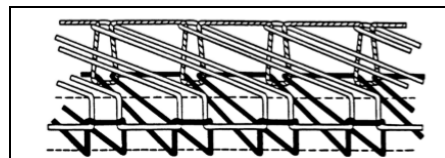


Figure 5. Stitch type 504 (Three thread overlock stitch) [14]

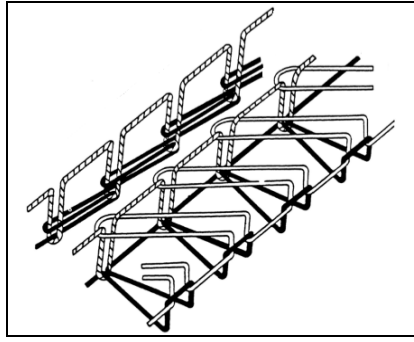


Figure 6. Stitch type 516 (Five thread overlock stitch) [14]

$$\text{Fabric Elongation (\%)} = [(B - A) / A] \times 100 \quad (1)$$

$$\text{Fabric Permanent Elongation (\%)} = [(C - A) / A] \times 100 \quad (2)$$

A: Original length of the fabric sample,

B: Benchmark length of the fabric under load,

C: Benchmark length of the fabric after load release [15]

A length of 25 cm was marked by leaving a distance of 6.5 cm from the edges on the fabric sample prepared with a size of 5 cm x 38 cm (A). Benchmark length of the fabric under load amount was determined while the sample was loaded (B) at the end of 30 minutes load application period. Benchmark length of the fabric after load release amount were determined according to the previously marked 25 cm dimension (C), after 5 minutes, 1 hour and 2 hours. Fabric elongation percentages of fabric samples and fabric permanent elongation percentages were calculated with the formulas in Equation 1 and 2 [15]. SPSS 21.0 statistical program was used to evaluate the test results. ANOVA and Student-Newman-Keuls (SNK) tests were applied to the results.

3. RESULTS AND DISCUSSION

The elongation behavior of elastane fabrics is desired to be between 10% and 30%. If the elongation behavior is lower than 10%, it indicates that the flexibility of the fabric is not good. Stretching and permanent elongation values in elastane fabrics are very important in determining its flexibility. The closer the permanent elongation gets to 0, the better the fabric's elasticity and recovery. As the permanent elongation value increases, it is revealed that the stretched fabric has difficulties in coming back and recovery. Percentage of permanent elongation of the fabrics should not be more than 3% after the application of stretching force and 2 hours withdrawal period [15]. The stitches applied to the elastane fabric should not adversely affect the elasticity and permanent elongation values of the elastane fabric. Table 3 and 4 show the permanent elongation (%) values at different time periods (after 5 minute, 1 hour and 2 hours) for different sewing threads with different stitch densities.

3.1 Statistical Results of Elongation (%) and Permanent Elongation (%) Values of Fabric Samples

The statistical results of the elongation (%) and permanent elongation (%) values (after 2 hours) of the stitched fabric

samples were examined. Table 5 shows the statistical results of the elongation and % permanent elongation values of the samples sewn using different sewing threads. There are significant differences on elongation (%) and permanent elongation (%) values of sewing thread types. It is seen that Eloflex-80, Eloflex-120 and Poly / poly -120 sewing threads have the highest elongation.

Polyester and nylon sewing threads are generally preferred for flexible stitches used at the fabrics. Medium thickness synthetic sewing threads show 15-20% elongation. In recent years, elastic sewing threads with very high elasticity rates at 40-50% elongation have also been produced and started to be used in sewing elastane fabrics [8, 12].

Table 6 shows the statistical results of the elongation (%) and permanent elongation (%) values of the samples sewn using different sewing types. There are significant differences on the elongation (%) and permanent elongation (%) values of the stitch types. It is seen that three thread overlock, five thread overlock and two thread chain stitch have the highest elongation (%), while lockstitch and zig zag stitch types have low elongation (%). Lockstitch (301), which is the most frequently used, is a stitch type with the least elasticity, the sewing elasticity values can be increased with the appropriate stitch density. However, this elasticity is not enough. The elasticity of two thread chain stitch is better compared to lockstitch. The best results can be achieved with 500 group overlock stitch types with high sewing elasticity [1, 18].

Table 7 shows the statistical results of the elongation (%) and permanent elongation (%) values of the samples sewn using different stitch densities. There are significant differences in stitch density on elongation (%) and permanent elongation (%) values. It is seen that stitch types with 3 stitches / cm stitch density have the highest elongation (%), followed by 4 stitches / cm and 5 stitches / cm. As the stitch density increases, the stretch of the stitched sample decreases.

Table 3. Permanent elongation (%) at different time periods (after 5 minute, 1 hour and 2 hours) for different sewing threads with different stitch densities

Stitch Type	Time	Spun PES-80 Stitch/cm			Poly/Poly-80 Stitch/cm			Nylon-80 Stitch/cm			Eloflex-80 Stitch/cm		
		3	4	5	3	4	5	3	4	5	3	4	5
Lock stitch	5 min	2.52	2.00	2.12	1.84	2.12	1.84	2.00	1.60	1.20	2.80	2.92	1.44
	1hour	1.84	1.44	1.72	1.44	1.72	1.32	1.20	0.92	0.80	1.60	1.20	0.80
	2hour	1.44	1.04	0.80	0.92	0.80	0.64	0.64	0.52	0.40	0.80	0.64	0.40
Zig Zag	5 min	2.52	1.60	2.40	3.20	2.40	2.80	2.40	1.84	2.00	2.40	2.24	3.60
	1hour	1.72	1.20	1.72	2.24	1.32	2.00	2.00	1.20	1.44	1.60	1.20	2.40
	2hour	1.20	0.80	1.04	1.60	0.80	1.20	1.44	0.80	0.80	0.64	0.92	1.60
Two Thread	5 min	2.00	1.32	1.44	2.00	2.40	1.84	2.00	1.60	1.44	2.00	1.60	1.60
	1hour	1.60	0.92	0.80	1.60	1.60	1.04	1.60	1.04	1.04	1.60	0.92	0.80
	2hour	0.80	0.52	0.40	1.20	0.80	0.40	1.04	0.40	0.40	0.80	0.52	0.40
Three Thread	5 min	2.00	2.00	2.00	1.72	1.84	1.84	2.52	1.84	1.72	2.24	2.24	2.00
	1hour	1.20	1.04	1.20	1.20	1.20	1.20	2.00	1.32	0.92	1.84	1.84	1.60
	2hour	0.80	0.64	0.52	0.8	0.52	0.40	1.32	0.92	0.40	1.20	1.04	0.92
Overlock	Five	2.00	2.00	2.00	2.00	2.00	1.20	2.00	2.00	1.60	2.00	1.60	1.60
	1hour	1.60	1.44	1.20	1.60	1.60	0.80	1.60	1.20	1.04	1.60	1.04	0.80
	2hour	0.80	0.64	0.52	1.04	1.04	0.40	0.92	0.64	0.40	0.80	0.64	0.40

Table 4. Permanent elongation (%) at different time periods (after 5 minute, 1 hour and 2 hours) for different sewing threads with different stitch densities (3-4-5)

Stitch Type	Time	Spun PES-120 Stitch/cm			Poly/Poly-120 Stitch/cm			Nylon-120 Stitch/cm			Eloflex-120 Stitch/cm		
		3	4	5	3	4	5	3	4	5	3	4	5
Lock stitch	5 min	2.52	2.40	2.40	2.00	1.84	2.00	1.44	1.84	1.20	2.00	1.32	2.00
	1 hour	2.00	1.72	1.60	1.44	0.92	1.32	1.04	1.20	0.80	1.44	0.92	1.20
	2 hour	1.44	1.04	0.92	0.80	0.64	0.52	0.64	0.52	0.40	0.80	0.52	0.40
Zig zag	5 min	2.12	2.40	2.40	1.84	1.72	2.64	2.00	1.84	2.00	1.32	2.24	1.60
	1 hour	1.44	1.60	1.60	1.44	1.04	1.84	1.20	1.20	1.20	0.80	1.44	1.20
	2 hour	1.04	0.80	0.92	1.04	0.52	0.80	0.80	0.64	0.80	0.40	0.64	0.80
Two thread	5 min	2.00	2.00	1.60	2.40	2.00	2.00	2.00	2.00	2.00	2.00	1.44	1.32
	1 hour	1.60	1.20	1.20	1.60	1.60	1.20	1.60	1.20	1.44	1.60	0.92	0.92
	2 hour	0.80	0.64	0.52	1.04	1.20	0.40	1.04	0.80	0.52	0.80	0.52	0.40
3 thread overlock	5 min	1.84	2.40	1.72	3.44	3.32	3.72	3.20	2.92	2.64	2.00	2.80	2.00
	1 hour	1.44	1.20	0.92	2.40	2.24	2.80	2.00	1.20	2.00	1.60	2.00	1.60
	2 hour	1.04	0.80	0.40	2.00	1.84	1.72	1.60	1.32	1.20	1.20	1.04	0.80
5 thread overlock	5 min	2.00	1.84	2.00	2.00	2.00	1.60	2.00	2.52	2.00	2.00	2.00	2.00
	1 hour	1.60	1.04	1.20	1.60	1.60	0.92	1.60	1.72	1.20	1.60	1.20	1.20
	2 hour	0.92	0.64	0.40	1.04	0.80	0.52	0.92	0.80	0.40	1.04	0.80	0.52

Table 5. (ANOVA ve SNK) (Statistical results of elongation (%) and permanent elongation (%) values of samples sewn with different sewing threads (ANOVA and SNK)

Sewing Thread Type	Elongation (%)	Permanent Elongation (%)
Spun PES - 80	16.73 c	0.83 a
Spun PES - 120	16.40 b	0.82 a
Poly/Poly - 80	16.84 c	0.82 a
Poly/Poly - 120	18.20 e	0.97 b
Nylon - 80	16.30 a	0.76 a
Nylon - 120	16.53 b	0.80 a
Eloflex - 80	19.91 f	0.79 a
Eloflex - 120	17.60 d	0.72 a

*: statistically significant ($P < 0.05$)

(a),(b),(c),(d),(e) and (f) represent the statistical difference ranges according to SNK test.

Table 6. Statistical results of elongation (%) and permanent elongation (%) values of samples sewn with different stitch types (ANOVA and SNK)

Stitch Type		Elongation (%)	Permanent Elongation (%)
Lockstitch		15.78 a	0.77 b
Zig zag stitch		16.64 b	0.91 c
Two thread chain stitch	0.00*	18.34 d	0.67 a
Three thread overlock		18.44 d	1.02 d
Five thread overlock		17.34 c	0.71 b

*: statistically significant ($P < 0.05$)

(a),(b),(c) and (d) represent the statistical difference ranges according to SNK test.

Table 7. Statistical results of elongation (%) and permanent elongation (%) values of samples sewn with different stitch density (ANOVA and SNK)

Stitch Density (stitch/cm)		Elongation (%)	Permanent Elongation (%)
3		18.25 c	1.03 c
4	0.00*	17.14 b	0.78 b
5		16.55 a	0.64 a

*: statistically significant ($P < 0.05$)

(a),(b) and (c) represent the statistical difference ranges according to SNK test.

3.2 Elongation (%) and Permanent Elongation (%) Values of Fabric Samples Sewn with Lockstitch

Figure 7 shows the elongation (%) values of the fabric samples sewn with lockstitch and in Figure 8, the permanent elongation (%) values (after 2 hours) are shown on the graphic. The statistical (ANOVA and SNK) results of the values obtained from the experiments are also included in Tables 5, 6 and 7. Table 5 shows the statistical results of the effects of different sewing threads on elongation (%) and permanent elongation (%) values. As can be seen from the results in this table and Figure 7, the highest elongation in lockstitch was obtained in Eloflex-80 and Eloflex-120 sewing threads. In Figure 8, it is seen that the permanent elongation values of the samples sewn with lockstitch are high in Spun Pes-80, Spun-Pes-120, Poly / Poly-80 and Poly / Poly-120 sewing threads.

Table 6 contains the statistical results of the effects of different stitch types (lockstitch, zig zag stitch, two thread chain stitch, three thread overlock stitch and five thread overlock stitch) on elongation (%) and permanent elongation (%) values. As can be seen from the results in this table, lockstitch samples show the least elongation. Permanent elongation values are also low. Among the five types of stitches determined in the experimental study, the stitch with the least stretch property is seen as lockstitch.

Table 7 shows the statistical results of the effects of different stitch densities (3 - 4 and 5 stitches / cm) on elongation (%) and permanent elongation (%) values. As can be seen from the results in this table, it is seen that the lockstitch fabric samples sewn with a stitch frequency of 3 stitches / cm showed the highest elongation (%) and permanent elongation (%), and the fabric samples sewn with 5 stitches / cm showed the lowest elongation (%) and permanent elongation (%) results.

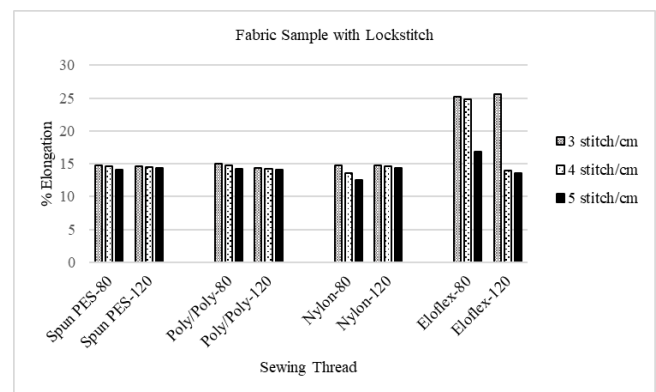


Figure 7. Elongation values (after 30 minutes) of the fabric sample with lockstitch

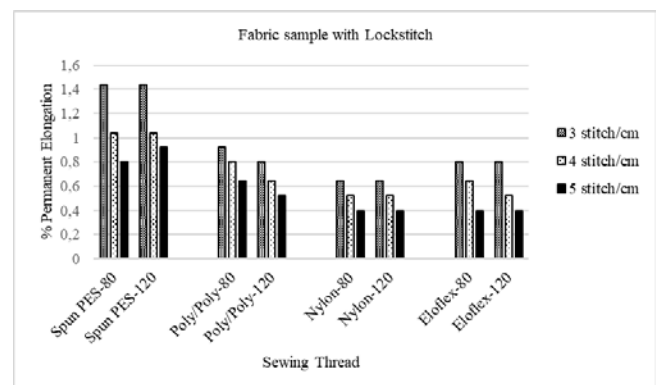


Figure 8. Permanent elongation values (after 2 hours) of the fabric with lockstitch

3.3 Elongation (%) and Permanent Elongation (%) Values of Fabric Samples Sewn with Zig Zag Stitch

Figure 9 shows the elongation (%) values of the fabric samples sewn with zig zag stitch and in Figure 10, the permanent elongation (%) values (after 2 hours) are shown on the graphic. The statistical (ANOVA and SNK) results of the values obtained from these experiments are also

included in Tables 5, 6 and 7. Table 5 shows the statistical results of the effects of different sewing threads on elongation (%) and permanent elongation (%) values. As can be seen from the results in this table and Figure 9, the highest elongation in zig-zag stitch was obtained in Eloflex-80 and Eloflex-120 sewing threads. In Figure 10, it is seen that the permanent elongation values of Spun Pes-80, Spun-Pes-120, Poly / Poly-80 and Poly / Poly-120 sewing threads of the samples sewn with zig zag stitch are high.

Table 6 contains the statistical results of the effects of different stitch types (lockstitch, zig zag stitch, two thread chain stitch, three thread overlock stitch and five thread overlock stitch) on elongation (%) and permanent elongation (%) values. As can be seen from the results in this table, the zig-zag stitched samples show the least elongation after straight stitching. Permanent elongation values are also low. Among the five stitch types determined in the experimental study, the second stitch with the lowest stretch is seen as the zig-zag stitch.

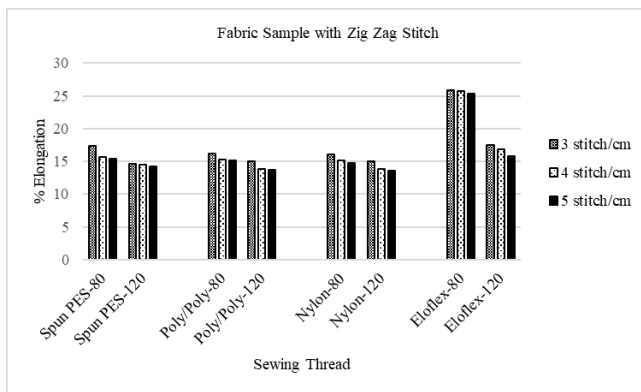


Figure 9. Elongation values (after 30 minutes) of the fabric sample with zig zag stitch

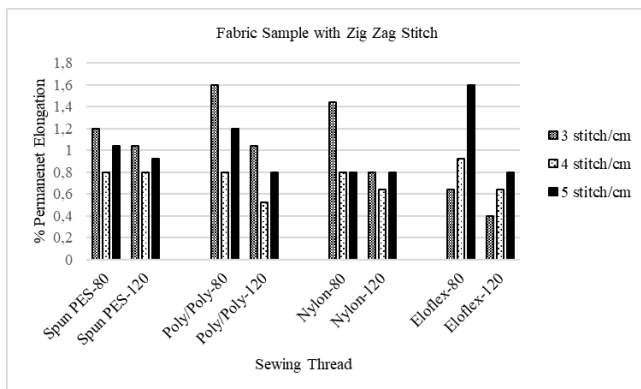


Figure 10. Permanent elongation values (after 2 hours) of the fabric with zig zag stitch

3.4 Elongation (%) and Permanent Elongation (%) Values of Fabric Samples Sewn with Two Thread Chain Stitch

Figure 11 shows the elongation (%) values of fabric samples sewn with two-thread chain stitch and the permanent elongation (%) values (after 2 hours) in Figure 12. The

statistical (ANOVA and SNK) results of the values obtained from these experiments are also included in Tables 5, 6 and 7. Table 5 shows the statistical results of the effects of different sewing threads on elongation (%) and permanent elongation (%) values. As can be seen from the results in this table and Figure 11, the highest elongation in two-thread chain stitch was obtained in Poly / Poly-80 and Poly / Poly-120 sewing threads. In Figure 12, it is seen that the permanent elongation values of Poly / Poly-80 and Nylon-120 sewing threads of the samples sewn with two-thread chain stitch are high.

Table 6 contains the statistical results of the effects of different stitch types (lockstitch, zig zag stitch, two thread chain stitch, three thread overlock stitch and five thread overlock stitch) on elongation (%) and permanent elongation (%) values. As can be seen from the results in this table, samples with two thread chain stitches show the greatest elongation. Permanent elongation values are also low. Among the five stitch types determined in the experimental study, one of the stitches with high stitch stretch is seen as a two-thread chain stitch.

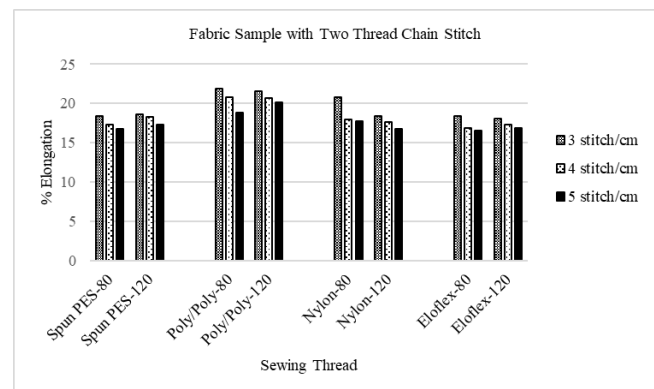


Figure 11. Elongation values (after 30 minutes) of the fabric sample with two thread chain stitch

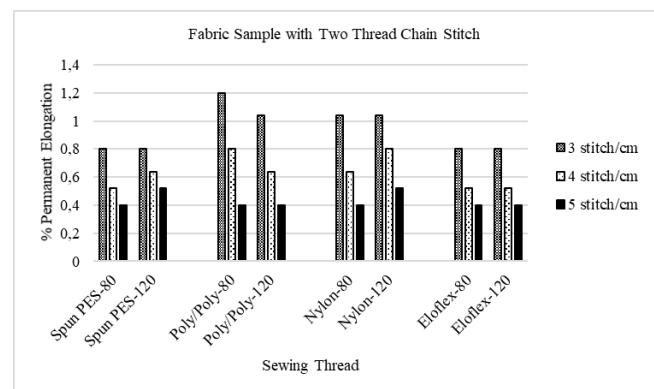


Figure 12. Permanent elongation values (after 2 hours) of the fabric sample with two thread chain stitch

Table 7 shows the statistical results of the effects of different stitch densities (3 - 4 and 5 stitches / cm) on elongation (%) and permanent elongation (%) values. As can be seen from the results in this table, the two thread

chain stitch fabric samples sewn with a stitch frequency of 3 stitches / cm showed the highest elongation (%) and permanent elongation (%), and the fabric samples sewn with 5 stitches / cm showed the lowest elongation (%) and permanent elongation (%) results is seen.

3.5 Elongation (%) and Permanent Elongation (%) Values of Fabric Samples Sewn with Three Thread Overlock Stitch

Figure 13 shows the elongation (%) values of fabric samples sewn with three-thread overlock stitch and the permanent elongation (%) values (after 2 hours) in Figure 14. The statistical (ANOVA and SNK) results of the values obtained from these experiments are also included in Tables 5, 6 and 7. Table 5 shows the statistical results of the effects of different sewing threads on elongation (%) and permanent elongation (%) values. As can be seen from the results in this table and Figure 13, the highest elongation in three-thread overlock stitch was obtained in Poly / Poly-120 and Nylon-120 sewing threads. In Figure 14, it is seen that the permanent elongation values of Poly / Poly-120 and Nylon-120 sewing threads of the samples sewn with three thread overlock stitch are high.

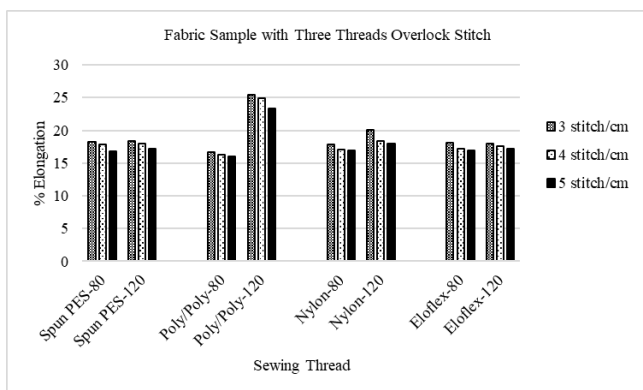


Figure 13. Elongation values (after 30 minutes) of the fabric sample with three thread overlock stitch

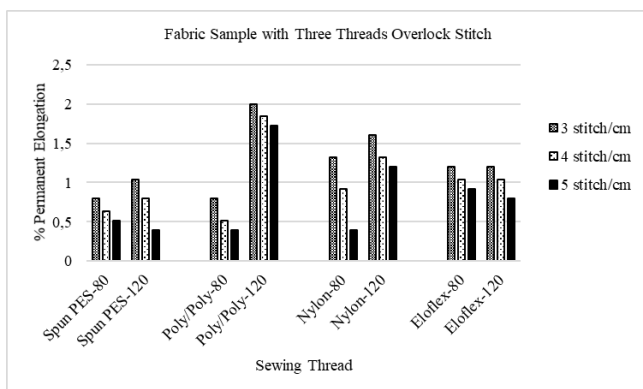


Figure 14. Permanent elongation values (after 2 hours) of the fabric sample with three thread overlock stitch

Table 6 contains the statistical results of the effects of different stitch types (lockstitch, zig zag stitch, two thread chain stitch, three thread overlock stitch and five thread overlock stitch) on elongation (%) and permanent

elongation (%) values. As can be seen from the results in this table, samples with three thread overlock stitches show the greatest elongation. Permanent elongation values are also high. Among the five types of stitches determined in the experimental study, the stitch stretch property is seen as the three thread overlock stitch as the highest.

Table 7 shows the statistical results of the effects of different stitch densities (3 - 4 and 5 stitches / cm) on elongation (%) and permanent elongation (%) values. As can be seen from the results in this table, it is seen that the three thread overlock stitched fabric samples sewn with a stitch frequency of 3 stitches / cm showed the highest elongation (%) and permanent elongation (%), and the fabric samples sewn with 5 stitches / cm stitch frequency showed the lowest elongation (%) and permanent elongation (%) results.

3.6 Elongation (%) and Permanent Elongation (%) Values of Fabric Samples Sewn with Five Thread Overlock Stitch

Figure 15 shows the elongation (%) values of the fabric samples sewn with five-thread overlock stitch and the permanent elongation (%) values (after 2 hours) in Figure 16. The statistical (ANOVA and SNK) results of the values obtained from these experiments are also included in Tables 5, 6 and 7. Table 5 contains the statistical results of the effects of different sewing threads on % elongation and % permanent elongation values. As can be seen from the results in this table and Figure 15, the highest elongation in five-thread overlock stitch was obtained in Eloflex-120, Nylon-120 and Spun Pes-120 sewing threads. In Figure 16, the permanent elongation values of the samples sewn with five-thread overlock stitch are high in Eloflex-120 and Poly / Poly-120 sewing threads.

Table 6 contains the statistical results of the effects of different stitch types (lockstitch, zig zag stitch, two thread chain stitch, three thread overlock stitch and five thread overlock stitch) on elongation (%) and permanent elongation (%) values. As can be seen from the results in this table, the five thread overlock stitched samples show the greatest elongation. Permanent elongation values are also high. Among the five types of stitches determined in the experimental study, it is seen as a five thread overlock stitch with stitch stretching feature in the middle.

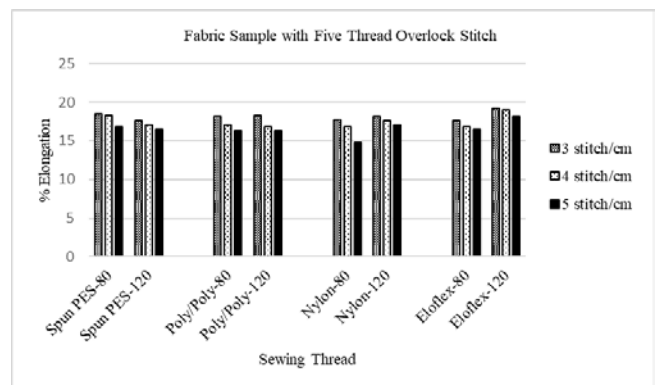


Figure 15. Elongation values (after 30 minutes) of the fabric sample with five thread overlock stitch

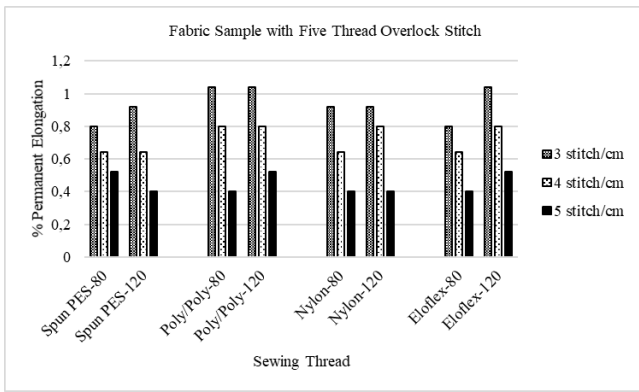


Figure 16. Permanent elongation values (after 2 hours) of the fabric sample with five thread overlock stitch

Table 7 shows the statistical results of the effects of different stitch densities (3 - 4 and 5 stitches / cm) on elongation (%) and permanent elongation (%) values. As can be seen from the results in this table, five thread overlock stitched fabric samples sewn with 3 stitches / cm stitch frequency showed the highest elongation (%) and permanent elongation (%), and fabric samples sewn with 5 stitches / cm stitch frequency showed the lowest elongation (%) and permanent elongation (%) is seen.

4. CONCLUSION

In the apparel industry, stitch should not prevent the fabric from stretching in the garments made of elastane woven fabrics. The elasticity of the stitches of the garments consisting of elastic fabrics is very important. In this study, it is aimed to investigate the elongation and permanent elongation properties of different stitch types of garments made of elastane woven fabrics. For this purpose, 5 different stitch types were selected as lockstitch, zig zag stitch, two thread chain stitch, three thread overlock stitch and five thread overlock stitch and these stitches were sewn at different stitch densities (3 - 4 and 5 stitches / cm) with different sewing threads (spun polyester, core spun (poly / poly), nylon and elastic sewing thread) with two different ticket numbers (80 and 120).

The elongation rate (%) of Eloflex-80 and Eloflex-120 elastic sewing threads and Poly / Poly-120 sewing thread were found to be high and the permanent elongation (%) was also low. Therefore, the elasticity of these sewing threads is evaluated as high. In recent years, elastic sewing threads with high elongation have also been produced for sewing elastic garments. Elastic sewing thread is an ideal thread for sportswear and body-fitting garments. These sewing threads have high elongation and high seam strength and provide stretch seams by preventing damages caused by seam stretch in elastic fabrics.

Besides sewing thread elongation, other important factors that support stitch elasticity are the correct choice of stitch type and stitch density. Although lockstitch (301), which is

the most frequently used stitch type, is a stitch type with the least elasticity, the sewing elasticity values can be increased with the appropriate stitch density. However, this elasticity is not enough. The elasticity of zig zag stitch type 304 is better compared to lockstitch. The best results can be achieved with 500 group overlock stitch types with high sewing elasticity.

The elongation (%) and permanent elongation (%) values of the sewn samples were tested in order to examine the stretch rates of the sewn fabric samples. From the results of the research, it was observed that the elongation rates (%) of three-thread overlock, five-thread overlock and two-thread chain stitches were high, while the elongation rates of lockstitch and zig-zag stitch were low. It has been determined that the permanent elongation values of the three-thread overlock and five-thread overlock stitches are also high. Elasticity of three-thread overlock, five-thread overlock and two-thread chain stitches is higher than lockstitch.

From the results obtained from this study, it was revealed that the stitch density also has an important effect on stitch flexibility. The elongation (%) and permanent elongation (%) values of all stitch types sewn with 3 stitches / cm stitch density were found to be high; The elongation (%) and permanent elongation (%) values of all stitch types sewn with a stitch density of 5 stitches / cm were found to be low. It is desired that the seams of the garments sewn with elastic sewing threads have high stretch properties. However, when the load on the stretched seam is removed, it is desired to be restored. Otherwise, the seam problems may be encountered. Therefore, permanent elongation values in seams are also important. The closer the permanent elongation value is to 0, the fabric does not become loose or bagged, and the stitches do not open or grin, and the sooner it reaches its former state. From the results obtained in this study, it was concluded that the best density value was 4 stitches / cm since the samples sewn with 4 stitches / cm showed an average elongation and permanent elongation values in all stitch types.

From the results obtained from this study, it was observed that the best elasticity was achieved with overlock and two-thread chain stitches, with a stitch density of 4 stitches / cm and elastic sewing threads and corespun (poly / poly) sewing threads applied to garments made of elastane woven fabric.

ACKNOWLEDGMENT

This study was supported by Tübitak 1002 Project with 119M028 number. We would like to express our sincere gratitude to TUBITAK for the support also we would like to thank Savcan Textile Factory, Bursa for fabric supply and Coats Factory, Bursa for sewing threads supply.

REFERENCES

1. Gürarda A. 2005. An investigation for sewing problems of elastic fabrics in clothing industry (doctoral dissertation). Bursa Uludag University, Graduate School of Natural and Applied Sciences, Department of Textile Engineering, Bursa, Turkey.
2. Gürarda A, Meriç B. 2005. The effects of silicone and pre-fixation temperature on the elastic properties of cotton/elastane woven fabrics. *AATCC Review* 9, 53-56.
3. Gürarda A. 2008. Investigation of the seam performance of pet/nylon- elastane woven fabrics. *Textile Research Journal* 78(1), 21-27.
4. Gürarda A, Meriç B. 2010. Slippage and grinning behaviour of lockstitch seams in elastic fabrics under cyclic loading conditions. *Tekstil ve Konfeksiyon* 20(1), 65-69.
5. Rashid MR, Ahmed F, Azad AK. 2012. An investigation about abrasion resistance and seam stretchability properties of weft knitted fabrics made from conventional ring and compact yarn. *International Journal of Scientific and Research Publications* 2(3), 2-6.
6. Akter M, Khan MR. 2015. The effect of stitch types and sewing thread types on seam strength for cotton apparel. *International Journal of Scientific & Engineering Research* 6(7), 198-205.
7. Zeto W, Dhingra RC, Lau KP, Tam H. 1996. Sewing performance of cotton/lycra knitted fabrics. *Textile Research Journal* 66(4), 282-286.
8. Carr H, Latham B. 1998. *The technology of clothing manufacture*, Oxford: BSP Professional Books, , 13-35.
9. Mehta PV. 1992. *An Introduction to quality control for the apparel industry*. Wisconsin: ASQC Quality Press, 80-83.
10. Demir A, Günay M. 1999. *Tekstil Teknolojisi*. İstanbul: Şan Ofset.
11. Wirth E. 2001. Dokuma makinasında elastan iplikle çalışma, *Melliand Türkiye* 3, 72-75.
12. Sewing Threads. 2021. January 10. Retrieved from <https://www.coats.com/tr/Products?type=Threads&type=Threads>.
13. Bubania JE. 2014. *Apparel quality*, England: Fairchild Books, 129-131.
14. ASTM D 6193, Standard Practice for Stitches and Seams, American Society for Testing and Materials, USA, 1990.
15. TS 6071, Dokunmuş Kumaşların Giyim Sebebiyle Torbalanma ve Uzamaya Karşı Mukavemetlerinin Tayini Metodu. Türk Standartları Enstitüsü, Türkiye, 1988.
16. ASTM D 3107-07, Standard Test Method for Stretch Properties of Fabrics Woven from Stretch Yarns, American Society for Testing and Materials, USA, 2015.
17. Gorjanc DS. 2006. Elastic properties of sewing threads after stretching. *Tekstilec* 49(10-12), 218-224.
18. Tylor DJ. 2008. *Carr and Latham's Technology of Clothing Manufacture*, Blackwell Publishing, 129-130.
19. Mandal S, Abraham N. 2010. An overview of sewing threads mechanical properties on seam quality. *Pakistan Textile Journal* 59(1), 40-43.
20. ASTM D 1776, Standard Practice for Conditioning and Testing Textiles, American Society for Testing and Materials, USA, 1990.
21. Flexi-Frame Stretch and Recovery Tester (James Heal). 2021, January 15. Retrieved from <https://www.james-heal.co.uk/instrument/flexiframe/>



Study on Single Jersey Knitted Fabrics Made from Cotton/ Polyester Core Spun Yarns. Part I: Thermal Comfort Properties

Vidhya M¹  *0000-0001-6036-6117

Parveen Banu K¹  0000-0001-8497-2752

Vasanth Kumar D²  0000-0001-9449-2517

Prakash C³  0000-0003-2472-6765

Subramaniam V⁴  0000-0001-5192-9280

¹ Periyar University/ Department of Textiles and Apparel Design / Salem 636 011, Tamil Nadu, India

² VIT Fashion Institute of Technology (VFIT)/ Vellore Institute of Technology - Chennai/ Chennai 600 127, Tamil Nadu, India

³ Indian Institute of Handloom Technology/Department of Handloom and Textiles/ Fulia, Ministry of Textiles, Govt. of India, Shantipur, Nadia 741 402, West Bengal, India

⁴ Jaya Engineering College /Department of Textile Technology /Chennai 602 024, Tamil Nadu, India

Corresponding Author: Vidhya M, E-mail: vidhyaarumugam2604@gmail.com

ABSTRACT

This study, mainly focused on the effect of core-sheath ratio, twist and stitch length on the thermal comfort properties of single jersey knitted fabrics produced from various ratios (100:0, 80:20 and 60:40) of cotton/ polyester core spun yarns. The Box-Behnken design tool was used to study core-sheath ratio, twist and stitch length on the thermal comfort properties of single jersey knitted fabrics and response surface equations were derived and design variables were optimized. From this study, the findings reveal that the decrease in cotton ratio among the fabrics made from core spun yarns decreases the fabric thickness and hence a more porous structure that results in higher thermal conductivity, air permeability, water-vapour transmission and less thermal resistance. It is also evidenced that, increase in the yarn twist (high) and the stitch length (tight) in the fabric structure makes thicker and less porous fabric which results in higher thermal resistance and lesser thermal conductivity, air permeability and water-vapour transmission.

1. INTRODUCTION

Cotton fibres are soft, cool, breathable, absorbent and natural hollow fibres and able to hold 24–27 times of water of their weight [1]. They are strong, absorbent, dyeable, and have high abrasion resistance. In general, cotton is considered one of the well-known and comfortable fibres amongst all the fibres [2]. Cotton has poor wrinkle resistance properties, due to this cotton can be mixed with polyester or some permanent finish can be applied to give

improved properties to cotton fabrics [3]. Hence to attain the best properties of the fibres, cotton fibres are often blended with polyester fibres [4-5].

Polyester fibre is one of the commonly used commercial fibres in the textile industry. These are strong synthetic fibres made by blending the alcohol and acid and initiating a sequence reaction [6-8]. Polyester filament yarns are commercially used interlocked fibres of continuous length

ARTICLE HISTORY

Received: 03.03.2021

Accepted: 25.10.2021

KEYWORDS

Air permeability, thermal comfort, core spun yarn, thermal conductivity and resistance, water vapour permeability.

To cite this article: Vidhya M, Parveen Banu K, Vasanth Kumar D, Prakash C, Subramaniam V. 2021. Study on single jersey knitted fabrics made from cotton/ polyester core spun yarns. Part I: Thermal comfort properties. *Tekstil ve Konfeksiyon*, 31(4), 295-305.

majorly used for weaving and knitting [9]. The polyester filament yarn is one of the finest and synthetic yarns that are used for various purposes like embroidery, sewing, knitting, weaving and core yarn spinning [10-11]. Generally, core spun yarns have two-component in their structure namely core and sheath [11]. Core spun yarns were used to improve strength, durability, comfort, aesthetics, and other functional properties [12]. Continuous filament yarn is used as a core and cotton staple fibres are used to spin the core spun yarns [13]. Filament-core yarns were produced to benefit both the filament and staple fibres properties by resulting in greater strength and good uniformity without sacrificing the surface characteristics of the staple fibre yarn. As the cotton was wrapped over the polyester filament, improvements were observed in yarn properties compared to synthetic yarns [14]. Various factors such as fibre type (natural, synthetic or blend), fabric type (woven or knitted) and fabric constructions (weave or knit structures) are considered as important properties and these properties affect the breathable and thermal properties of the fabrics. From a physiological perspective, comfort properties are majorly affected by the thermal insulation, breathability, moisture transmission properties of the fibres. Commonly polyester fibres have good wicking behaviour and moisture transmission properties and hence polyester fibres and their blends were most widely used in sports wears in recent years [15]. Consumers are more and more interested in knitted fabrics because of such advantages as good fit and softness. Still lot of researches are happening on the usage of core spun yarns for knitted fabric application [16-17].

Clothing comfort is one of the fundamental needs and universally required for the end-users. Such clothing comfort involves both the thermal and non-thermal components and depends on the wearer situation. Clothing comfort is considered as one of the fundamental properties when a textile product is valued. The comfort properties of the fabric are influenced by various parameters such as fibre type, fabric structure, areal density, moisture absorption, heat transmission and skin perception properties [18]. Textile materials can be valued by their comfort level. Such clothing comfort can be classified into two type's namely sensorial comfort and non-sensorial comfort. Sensorial comfort deals with the fabric hand properties such as bending, shear, tensile, thickness and compression, drape, friction and roughness. Non-sensorial comfort deals with the thermal and moisture transmission properties which include air permeability and water-vapour transmission [19]. When a human mind expresses satisfaction when exposed to the thermal environment is defined as thermal comfort. In general, when the body temperature is about 37°C (98.6°F); this is achieved by balancing the amount of heat generated with the amount lost from the body. To maintain a stable body temperature, heat loss is needed to balance the heat production. If the body temperature is unstable, then the body core temperatures will change accordingly [20]. So the clothing

and textile materials require the best thermal insulation properties accordingly for the cold and hot climates. Hence the thermal insulation depends on various factors such as fibre density, fabric thickness, drape and number of layers [21-22]. Mostly the thickness of the fabric is considered as one of the major factors because the fabric thickness encloses still air and restricts the external air movement. The thermal insulation of the fabric can be determined by the entrapped air and which is considered as one of the most significant factors. Micro layers and macro layers of air enclosed within an assembly increase, the thermal insulation of the material increases. Hence the characteristics of fibre, type of fibre, yarn and fabric structure provide a key influence towards the thermal comfort properties [23-24].

During any sports activity, the physiological and psychological comfort of the clothing can be comprehensively balanced by the environment, clothing performance and human body. The comfort properties of the sportswear play a vital role and mainly concentrate on the performance and wearer comfort of the sportswear [25]. The significance of functional clothing used for various activities such as sports, outdoor and other protective garments has got increased in the last decades. Hence thermal properties, moisture transmission and air permeability properties of the clothing should be improved to meet the requirements of sportsperson and athletes [26]. In general, during any sports activity, a human body can able to generate more than 1000W of heat and the generated heat has to be transferred to the environment so that makes the wear comfortable by staying in the thermal equilibrium. For transferring such heat to the environment clothing is necessary for sports for identification, ethical reasons and also to protect our body against impact [27]. Gokarneshan [2019] investigated the thermal comfort properties of single jersey knitted fabrics made from the intimate blends of recycled polyester and cotton fibres. It is also reported that, increase in the ratio of recycled polyester fibres among the blends the fabric becomes thin, porous and lightweight and results in lesser thermal resistance and higher thermal conductivity, relative water-vapour permeability and air permeability properties [28-29]. Jhanji et al [2015] examined the thermo-physiological properties of polyester-cotton plaited fabrics by varying the fibre linear density and yarn type and reported that the plaited fabrics made from carded yarns of polyester fibres have higher linear density and resulted in higher thermal resistance and lower thermal absorptivity which in line makes the wearer feel comfortable [30]. Similarly, the fabrics made from the core yarn result in higher moisture transmission and air permeability properties with the combination of combed cotton yarn in the sheath and coarser polyester yarn in the core.

Aytac and Unal [2017] investigated the comfort properties of plain knitted fabrics made of core spun yarns, by blending the cotton, viscose and PES fibres in the sheath

and different ratios of PVA within the core. The researchers concluded that the permeability properties of the knitted fabrics produced with cotton, viscose, and PES fibres in the sheath and PVA in the core were positively affected [31]. Khalil et al [2020] studied the thermal comfort properties of 100% cotton, cotton with full-platted Lycra, Core, and Dual Core spun yarns (DCS). It is concluded that the core spun and DCS show the highest elongation 27% increased thermal conductivity 18% decreased water-vapour permeability which gives extensibility and comfort at the same strength compared to 100% cotton samples [32]. Prakash and Ramakrishnan [2013] reported that, as the loop length increases, the thermal conductivity also increases due to the fabric packing density and also an increase in the loop length decreases the flow rate of water-vapour [33]. Atalie et al [2019] proved that an increase in the yarn twist increases the fabric permeability due to more air gaps in the fabric structure thus enhancing the overall sensorial comfort [34]. Although many researchers investigated the comfort properties of fabrics with different blend compositions, linear density, fabric structure and few researchers only investigated the comfort properties of knitted fabrics made from core spun yarns. Hence, this study is mainly intended to study the thermal comfort properties of single jersey knitted fabrics made from cotton/ polyester core spun yarns.

Latif et al [2018] examined the comfort properties of fabrics made from cotton fibres blended with various regenerated fibres such as viscose, Tencel, modal, bamboo and proved that when cotton blended with any regenerated fibres could replace the usage of 100% cotton in the clothing applications to meet the requirements of growing demands of the clothing [35]. Likewise, Medar and Mahale [2018] reported that the comfort properties of union knitted fabrics made from cotton and bamboo/ tencel fibre blends were analyzed. This study reveals that the comfort properties of the union knitted fabrics made from bamboo and tencel fibres blended with cotton fibres resulted in superior comfort properties by enhancing the wearer's physiological needs this further enhances their personality and their working efficiency [36]. Oglakcioglu and Marmarali [2007] investigated the thermal comfort properties of knitted fabrics made of various structures and evidenced that the relative water vapour permeability of the single jersey structure is higher than 1 X 1 rib and interlock structure and keeps the wearer warmer and comfortable due to the lower thermal absorptivity properties. Due to the structural nature, single jersey fabrics remarkably results in lower thermal conductivity and higher relative water vapour permeability of 1 X1 rib and interlock fabrics [37]. Khalil et al [2017] reported that the thermal comfort properties of single jersey knitted fabric produced from different lycra states and proved that the knitted fabrics are characterized by comfort when compared to woven fabrics due to their higher extensibility, air permeability and heat retention properties which consequences in dimensional instability after repeated cycles of washing [38]. Hence to maintain

the dimensional stability of the knitted fabrics, additional lycra yarns (spandex) are either half or fully plaited with 100% cotton yarns. It is also suggested that, instead of full plaited fabrics, knitted fabrics made from lycra (in core) and cotton in the sheath can also be used. Vadicherla and Saravanan [2017] examined the thermal comfort properties of single jersey knitted fabrics made from different blend ratios, linear density and loop lengths of recycled polyester and cotton blended yarns and proved that increase in the recycled polyester ratio and loop length among the blends the fabric becomes thin, porous and lightweight results in higher thermal resistance, air permeability, relative water-vapour permeability and lesser thermal conductivity [39]. Similarly when the recycled polyester ratio decreases and the cotton ratio increases the fabric becomes thick, heavier and less porous fabric with higher thermal conductivity, lesser air permeability and thermal resistance and high relative water-vapour permeability at medium linear densities.

It is noticed from the literature that although core spun yarns have been produced and studied for their various properties, their exploitation in knitted fabrics is obscure. The influence of core-sheath ratio, twist and stitch length on the thermal comfort properties of the single jersey knitted fabrics produced from core spun yarns have not been studied yet. The novelty of this study is to produce a cost-effective core spun yarn by using a unique core spin attachment on the ring-spinning machine. A very few researches were carried out in this area, hence based on the literature which inspired the researchers to take up this study on the effect of core-sheath ratio, yarn twists and the stitch length on the thermal comfort properties of the single jersey knitted fabrics.

2. MATERIAL AND METHOD

2.1 Material

For this study, MCU 5 cotton fibres with 31mm fibre length, 4.1 $\mu\text{g}/\text{in}$ fibre fineness, 22.5 g/tex fibre strength, the linear density of 0.17 tex, 8.5% moisture regain and 6% elongation were used in the sheath (cotton staple fibres) and for the core polyester monofilaments with 50 and 65 deniers were used during the core-yarn spinning process. Core sheath proportions of 100:0, 80:20 and 60:40 of cotton/ polyester core spun yarns were produced by varying different levels of the yarn twists (low, medium and high). Single jersey knitted fabrics were produced by varying the stitch length (loose, medium and tight) in the fabric structures and the thermal comfort properties were studied.

2.2 Method

2.2.1 Yarn production

As shown in Figure 1, the yarn production process starts with fibre mixing, lap production, carding, drawing, rove-preparation and ring spinning. This study is aimed to optimize and produce three different yarns (100% cotton, 80:20 and 60:40 cotton/polyester core spun yarns) with a linear density of 14.76 tex by varying

three different twist levels (940, 1020, 1100). For producing 100% cotton yarns, a ring frame machine was used, similarly, for producing core spun yarns Trytex Core Lycra ring frame with a core spin attachment above the drafting unit was used (as shown in Figure 2). In the core spin attachment, a polyester monofilament was passed through the front drafting roller and the core spun yarns were produced with the blend ratio of 80:20 (50 denier polyester monofilament was used in the core) and similarly for 60:40 (65 denier polyester monofilament was used in the core).

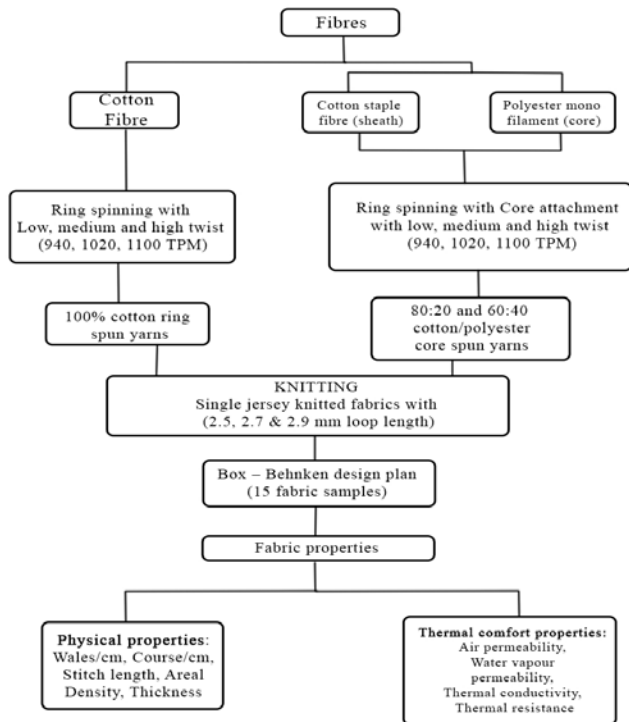


Figure 1. Experimental plan

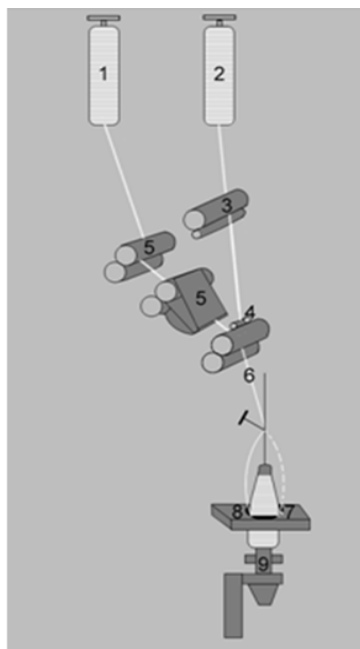


Figure 2. Core spinning process diagram 1. Cotton roving, 2. Polyester filament, 3. Positive feed roller 4. Feeding roller, 5. Drafting roller, 6. Core spun yarn 7. Traveller, 8. Ring, 9. Drive

2.2.2 Fabric production

Box-Behnken, (three-level - three variable factorials) design tool was used in this study. The input parameters under study were the core-sheath ratio of cotton and polyester (100%, 80:20, and 60:40), twists per metre (940, 1020, and 1100) and loop length (2.5, 2.7, 2.9 mm). The knitted fabric samples were shown in Figure 3. The coded factors were calculated using the following Equation (1),

$$x_c = \frac{(x-\bar{x})}{\Delta x} \quad \text{Equation (1)}$$

where x is the actual value of the factor, (low or centre or high level), \bar{x} is the mean value of all levels of the factor, and Δx is the difference between the levels of the factor.

Fifteen single jersey knitted fabric samples with a yarn linear density of 14.76 tex were knitted as per the combination as shown in Tables 1 and 2. The fabrics were knitted using a smart machinery knitting machine with the following specifications; gauge- 32inch, 24-inch dia, 4 feeders/inch, 35 rpm speed and 1800 needles. Single jersey knitted fabric samples (as mentioned in Figure 3.) were subjected to the dry, wet and full relaxation treatments as per the procedure set out by the 'Starfish' recommendations. The fabrics were then subjected to scouring and then conditioned in the standard atmospheric conditions of $27^\circ\text{C} \pm 2^\circ\text{C}$ at a relative humidity of $65\% \pm 2\%$ prior to testing.

Table 1. Variables and levels used in Box-Behnken design

Variables	Levels		
	- 1	0	1
Core sheath ratio % (A)	100	80:20	60:40
TPM (B)	940	1020	1100
Loop length in mm (C)	2.5	2.7	2.9

Table 2. Box-Behnken design sample plan

Std.	Run	Factor 1 A: Core sheath ratio	Factor 2 B: TPM	Factor 3 C: Loop length
8	1	1	0	1
7	2	-1	0	1
9	3	0	-1	-1
13	4	0	0	0
15	5	0	0	0
3	6	-1	1	0
5	7	-1	0	-1
1	8	-1	-1	0
4	9	1	1	0
2	10	1	-1	0
10	11	0	1	-1
14	12	0	0	0
12	13	0	1	1
11	14	0	-1	1
6	15	1	0	-1

2.2.3 Test Methods

Single jersey knitted fabrics produced from the cotton/polyester core spun yarns were tested for areal density (ASTM D 3776), thickness (ASTM D 1777-96) under the standards respectively. Air permeability (ASTM D737-96) of the single jersey knitted fabric samples were investigated using Textest FX 3300 tester at a pressure of 100 Pa and measurements of the samples were carried out ten times and the average and standard deviation of the values were reported. Water-vapour transmission of single jersey knitted fabrics was determined using the Permetest instrument (ISO 11092). The Permetest instrument works on the principle of heat flux sensing and it measures the heat flow caused by the evaporation of water passing through the tested sample and the average values of five readings were reported. Alambeta testing instrument was used to measure the thermal conductivity and thermal resistance of the fabrics. The thermal resistance of the textile materials depends on the thickness and porosity of the particular layer of fabrics. The sample is kept between two plates (one is hot and another is cold) provided in the instrument, according to ISO 11092 standards and measurements of the samples are carried out five times and the average values were reported

3. RESULTS AND DISCUSSION

3.1 Physical properties

Table 3 exhibits the physical properties of single jersey knitted fabrics made from 100% cotton and cotton/polyester core spun yarns. As per the standards, wales/cm, course/cm, stitch length, areal density and thickness of the single jersey knitted fabrics were tested. Optimized values of A = 78:22, B= 1080, C = 2.8.

Figures 4 to 9 represents, 3-D graphs indicating the interactive effects of (a) Core ratio and TPM (b) Core ratio

and Loop length; and (c) TPM and Loop length on the air permeability of cotton/polyester core spun knitted fabrics.

From Figures 4 and 5, it was observed that the increase in polyester content decreases the thickness and fabric weight. Table 4 reveals the statistical significance with high F-value and low *p*-values. From statistical analysis, the response surface equation derived for areal density and thickness was found to be

$$\text{Areal density} = 107+1.5*A+2.625*B-0.875*C+0.0000*AB+0.0000*AC+0.25*BC-1.125*A^2-0.375*B^2-0.375*C^2$$

$$\text{Thickness} = 0.5600+0.0125*A+0.0212*B-0.0087*C-0.0075*AB+0.0025*AC+0.0000*BC+0.0075*A^2-0.0050*B^2-0.0050*C^2$$

100% cotton knitted fabrics with a high twist and low loop length show the highest areal density and thickness values. As per the studies [39-41], polyester is a finer fibre that has low bending rigidity, enhances packing fraction which enhances the compressibility of knit loops and makes thinner and lighter fabrics. Low twist and increased loop length in fabrics show lower GSM and thickness which agrees with the findings of the researchers [42-47].

3.2 Thermal comfort properties of knitted fabrics produced from cotton/polyester core spun yarns

Thermal comfort properties of cotton/polyester core spun knitted fabrics were shown in Table 5. "Design Expert" software was used to perform the experimental study and the interactive effects of these variables and their response surface equations were derived. ANOVA quadric model was used for statistical analysis and results are summarized in Table 6, which reveals the statistical significance with high F-value and low *p*-values.

Table 3. Physical properties of knitted fabrics produced from cotton/polyester core spun yarns

Sample code [Core sheath ratio (Cotton: Polyester) – TPM – Loop length]	Wales/cm	Course/cm	Stitch length	Areal density (g/m ²)	Thickness (mm)
100:0 - 940 - 2.7	17	21	0.149	104	0.56
100:0 - 1020 - 2.9	16	22	0.133	106	0.57
100:0 - 1020 - 2.5	18	23	0.149	108	0.58
100:0 - 1100 - 2.7	17	22	0.148	109	0.59
80:20 - 940 - 2.9	17	21	0.137	103	0.53
80:20 - 940 - 2.5	19	23	0.145	105	0.54
80:20 - 1020 - 2.7	18	22	0.138	106	0.53
80:20 - 1020 - 2.7	18	22	0.138	106	0.53
80:20 - 1020 - 2.7	18	22	0.138	106	0.53
80:20 - 1100 - 2.9	17	21	0.133	107	0.54
80:20 - 1100 - 2.5	18	23	0.145	108	0.55
60:40 - 940 - 2.7	18	22	0.137	102	0.52
60:40 - 1020 - 2.9	17	21	0.130	103	0.51
60:40 - 1020 - 2.5	19	23	0.138	104	0.53
60:40 - 1100 - 2.7	18	22	0.141	105	0.52

Table 4. Analysis of variance

	Degrees of freedom	F-value	<i>p</i> -value
Areal density	9	37.67	0.0005
Thickness	9	136.63	< 0.0001

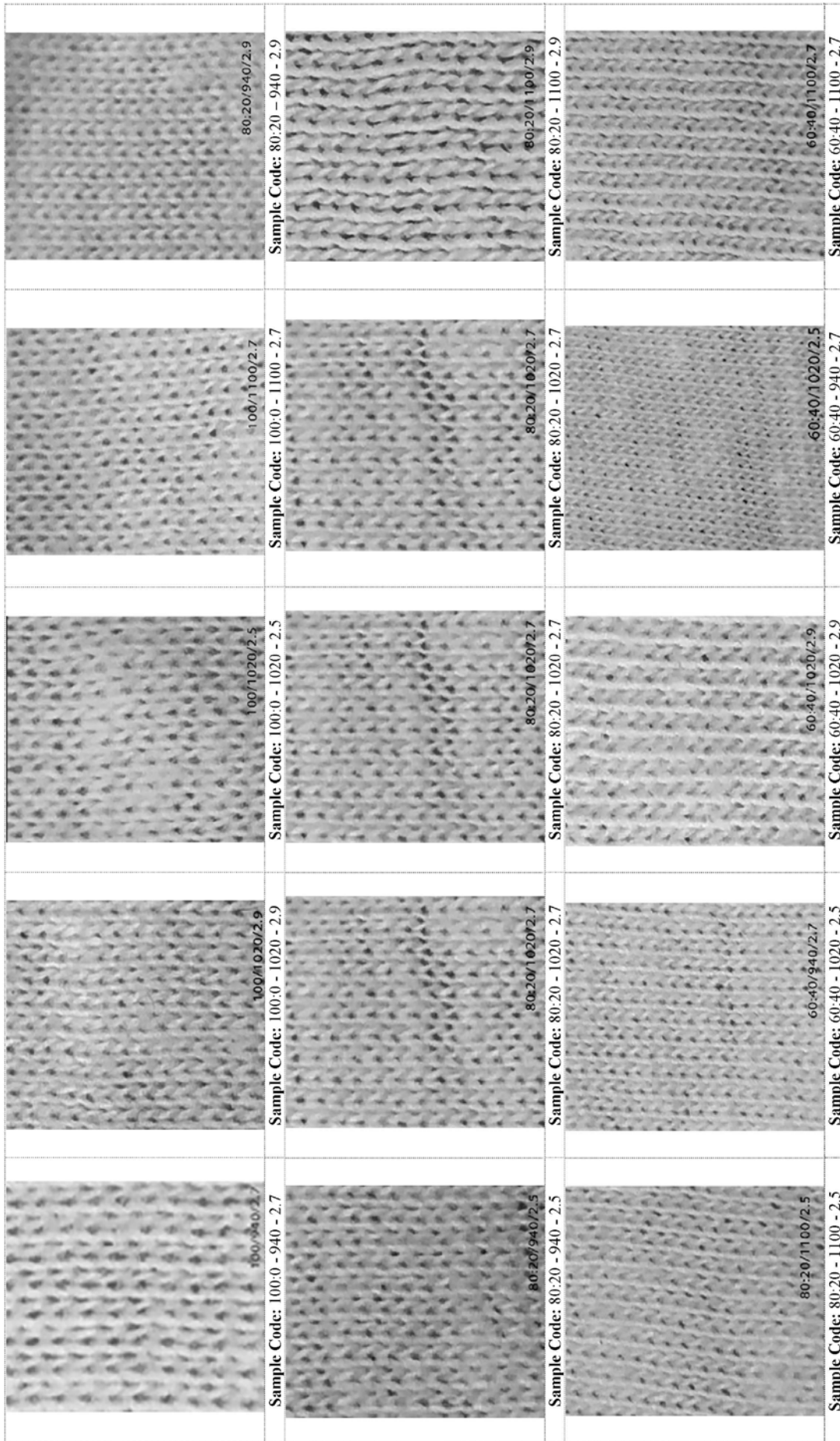


Figure 3. Cotton and Cotton/ Polyester core spun knitted fabric samples

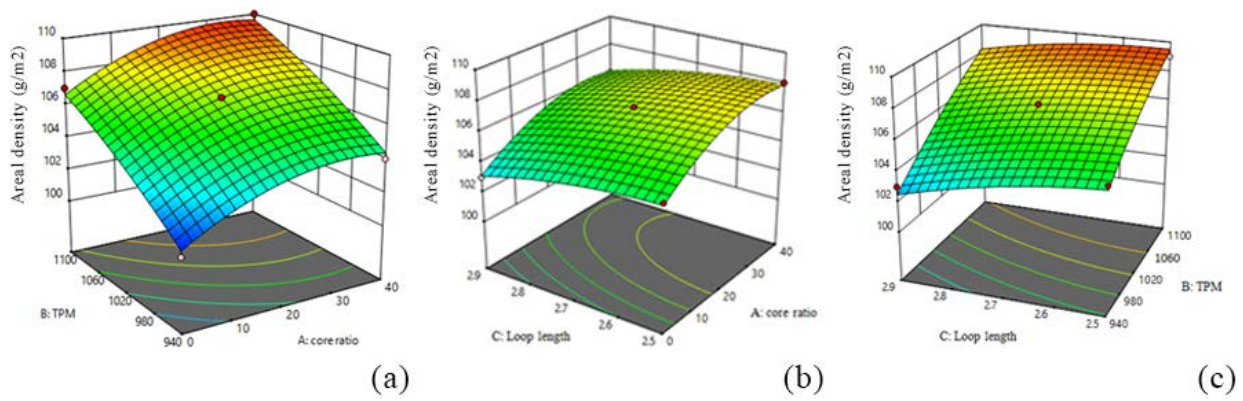


Figure 4. Areal density of knitted fabrics produced from cotton/polyester core spun yarns

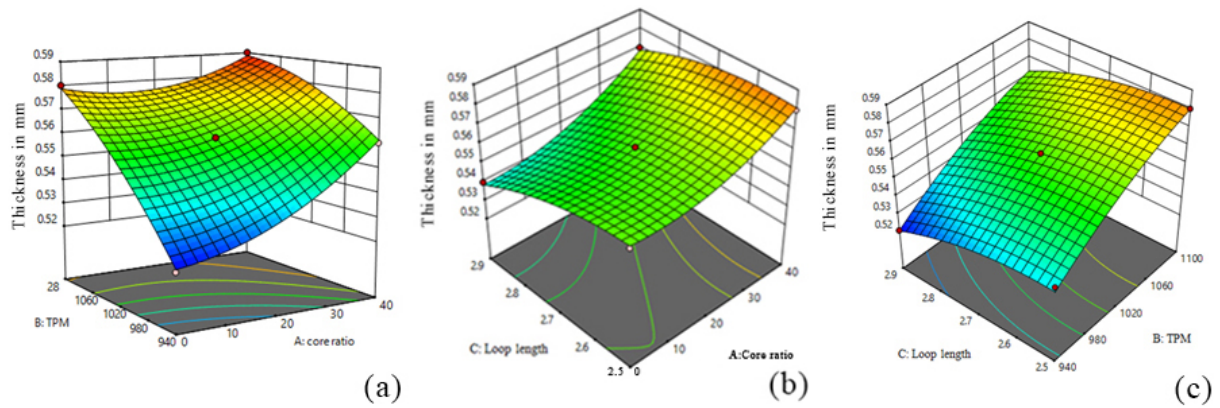


Figure 5. Thickness of knitted fabrics produced from cotton/polyester core spun yarns

Table 5. Thermal comfort properties of knitted fabrics produced from cotton/polyester core spun yarns

Sample code [Core sheath ratio (Cotton: Polyester) – TPM – Loop length]	Response 1 Air permeability in c.c/cm.sq/sec (ASTM D 737-04) (2016)	Response 2 Water vapour transmission (Breathability) (g/m ² /24h)	Response 3 Thermal conductivity (W/mK)	Response 4 Thermal resistance (m ² K/W×10 ⁻³)
100:0 - 940 - 2.7	92.5	2098.46	0.0322	17.08
100:0 - 1020 - 2.9	115	1809.73	0.0317	17.67
100:0 - 1020 - 2.5	102	1732.39	0.0319	17.24
100:0 - 1100 - 2.7	121	2037.62	0.0315	18.1
80:20 - 940 - 2.9	115	2103.19	0.0328	16.15
80:20 - 940 - 2.5	102	1732.39	0.0319	17.24
80:20 - 1020 - 2.7	118	1821.5	0.0325	16.31
80:20 - 1020 - 2.7	118	1821.5	0.0325	16.31
80:20 - 1020 - 2.7	118	1821.5	0.0325	16.31
80:20 - 1100 - 2.9	141	1887.07	0.0321	18.69
80:20 - 1100 - 2.5	108	1726.98	0.0387	13.71
60:40 - 940 - 2.7	93.1	1843.25	0.0408	12.75
60:40 - 1020 - 2.9	115	2103.19	0.0328	16.15
60:40 - 1020 - 2.5	108	1726.98	0.0387	13.71
60:40 - 1100 - 2.7	130	1675.96	0.0374	15.78

Table 6. Analysis of variance

	Degrees of freedom	F-value	p-value
Air permeability	9	26.06	0.0011
Water-vapour transmission	9	23.71	0.0014
Thermal conductivity	9	62.32	0.0001
Thermal resistance	9	426.91	<0.0001

3.2.1 Air Permeability

Table 5 shows the air permeability result and the 3-D graphs (Figure 6.) indicates the effect of variables on the air permeability of single jersey knitted fabrics produced from core spun yarns. The response surface equation obtained for air permeability is mentioned as follows,

$$\text{Air permeability} = 118 - 3.45*A + 14.3625*B - 9.4375*C + 2.1*AB - 1.5*AC - 0.625*BC - 6.4875*A^2 - 2.3625*B^2 + 1.4875*C^2$$

From Figure 6 it was observed that the fabrics with a higher twist and higher loop length show higher air permeability values. When the twist increases, fibres are bound compactly to the yarn body that reducing the hairiness brings high air permeability. The lower hairiness of the yarn contributes towards higher air permeability. Air will flow primarily through the inter-yarn pores because of the high twist in the yarn and the compression of the yarn near the binding points [25-26]. When the loop length increases, the fabric porosity and the air permeability also increase. With the increase in the loop length, the looser the structure leads to higher air permeability. The highest air permeability value of 141 c.c/cm.sq/sec was obtained in 80:20 cotton/polyester core spun knitted fabrics with a high twist and high loop length. An increase in polyester core ratio decreases the fabric thickness and it becomes lighter and more porous with high air permeability which agrees with the study [39]. The lower thickness accompanied by weight per square meter and facilitate the passage of air through the fabric and thus correlates with the earlier studies [42-44].

3.2.2 Water-vapor transmission

Water-vapour transmission is the ability of a fabric to permit the water vapour to pass through the body and to prevent the entry of water. It highly depends upon the macro-porous structure of the fibres in the yarn [30]. From statistical analysis, the response surface equation derived for water vapour transmission is

Moisture Vapour

$$\text{Transmission} = 1821.50 + 83.52*A - 112.35*B + 32.23*C + 49.70*AB - 66.19*AC - 97.21*BC - 23.68*A^2 + 39.70*B^2 + 36.72*C^2$$

The lowest water-vapour transmission rate of 1675.96g/m² for 24hours was obtained in a 60:40 cotton/polyester blend with the TPM and loop length of 1020 and 2.7mm respectively as shown in Figure 7. When the TPM and loop length of 80:20 cotton/polyester core spun knitted fabrics were 940 and 2.9, the water vapour transmission rate was highest as 2103.19 g/m² for 24 hours. An increase in polyester in the core reduces the yarn diameter, better packing fraction, increases the pores that contribute to the higher water vapour transmission rate. The low twist and the high loop length, makes the fabric more porous and thinner which results in an increased water vapour transmission rate. Polyester fibres transport the water vapour from the body at a higher rate than cotton fibres [46]. They attributed these differences to the fact that hydrophilic fibres retained water molecules and could even swell to reduce the porosity of the fabrics [47-48]. 100% cotton fabrics show 2098.46 g/m²/24h at low twist with 2.7mm loop length. Water-vapour transmission rate was strongly correlated with the cross-section of the fibre, fabric thickness and moisture-absorbing properties did not play a significant role [49]. From the literature, it is proved that air permeability has a close relationship with the water-vapour transmission.

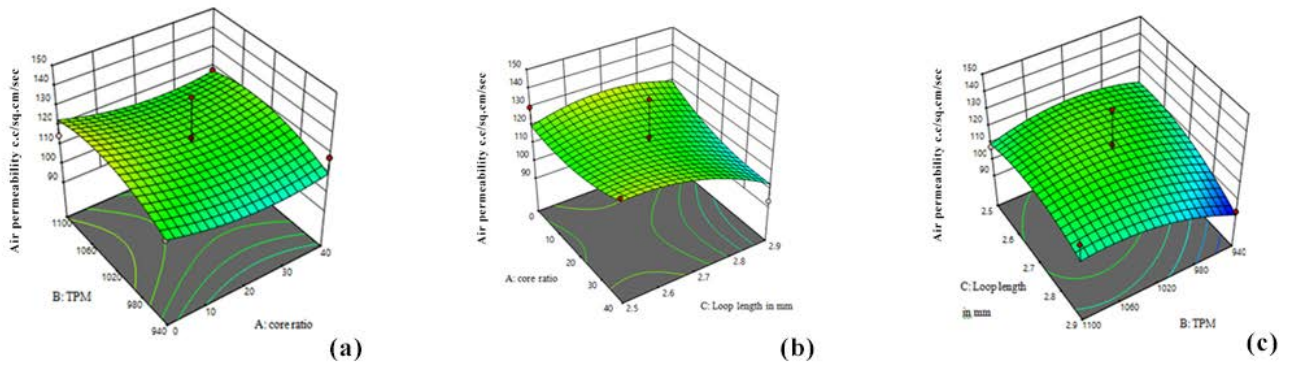


Figure 6. Air permeability of knitted fabrics produced from cotton/polyester core spun yarns

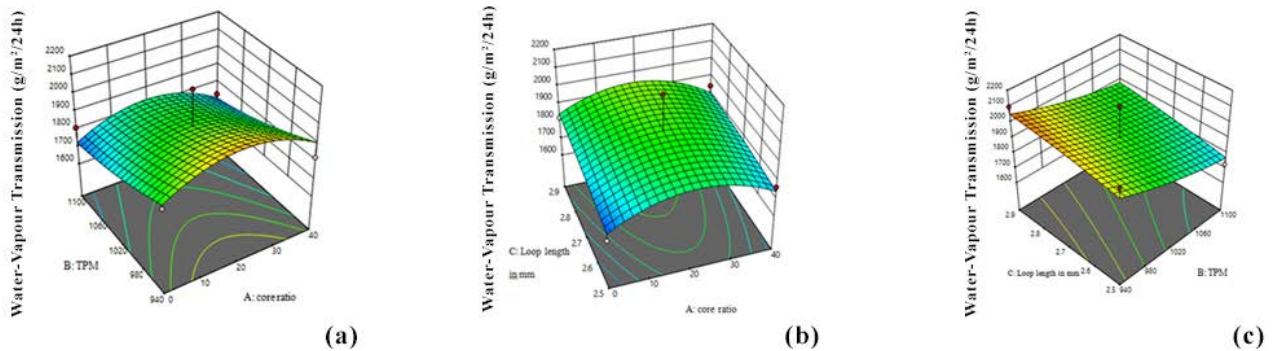


Figure 7. Water-vapour transmission of knitted fabrics produced from cotton/polyester core spun yarns

3.2.3 Thermal conductivity

The ability of a fabric to conduct heat is referred to as thermal conductivity. The thermal conductivity of the fabric depends on the air entrapped within it than on the fibre conductivity. Response surface equation for thermal conductivity as

$$\begin{aligned} \text{Thermal} \\ \text{conductivity} = & 0.0325 + 0.0325 * A - 0.0007 * B + 0.0001 * C - \\ & 0.0007 * AB + 0.0001 * AC + 0.0000 * BC + \\ & 0.0028 * A^2 + 0.0002 * B^2 - 0.0002 * C^2 \end{aligned}$$

It is apparent from Figure 8, 60:40 cotton/polyester core spun fabrics show a higher thermal conductivity value of 0.0408 W/mK at low twist and medium loop length. 100% cotton fabrics with a high twist and medium loop length show the lowest value of 0.315 W/mK. The thermal conductivity of the knitted fabrics can be influenced by the increased twist and stitch length of the fabrics. An increase in the cotton fibre content on the fabric leads to a decrease in the thermal conductivity of the fabrics. This is attributed to the lower fabric cover that allows more air gaps in the fabric structure, thus improving the resultant thermal conductivity through the fabric [50]. This study shows a well-known fact that thermal conductivity is inversely proportional to the thermal resistance of the fabrics. This is

in substantial agreement with the findings of previous works [51- 52].

3.2.4 Thermal resistance

The thermal resistance properties of cotton/polyester knitted fabrics were shown in Table 5 and Figure 9. Response surface equation derived for thermal resistance is

$$\begin{aligned} \text{Thermal} \\ \text{resistance} = & 16.31 - 1.64 * A + 0.9837 * B - 0.4225 * C + 0.5025 * AB - \\ & 0.1400 * AC - 0.3150 * BC - 0.7412 * A^2 + 0.3588 * B^2 + \\ & 0.2612 * C^2 \end{aligned}$$

An increase in the stitch length of the fabric increases the thermal resistance properties and this is due to an increase in the air gaps in the fabric structure. Air is considered a good thermal insulator and hence the air gaps increases result in enhanced thermal resistance of the knitted fabrics. The increase in thermal resistance at the same time by an increase in loop length is explained due to a decrease in fabric thickness proportionally and a change in pore structure [53-54]. The thermal resistance of the knitted fabric decreases with the decrease in the fabric density. Due to the decrease in the fabric density, the air trapped in the holes of the knitted fabrics will be higher. The higher the thermal resistance value of the air compared to the textile fibres, the lower the total heat transfer in the fabric and the higher the thermal resistance [55-56].

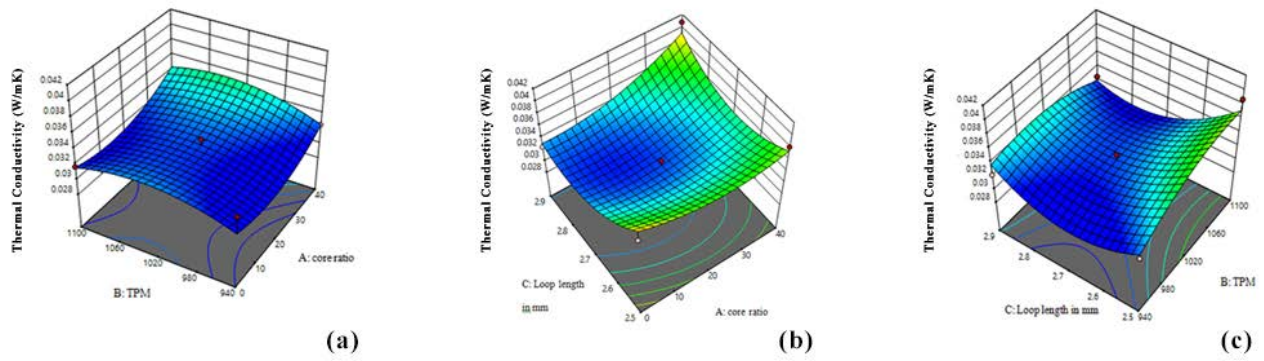


Figure 8. Thermal conductivity of knitted fabrics produced from cotton/polyester core spun yarns

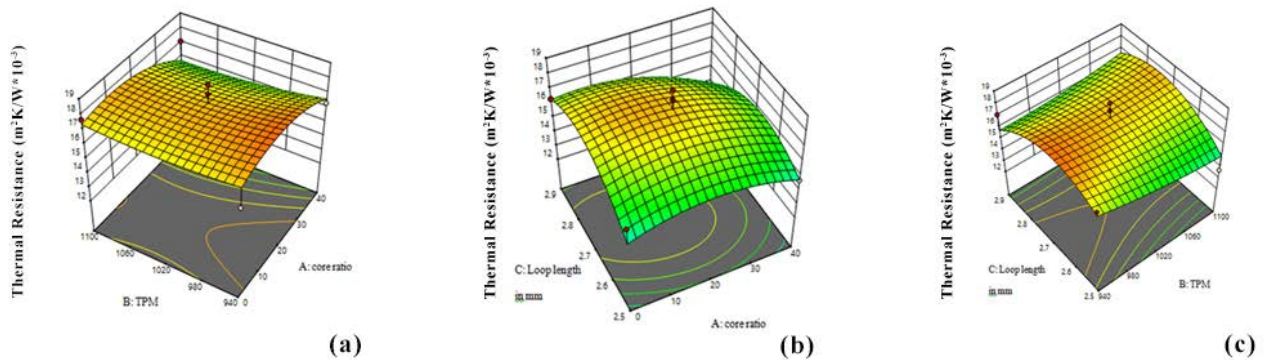


Figure 9. Thermal resistance of knitted fabrics produced from cotton/polyester core spun yarns

4. CONCLUSION

The thermal comfort properties of 100% cotton, 80:20 and 60:40 knitted fabrics produced from cotton/polyester core spun yarns were investigated in this study. It was found that the core-sheath ratio, twist and stitch length have a significant influence on the thermal comfort properties of the knitted fabrics. It is also noticed that the decrease in cotton ratio decreases the fabric thickness and results in lighter and more porous fabric structure leads to higher thermal conductivity, thermal resistance, air permeability and lower water-vapour transmission properties [39]. An increased twist in the yarn and tight loop structure in the fabric makes the fabric thicker and less porous with higher thermal resistance and lower thermal conductivity, air

permeability and water-vapour transmission rate [44-45]. This is a fragmented part of our research work and this paper (Part I) mainly focused on the thermal comfort properties of knitted fabrics produced from cotton/polyester core spun yarns. In continuation to this research work, the next paper (Part II) is mainly focused on the moisture management properties of knitted fabrics produced from cotton/polyester core spun yarns. Compared to the knitted fabrics made from 100% cotton yarn, loose structured 80:20 cotton/polyester core spun knitted fabrics shows higher thermal resistance, air permeability, water-vapour transmission and lesser thermal conductivity and are more suitable for various end uses with enhanced thermal comfort properties.

REFERENCES

1. Mather RR, Wardman RH. 2015. *The chemistry of textile fibres*. UK: Royal Society of Chemistry.
2. Paul R. 2015. *Functional finishes for textiles: Improving comfort, performance and protection*. UK: Woodhead Publishing Private Limited.
3. Gordon S, Hsieh YL. 2007. *Cotton: Science and technology*. UK: Woodhead Publishing.
4. Ravandi SH, Valizadeh M. 2011. *Properties of fibers and fabrics that contribute to human comfort*. UK: Woodhead Publishing Series in Textiles.
5. Rathod AR, Kolhatkar AW. 2010. Comparison of bamboo and cotton yarn. *Asian Textile Journal* 19(1), 44- 46.
6. Hearle JWS, Morton WE. 2008. *Physical properties of textile fibres*. UK: Woodhead Publishing Private Limited.
7. McLoughlin J, Sabir T. 2018. *High-Performance apparel: Materials, development, and applications*. UK: Woodhead Publishing Private Limited.
8. Lawler B, Wilson H. 2002. *Textiles technology*. Oxford: Heinemann Educational Publishers.
9. Lewin M, Pearce EM. 1998. *Handbook of fiber chemistry*. New York: Marcel Dekker Inc.
10. Camlibel NO. 2018. *Polyester: Production, characterization and innovative applications*. Croatia: Intech.

11. Miao M, Xin JH. 2018. *Engineering of high-performance textiles*. UK: Woodhead Publishing Private Limited.
12. Gong RH. 2011. *Specialist yarn and fabric structures: Developments and applications*. New Delhi: Woodhead Publishing India Private Limited.
13. Lawrence CA. 2010. *Advances in yarn spinning technology*. New Delhi: Woodhead Publishing India Private Limited.
14. Pramanik P, Patil VM. 2009. Physical characteristics of cotton/polyester core spun yarn made using ring and air-jet systems *Autex Research Journal* 9(1), 14-19.
15. Daanen H. 2015. *Physiological strain and comfort in sports clothing. Textiles for Sportswear*. UK: Woodhead Publishing Series in Textiles, 153-168.
16. Spencer DJ. 2001. *Knitting technology: A comprehensive handbook and practical guide*. England: Woodhead Publishing Ltd.
17. Au KF. 2011. *Advances in knitting technology*. New Delhi: Woodhead Publishing India Private Limited.
18. Song G. 2011. *Improving comfort in clothing*. New Delhi: Woodhead Publishing India Private Limited.
19. Pan N, Sun G. 2011. *Functional textiles for improved performance, protection and health*. New Delhi: Woodhead Publishing India Private Limited.
20. Havenith G. 2005. *Temperature regulation, heat balance and climatic stress*. Berlin: Springer.
21. Kothari VK. 2006. Thermo-physiological comfort characteristics and blended yarn woven fabrics. *Indian Journal of Fiber and Textile Research* 31, 177-186.
22. Li Y, Wong ASW. 2006. *Clothing biosensory engineering*. England: Woodhead Publishing Private Limited.
23. Tochihara Y, Ohnaka T. 2005. *Environmental ergonomics- The ergonomics of human comfort, health, and performance in the thermal environment*. UK: Elsevier Science.
24. Angelova RA. 2016. *Textiles and human thermophysiological comfort in the indoor environment*. New York: CRC Press.
25. Bartels VT. 2005. *Textiles in sport*. UK: Woodhead Publishing Series in Textiles, 177-203.
26. Xiaofei W. 2020. Evaluation of the comfort of sportswear. *Journal of Physics: Conference Series* 1790(1), 1-7.
27. Özkan ET, Kaplangiray BM. 2019. Investigating thermophysiological comfort properties of polyester knitted fabrics. *Journal of Textile Engineering and Fashion Technology* 5(1),50-56.
28. Gokarneshan N. 2019. Comfort properties of textiles: A review of some breakthroughs in recent research *Juniper Online Journal Material Science* 5(3), 1-5.
29. Kumar DV, Raja D. 2021. Study of thermal comfort properties on socks made from recycled polyester/virgin cotton and its blends *Fibers Polymers* 22(3), 841-846.
30. Jhanji Y, Gupta D, Kothari V K. 2016. Thermo-physiological properties of polyester-cotton plated fabrics in relation to fibre linear density and yarn type. *Fashion and Textiles* 2, 16.
31. Aytaç I, Ünal PG. 2017. The effect of core-sheath proportion on the characteristics of fabrics produced with hollow yarns: part II comfort and mechanical properties. *The Journal of The Textile Institute* 109(7), 975-982.
32. Khalil A, Fouda A, Tešinová P, Eldeeb AS. 2020. Comprehensive assessment of the properties of cotton single jersey knitted fabrics produced from different lycra states *AUTEX Research Journal* 21(1), 71-78.
33. Prakash C, Ramakrishnan G. 2013. Effect of blend ratio, loop length, and yarn linear density on thermal comfort properties of single jersey knitted fabrics. *International Journal of Thermophysics* 34(1), 113-121.
34. Atalie D, Ferede A and Rotich GK. 2019. Effect of weft yarn twist level on mechanical and sensorial comfort of 100% woven cotton fabrics *Springer Open* 6(3), 1-12.
35. Latif W, Basit A, Ali Z, Baig SA. 2018. The mechanical and comfort properties of cotton and regenerated fibers blended woven fabrics. *International Journal of Clothing Science and Technology* 30 (1), 112-121.
36. Medar R, Mahale G. 2018. Quality analysis of comfort properties of cotton and bamboo/tencel union fabrics. *Indian Journal of Pure & Applied Biosciences* 6 (5), 827-831.
37. Oglakcioglu N, Marmarali A. 2007. Thermal comfort properties of some knitted structures. *Fibres & Textiles in Eastern Europe* 15 (5), 64 – 65.
38. Khalil A, Tešinová P, Aboalasaad AR. 2019. Thermal comfort properties of single jersey knitted fabric produced at different Lycra. *States ICNF Conference Porto Portugal*.
39. Vadicherla T, Saravanan D. 2017. Thermal comfort properties of single jersey fabrics made from recycled polyester and cotton blended yarns. *Indian Journal of Fibre & Textile Research* 42, 318-324.
40. Sitotaw DB. 2016. Effect of twist multipliers on Air permeability of single jersey and 1×1 rib fabrics. *Journal of Textile and Apparel Technology and Management* 10(1), 1- 8.
41. Havlová M, Špánková J. 2017. Porosity of knitted fabrics in the aspect of air permeability – discussion of selected assumptions. *Fibres & Textiles in Eastern Europe* 25, 3(123), 86-91.
42. Bhattacharya SS, Ajmeri JR. 2014. Air permeability of knitted fabrics made from regenerated cellulosic fibres. *International Journal of Engineering Research and Development* 10(7), 16-22.
43. Bivainyte A, Mikucioniene D. 2011. Investigation on the air and water vapour permeability of double-layered weft knitted fabrics. *Fibres & Textiles in Eastern Europe* 19, 3(86), 69-73.
44. Prakash C, Ramakrishnan G, Koushik CV. 2012. Study of thermal comfort properties of cotton/regenerated bamboo knitted fabrics. *African Journal of Basic & Applied Sciences* 4(2), 60-66.
45. Karthikeyan G, Nalanilli G, Shanmugasundaram OL, Prakash C. 2016. Thermal comfort properties of bamboo tencel knitted fabrics. *International Journal of Clothing Science and Technology* 28(4), 420 – 428.
46. Dhinakaran M, Sundaresan S, Dasaradan BS. 2014. Comfort properties of apparels. *The Indian Textile Journal* 5, 45-48.
47. Ito H, Muraoka Y. 1993. Water transport along textile fibers as measured by an electrical capacitance technique, *Textile Research Journal* 63, 414-420.
48. Halgas BW, Danych R, Wiecek B, Kowalski K. 2006. Air and water vapour permeability in double-layered knitted fabrics with different raw materials. *Fibres & Textiles in Eastern Europe* 57, 14(3), 77-80.
49. Prahsarn C. 2005. Moisture vapor transport behaviour of polyester knit fabrics. *Textile Research Journal* 75(4), 346-351.
50. Ramratan A, Choudhary AK. 2018. Thermo-physiological study of active knitted sportswear A critical review. *Asian Textile Journal* 5, 53- 64.
51. Afzal A, Ahmad S, Rasheed A, Ahmad F, Ifikhar F, Nawab Y. 2017. Influence of fabric parameters on thermal comfort performance of double layer knitted interlock fabrics. *Autex Research Journal* 17(1), 20- 26.
52. Varghese N, Thilagavathi G. 2014. “Handle and comfort characteristics of cotton core spun lycra and polyester/lycra fabrics for application of blouse. *Journal of Apparel, Technology and Management* 8(4), 1-13.
53. Onofrei E, Rocha AM, Catarino A. 2014. The influence of knitted fabrics’ structure on the thermal and moisture management properties. *Journal of Engineered Fibers and Fabrics* 6(4), 14-20.
54. Özdil N, Marmarali A, Kretschmar SD. 2007. Effect of yarn properties on thermal comfort of knitted fabrics. *International Journal of Thermal Sciences* 46, 1318-1322.
55. Pant S, Jain R. 2014. Comfort and mechanical properties of cotton and cotton blended knitted khadi fabrics. *Studies on Home and Community Science* 8(2-3), 69-74.
56. Erdumlu N, Saricam C. 2016. Investigating the effect of some fabric parameters on the thermal comfort properties of flat knitted acrylic fabrics for winter wear. *Textile Research Journal* 87(11), 1349- 1359.



One-Bath Dyeing and Finishing Process of Polyester Fabrics

Gamze Gülşen Bakıcı¹  0000-0002-4241-7096

Füsün Doba Kadem²  0000-0002-7764-5910

¹Çukurova University / Adana Organized Industrial Zone Vocational School of Technical Sciences / 01350, Adana, Turkey

²Çukurova University / Department of Textile Engineering / 01330, Adana, Turkey

ABSTRACT

The purpose of this study is to provide some finishing properties of polyester fabrics in dyeing baths. One bath dyeing and finishing process of 100% polyester fabrics are carried out with exhaust method. A commercial finishing agent is added with different concentrations in the dyeing baths. Fabrics are evaluated concerning hydrophilicity, volumetric resistivity, colour measurement, colour fastness, soil-releasing and fabric performance tests like bending strength, crease recovery, air permeability and thickness. Test results are analyzed by Kruskal Wallis Analysis using version 25 of IBM SPSS Statistics. As a result, the addition of a finishing agent to the dyeing bath has improved hydrophilicity, soil-release, crease recovery and bending strength properties of the fabrics, but has not affected the colour fastness of the fabrics. As the concentration of the finishing agent has increased, the air permeability and the surface resistance of the fabrics have decreased and the thickness has increased.

ARTICLE HISTORY

Received: 24.07.2020

Accepted: 08.11.2021

KEYWORDS

Polyester, One-Bath, Dyeing, Finishing, Colour

1. INTRODUCTION

Polyester (PES) dominates the world market for synthetic textile fibers [1]. The use of polyester fibres in many textile applications is growing very rapidly due to their high strength, good elastic recovery, dimensional stability after heat setting, as well as suitability for blending with natural fibres. However, the main drawbacks in polyester-based textiles, for example, low moisture content, static accumulation, soiling, uncomfortable feel, pilling tendency, and difficulty in dyeing, attributed to their high crystallinity, compactness, hydrophobic nature, and absence of chemically reactive groups. Therefore, considerable efforts and technical developments have been done to upgrade their quality and usefulness, for example, antistatic finish, soil-release finish, water-repellent finish, anti-pilling finish, flame-retardant finish, and silk-like finish [2].

Moreover the combined dyeing and finishing processes offer a saving in energy and water consumption, which is important from both an economical and ecological point of view [3]. Dyeing and finishing of polyester fabrics were applied in one bath to give some finishing properties during disperse dyeing of polyester fabrics in this study. Disperse dyes have very limited solubility in water at room temperature and have substantivity for one or more hydrophobic fibres; e.g., polyesters and nylons. A general rule of thumb has the starting temperature about 70-80°C, the rate of temperature rises at 1.5-2 °C per minute, the dyeing temperature between 115-130°C and the time of dyeing at temperature from 15-60 minutes [4]. Most disperse dyes have a high exhaustion on polyester, often achieving 95% or higher. However, to achieve the best levels of wet-fastness, it is necessary to remove the residual dye from the polyester surface after dyeing to prevent it from staining other fibres. This is normally achieved by a

To cite this article: Bakıcı GG, Kadem FD. 2021. One-bath dyeing and finishing process of polyester fabrics. *Tekstil ve Konfeksiyon* 31(4), 306-317.

reduction clearing treatment using caustic soda and hydrous (sodium dithionite), which reduces the surface dye [5].

Studies in the literature are focused on dyeing of polyester / cotton fabrics in one bath [6-8]. In one of the studies, the effects of corona discharge (CD) and chitosan treatment on the dyeability of polyester / cotton blends with direct and reactive dyes were investigated. The results have opened up the possibility of a new method for dyeing polyester / cotton blends in a single bath using a class of dyes commonly used for dyeing textile material of cellulosic origin [6]. In another study, the dyeing process of polyester / cotton fabrics using disperse / reactive dyes in one-bath dyeing method was examined. It was pretreated in NaOH solutions to improve the adhesion of chitin to the surface of polyester / cotton fibers. The colour and friction fastness properties of the chitin deposited polyester / cotton fabrics were evaluated. The colour difference between the stained voids and the stained voids in the NaOH and / or different viscosity chitin treatment was estimated. The data obtained show that it is possible to dye polyester / cotton fabrics finished with chitin with only one dispersion / reactive dye. The rubbing and washing colour fastness of the dyed samples were found to be good [7]. Maeda et al. conducted an experimental study on dyeing polyester / cotton blends with reactive disperse dyes in one bath. Supercritical carbon dioxide (SC-CO₂) was used as solvent in the range of 353 to 393 K and 10 to 20 MPa, and a successful result was achieved in dyeing polyester / cotton blends in one bath. The dyeing behavior was compared with the thermosol dyeing method using the same dye, and the colour fastness properties of the fabrics dyed with SC-CO₂ gave a better result than the fabrics dyed with the thermosol dyeing method [8]. Afifi and Sayed carried out an experimental study aimed at researching and developing a one-bath dyeing process for the most common blended fibers that would replace the traditional two-step process to dye each fiber component individually. They applied the dyeing of polyester / wool mixture with disperse dyes in a single bath, aiming to save raw materials, dyes, auxiliary substances and energy [9].

Fan et al. (2019) for the antistatic properties of polyester fabric, demonstrated that dyeing and antistatic finishing in which a new functional disperse dye is doped with graphene oxide can be obtained simultaneously with a single bath method. Functional dyes were used to dye polyester fabric by a high-temperature, high-pressure dyeing method. The dyeing concentration of the disperse dye for polyester fabric was 2%. The concentrations of GO were 0.5%, 1%, 2%, 3%, and 4% respectively. The original disperse Dye, GO, and the Dye-GO-treated polyester fabric were characterized by scanning electron microscopy. Raman spectrum, the colour performances of dyed polyester fabrics and effects of GO concentration and reduction time on antistatic properties were analysed. Increase in the amount of GO in functional

disperse dye in terms of rubbing and washing fastness when tested, washing fastness of polyester fabric while it is at a good level, it was observed that the friction fastness decreased a little. The surface electrical resistance of the dyed fabric was obtained at a condition of 2% GO with a reduction time of 30 min and achieved an excellent antistatic standard. **It means that the dyeing and antistatic finishing can be simultaneously obtained by a one-bath method** [10].

In a study conducted in 2019, the simultaneous alkali deweighting and dyeing of polyester fabric was carried out in one-bath and one-step process. In the study, three highly alkali-resistant (HA) disperse dyes were successfully applied to the simultaneous alkali deweighting and dyeing of polyester fabric by a one-bath and one-step process. All the dyeing and finishing experiments were carried out in sealed and conical flasks immersed in a universal dyeing machine using a 50:1 liquor ratio. Colour measurement, mechanical performance, scanning electron microscopy observation, fastness to washing and rubbing were evaluated according to related standards. HA disperse dyes had very good dyeing performance and good fastness on polyester fabrics. Compared to the traditional method one-bath and one-stage process it has been determined that it has the potential to increase production efficiency. Thus, water, chemical and energy consumption decreases it is thought that economic and environmental benefits can be achieved [11].

Touhid et al. (2020) investigated a dyeing process that can provide functional properties to polyester fabric. In the study in question, a production-scale semi-continuous dyeing process was used for the production of reduced graphene oxide (rGO) and titanium dioxide (TiO₂) on polyester fabric. The micro-flowers (MFs) were successfully decorated on the fiber surface through a simple binder-free approach. The MFs blessed fabric showed improved adhesion and washing stability for antibacterial performance using eco-friendly cold O₂ plasma technique. Surface morphology analysis and elemental analysis such as FTIR analysis, X-ray diffraction analysis, Raman spectra analysis, Thermal analysis (TGA-DTG), XPS spectra analysis were performed experimental samples. The hydrophilicity of the as plasma modified polyester fabric was analyzed before and after surface modification. After treatment with pristine TiO₂ and rGO-TiO₂ the water contact angle (WCA) was increased from 20° to 85°, 115°, 125°, and 135° respectively. The antibacterial performance for the functionalized polyester fabric was analyzed. The antibacterial performance of the resultant fabric coated of TiO₂- rGO was enhanced from 60% to 99.5% with the increase of GO and TiO₂ content % as compared to a pristine coated fabric. The overall efficiency of TiO₂-rGO MFs against the gram-positive (*S. aureus*) and gram-negative (*E. coli*) bacteria was recorded 99.5% and 98.0%, respectively [12].

Dyeing and finishing processes of 100% polyester fabrics with disperse dyestuff are carried out using the exhaust dyeing method in one bath in this study. Fabrics are evaluated concerning hydrophilicity, volumetric resistivity, colour measurement, colour fastness, soil-releasing test and fabric performance tests like bending strength, crease recovery, air permeability and thickness. Test results are analyzed by Kruskal Wallis Analysis using version 25 of IBM SPSS Statistics.

2. MATERIAL AND METHOD

2.1 Material

2.1.1. Fabric

100% polyester fabrics that are prefinished are obtained from Zorlu Textile (Turkey). The physical properties of the fabric are given in Table 1.

2.1.2. Disperse dye

Disperse Blue 79, whose chemical structure is shown in Figure 1, is provided by Setaş Chemical Company (Adana, Turkey).

2.1.3. Finishing agent

A commercial finishing agent (Reapret SR) is provided from Bozetto Group (Izmir, Turkey). The finishing agent gives softness, slipperiness, anti-static, dirt/stain resistant and hydrophilic properties to the polyester fabric. FT-IR analysis of the finishing agent is given in Figure 2.

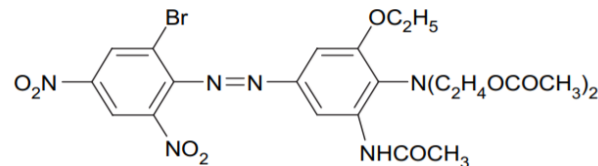


Figure 1. C.I. Disperse blue 79 (Şahin vd. 2007)

Table 1. Physical properties of polyester fabric

Weave Structure		Satin
Weight (g/m ²)		160
Density (yarns per cm)	Weft	25
	Warp	56
Linear Densities of Yarns (denier)	Weft	300
	Warp	100

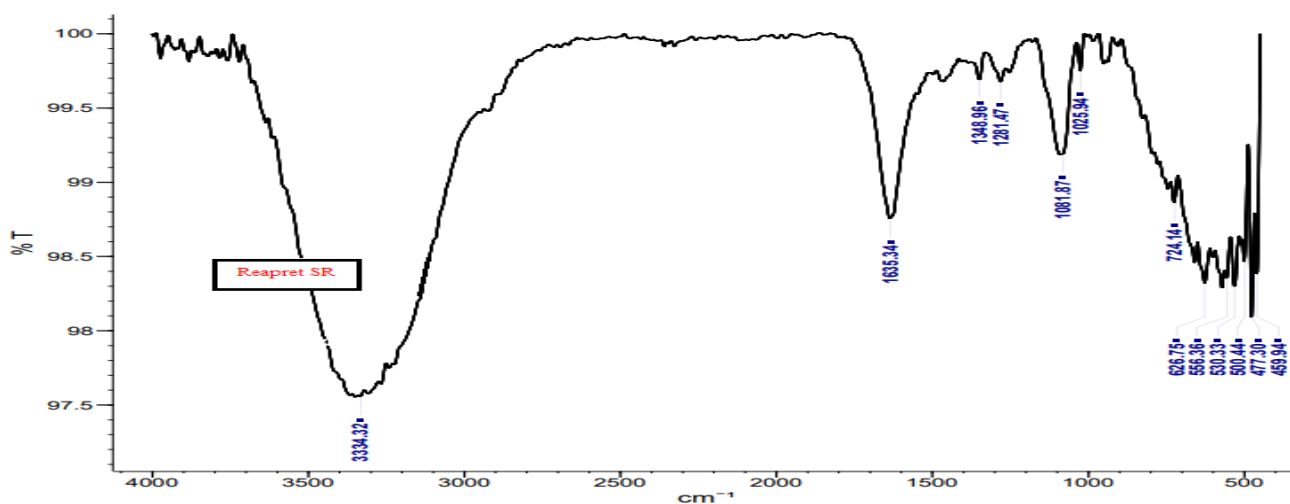


Figure 2. FT-IR analysis of the commercial finishing agent (Reapret SR)

In FT-IR analysis (Figure 2), wide O-H H₂O band at 3300 cm⁻¹, C = O at 1600 cm⁻¹ and etheric bond C-O-C peaks at 1100 cm⁻¹ are seen. The chemical structure of the commercial finishing agent is given in Figure 3.

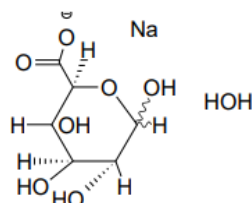


Figure 3. Chemical structure of the commercial finishing agent (Reapret SR)

The chemical structure of this material, used to reduce the static electrification of polyester fabric and to give it a hydrophilic feature, is given in Figure 3. This material, in the form of light brown cloudy liquid, is thought to be a water-based material. While the OH group in the structure gains hydrophilicity, conductivity is provided with H₂O and Na (due to its ionic character).

2.1.4. Auxiliary chemicals

Dispergator and pH regulating agent (Belsit Emu), anti-creasing agent (Belfalt Oyt) and wetting agent (Belwett-Mr-Ex) are provided by Belice Chemical Company (Gaziantep, Turkey).

2.2 Method

100% polyester fabrics are treated in dyeing baths containing different concentrations of a commercial finishing agent. The finishing agent is added in different concentrations to the dyeing bath. Some properties of the fabrics are tested after the dyeing process. Hydrophilicity, volumetric resistivity, colour measurement, colour fastness, soil-release and some performance properties (bending strength, crease recovery, air permeability, thickness) are tested respectively.

2.2.1. Disperse dyeing

Disperse dyeing processes containing different concentrations of a finishing agent are carried out with exhaust method. C.I. Disperse Blue 79 dyestuff is used in all dyeing processes. The finishing agent is added to the dyeing bath as 2%, 4% and 6% owf (on the weight of fabric). Disperse dyeing recipes are given in Table 2.

Disperse dyeing baths are prepared according to four different recipes as shown in Table 2. Fabric weights are taken as 10 grams. The pH values of the dyeing solutions are adjusted to 5 with acetic acid. Dyeing processes are carried out for 60 minutes at 130°C. Disperse dyeing processes for all samples are carried out in a laboratory-type dyeing machine (Ataç HT) at 20:1 liquor ratio (Figure 4).



Figure 4. Laboratory-type dyeing machine [13]

Reductive washing processes of samples are carried out with exhaust method after the dyeing process. Reductive washing recipes are prepared with hydrosulphite (2 g/L) and sodium hydroxide (2 g/L). Reductive washing processes are carried out for 20 minutes at 85°C in a laboratory-type dyeing machine (Figure 4) at 20:1 liquor ratio. Samples are neutralized for 10 minutes at 50°C in the neutralizing solution prepared by 1 g/L acetic acid after reductive washing processes.

2.2.2. Hydrophilicity test

Hydrophilicity tests are performed according to TSE 866 [14].

2.2.3. Volumetric resistivity tests

Volumetric resistivity measurements are carried out on the samples through a two-probe method using Keithley 6517B Electrometer/High resistance meter. Keithley 6517B electrometer is a multifunctional electrometer that usually works with low current and high resistance. This electrometer can be controlled through interfacing. Volumetric resistivity tests are performed according to ASTM D257-14 [15]. Test parameters are given in Table 3.

2.2.4. Colour measurement

Colour measurements of fabrics are made using a spectrophotometer (X-Rite Ci 4200UV) according to the CIE Lab system with d/8° measurement geometry and D65 daylight.

2.2.5. Colour fastness tests

Colour fastness tests to rubbing, washing and water are carried out according to TS EN ISO 105-X12, TS EN ISO 105-C06 and TS EN ISO 105-E01 respectively [16-18].

2.2.6. Soil-release tests

Soil-release tests are performed according to ASTM D4265 [19]. Firstly samples are contaminated with standard soils as seen in Table 4.

White circles 2,5 cm in diameter are drawn on the fabrics. Drawn areas are contaminated with the standard soils (Figure 5).

Table 2. Dyeing recipes

Dyeing Recipes	Reference	2% finishing agent	4% finishing agent	6% finishing agent
Weight of fabric (g)	10	10	10	10
Liquor ratio	1:20	1:20	1:20	1:20
Finishing agent (%) (Reapret SR)	0	2	4	6
Disperse dyestuff (%)	1	1	1	1
Dispergator and pH regulating agent (g/L)	1	1	1	1
Anti-creasing agent (g/L)	1	1	1	1
Wetting agent (g/L)	1	1	1	1

Table 3. Volumetric resistivity test parameters

Pre-discharge (s)	10
Bias voltage (V)	100
Bias time (s)	1
Measure voltage (V)	500
Measure time (s)	60

Table 4. Standard soil types

Soil	Standard Soil Types	Applied Amount (g)
Soil 1	%75 Tomato paste +%25 Pure olive oil	0.5
Soil 2	Mustard sauce	0.5
Soil 3	Ink	0.056

**Figure 5.** Samples contaminated with soil 2 (mustard sauce)

Soils transferred onto fabric samples are kept for 10 minutes under standard atmospheric conditions. Samples are washed 5 minutes under tap water at 29° dH hardness and left to dry at room temperature. Colour measurements of the samples are made with a spectrophotometer and the colour differences between the samples after and before soil-release tests are obtained.

2.2.7. Fabric performance test

Bending strength, crease recovery, air permeability and thickness tests are performed according to TS 1409, TS 390 EN 22313, TS 391 EN ISO 9237 and TS 7128 EN ISO 5084 respectively [20-23].

3. RESULTS AND DISCUSSION

3.1 Hydrophilicity Test Results

Hydrophilicity is the duration of absorbed drops by the fabric dropped onto the fabric. Hydrophilicity test results

are given in Table 5. The hydrophilicity values given for each sample are the average value of 10 measurements.

As seen in Table 5, the hydrophilicity value of the reference sample (dyed without the finishing agent) is found as 5.87 seconds. It can be said that the addition of the finishing agent to the dyeing bath has improved the hydrophilicity of the fabric. 71%, 86%, 90% better hydrophilicity obtained than the reference sample respectively with the addition of 2%, 4% and 6% finishing agent to the dyeing bath. Test results are analyzed using version 25 of IBM SPSS Statistics.

The compliance of the data to the normal distribution is tested with Kolmogorov-Smirnov and Shapiro-Wilk. Test results are given in Table 6.

Table 5. Hydrophilicity test results

Samples	Hydrophilicity (s)
Reference	5.87
2% finishing agent	1.70
4% finishing agent	0.80
6% finishing agent	0.53

Table 6. Kolmogorov-smirnov and shapiro-wilk test results of hydrophilicity values

Sample Code	Kolmogorov-Smirnov ^a			Shapiro-Wilk		
	Statistic	df	Sig.	Statistic	df	Sig.
Reference	.375	10	.000	.682	10	.001
2% finishing agent	.285	10	.021	.757	10	.004
4% finishing agent	.213	10	.200*	.920	10	.354
6% finishing agent	.154	10	.200*	.935	10	.494

*. This is a lower bound of the true significance.

a. Lilliefors Significance Correction

Since some data groups don't conform to a normal distribution and the number of samples is insufficient, a non-parametric test is used. Kruskal Wallis k-independent sample test is a nonparametric test that evaluates whether more than two groups are different from each other. It is used to reveal the difference between the groups with different concentrations (reference, 2% finishing agent, 4% finishing agent and 6% finishing agent) and the following hypothesis are established.

H₀: There is no difference between the groups that are treated with different concentrations of finishing agent

H₁: There is a difference between the groups that are treated with different concentrations of finishing agent

Kruskal Wallis test results of hydrophilicity are given in Table 7.

It is seen that comparison of groups treated with different concentrations of finishing agents in terms of hydrophilicity in Table 7. A statistically significant difference is found between the groups in terms of hydrophilicity values ($p < 0.05$). Mann-Whitney U test is used for the pairwise comparison of groups (Table 8). According to Table 8,

there is a difference in pairwise comparison between groups treated with different concentrations of finishing agents.

3.2. Volumetric Resistivity Test Results

Volumetric resistivity test results are given in Table 9. The volumetric resistivity value given for each sample is the average value of 4 measurements.

As seen in Table 9, the group dyed with 6% finishing agent has the lowest volumetric resistivity. The increase in concentration has reduced the surface resistivity, in other words, has increased the conductivity. However, we can say that the fabric is still insulating since it does not fall below the value of 5×10^{10} .

3.3. Colour Measurement Results

Colour measurements of fabrics are made using a spectrophotometer (X-Rite Ci 4200UV) according to the CIE Lab system with $d/8^\circ$ measurement geometry and D65 daylight. The L, a, b, ΔE values obtained for each sample are the average values of 3 measurements taken on the same fabric sample. Colour measurement results are given in Table 10.

Table 7. Kruskal Wallis test results of hydrophilicity values

Sample Code	n	p	χ^2
Reference	10	0.000	28.561
2% finishing agent	10		
4% finishing agent	10		
6% finishing agent	10		

Table 8. Mann-Whitney U test results of hydrophilicity values

Sample Code	p	Mann-Whitney U	Wilcoxon W
Reference-2% finishing agent	0.049	24.000	79.000
Reference-4% finishing agent	0.000	2.000	57.000
Reference-6% finishing agent	0.000	0.000	55.000
2% finishing agent-4% finishing agent	0.029	21.000	76.000
2% finishing agent-6% finishing agent	0.000	1.500	56.500
4% finishing agent-6% finishing agent	0.001	8.000	63.000

Table 9. Volumetric resistivity test results

Samples	Volumetric Resistivity (ohm.cm)
Reference	363×10^{11}
2% finishing agent	67.2×10^{11}
4% finishing agent	11.8×10^{11}
6% finishing agent	2.18×10^{11}

Table 10. Colour measurement test results

Sample Code	L*	a*	b*	C*	h	ΔE^*	K/S
Reference	26.20	0.95	-19.34	19.36	272.82		
2% finishing agent	25.80	1.37	-18.94	18.99	274.14	0.58	102.20
4% finishing agent	25.84	1.09	-19.48	19.51	273.20	0.29	102.94
6% finishing agent	24.76	1.62	-18.13	18.20	275.10	1.44	111.30

Colour differences between the group dyed with 2% finishing agent, the group dyed with 4% finishing agent, the group dyed with 6% finishing agent and the reference group is calculated as 0.58, 0.29 and 1.44 respectively. These colour differences are within acceptable limits for production in the textile industry. As the finishing agent concentration has increased, the colour strength (K/S) values have increased, as expected.

3.4. Colour Fastness Test Results

Colour fastness tests to washing and water are carried out using the relevant standards. Here, colour change on the fabric and colour staining on the multifiber fabric (acetate, cotton, polyamide, polyester, acrylic and wool) are investigated. Test results are given in Table 11.

Colour change values for all samples is found as 5 levels. In other words, no change is observed in the colour of the samples after colour fastness tests to washing and water. When the values of colour staining on the multifiber is examined, it is observed that the values are generally at the level of 4/5 and 5. It can be said that the highest colour staining value is to wool fibre.

Colour fastness to rubbing tests is made in two ways, dry and wet. Colour fastness test results to rubbing are given in Table 12.

As seen in Table 15, the colour staining values in the weft and warp directions are 5 levels for all samples in the dry rubbing fastness test. When the wet rubbing fastness test results is examined, it is seen that the fastness values of all samples are at the level of 4/5. As expected, the wet rubbing fastness values of the fabrics are slightly lower than the dry rub fastness values. As a result, it can be said that the increase in finishing agent does not affect the colour fastness of the fabrics.

3.5. Soil-Release Test Results

Soil-release tests are performed according to ASTM D4265. Colour measurements of the samples are made with a spectrophotometer after soil release treatment with soil 1, soil 2 and soil 3 to observe changes in colours of the fabrics. The L, a, b, ΔE values for each sample are the average values of 3 measurements taken on the same fabric (Table 13).

Table 11. Colour fastness test results to washing and water

Fastness	Colour fastness to washing				Colour fastness to water			
	Referenc e	2% finishing agent	4% finishing agent	6% finishing agent	Referenc e	2% finishing agent	4% finishing agent	6% finishing agent
Colour change	5	5	5	5	5	5	5	5
Colour staining								
-Acetate	5	5	5	5	5	5	5	5
-Cotton	5	5	5	5	5	5	5	5
-Polyamide	5	5	5	5	5	5	5	5
-Polyester	5	4/5	4/5	4/5	5	5	5	5
-Acrylic	5	5	5	5	5	5	5	5
-Wool	4/5	4/5	4/5	4/5	5	4/5	4/5	4/5

Table 12. Colour fastness to rubbing

Sample Code	Colour staining			
	Dry		Wet	
	Warp	Weft	Warp	Weft
Reference	5	5	4/5	4/5
2% finishing agent	5	5	4/5	4/5
4% finishing agent	5	5	4/5	4/5
6% finishing agent	5	5	4/5	4/5

Table 13. Colour measurement test results after soil-release treatment

Soil Type	Sample Code	L	a	b	ΔE^*
Soil 1	Reference	21.70	1.10	-12.50	
	2% finishing agent	22.50	1.08	-15.09	2.71
	4% finishing agent	23.51	0.83	-16.26	1.57
	6% finishing agent	23.65	1.14	-18.67	2.43
Soil 2	Reference	23.39	1.17	-19.16	
	2% finishing agent	22.67	1.30	-18.57	0.94
	4% finishing agent	22.43	1.54	-19.45	0.94
	6% finishing agent	24.45	1.03	-19.57	2.09
Soil 3	Reference	23.45	3.94	-18.68	
	2% finishing agent	24.85	2.72	-19.96	2.26
	4% finishing agent	25.74	2.61	-20.53	1.06
	6% finishing agent	24.79	2.44	-20.50	0.97

The group dyed with 4% finishing agent also have the lowest colour difference after the soil release test which is done with soil 1 (%75 Tomato paste +%25 Pure olive oil). The group dyed with 2% finishing agent and the group dyed with 4% finishing agent have the lowest and acceptable colour difference values after the soil release test which is done with soil 2 (mustard). It can be said that 2% finishing agent impregnation is enough to get soil release effect for mustard. As the concentration of the finishing agent has increased, the colour difference has decreased. The minimum colour difference with the reference group is observed in the sample which added 6% finishing agent to dyeing bath for soil 3.

3.6. Fabric Performance Test Results

Fabrics are evaluated concerning bending strength, crease recovery, air permeability and thickness. The bending strength value for each sample is a value calculated with these data obtained by measuring the droop lengths of 16 samples in the warp and weft directions. The crease recovery value for each sample is the average value of the measurement obtained from 10 samples in the warp and weft directions. Air permeability and thickness values represent the average value of 5 measurements for each sample. Fabric performance test results are given in Table 14.

Bending strength is the degree of deviation from the horizontal axis of the fabric with its weight. When the bending strength of fabric increases, stiffness of fabric also

increases but drape and softness of fabric decrease. As seen in Table 14, the reference sample has the highest bending strength. As the concentration of the finishing agent has increased, the bending strength has decreased and softness has increased. Crease recovery angle can be defined as the ability to revert fabric folded for a certain period under a given force. The high crease recovery angle means that the wrinkle properties of the fabric are good. Generally, it can be said that increased finishing agent concentration increased the crease recovery angles of the samples compared with the reference sample. It means that the addition of a finishing agent to the dyeing bath has improved the crease recovery property of the fabrics. Air permeability expresses the passing ability of air through fibers and yarns constituent of a fabric [24]. Air permeability is calculated as the time required for a certain volume of air to pass through the fabric. High air permeability values mean deterioration of the air permeability property of the fabric. As seen in Table 14, a certain volume of air has passed through the reference sample in the lowest time. It is observed that this sample has had the lowest thickness and the best air permeability. As the concentration of the finishing agent has increased, the thickness of the samples has increased and has deteriorated the air permeability of the samples slightly.

The compliance of the data to the normal distribution is tested with Kolmogorov-Smirnov and Shapiro-Wilk tests. Tests of normality of fabric performance test results are given in Table 15.

Table 14. Fabric performance test results

Samples	Bending Strength (mg.cm)	Crease Recovery Angle (°)	Air Permeability (s)	Thickness (mm)
Reference	28.92	139.50	144.80	0.31
2% finishing agent	26.73	136.35	154.20	0.32
4% finishing agent	25.93	141.00	156.40	0.32
6% finishing agent	16.16	144.55	172.80	0.33

Table 15. Kolmogorov-smirnov and shapiro-wilk test results of fabric performance values

Test Results	Sample Code	Kolmogorov-Smirnov ^a			Shapiro-Wilk		
		Statistic	df	Sig.	Statistic	df	Sig.
Bending Length (Weft Direction)	Reference	.194	16	.109	.902	16	.085
	2% finishing agent	.169	16	.200*	.947	16	.438
	4% finishing agent	.217	16	.043	.873	16	.031
	6% finishing agent	.269	16	.003	.725	16	.000
Bending Length (Warp Direction)	Reference	.137	16	.200	.960	16	.659
	2% finishing agent	.174	16	.200	.934	16	.287
	4% finishing agent	.259	16	.005	.898	16	.075
	6% finishing agent	.274	16	.002	.671	16	.000
Crease Recovery (Weft Direction)	Reference	.217	10	.200*	.931	10	.458
	2% finishing agent	.205	10	.200*	.881	10	.133
	4% finishing agent	.209	10	.200*	.922	10	.376
	6% finishing agent	.191	10	.200*	.865	10	.088
Crease Recovery (Warp Direction)	Reference	.274	10	.032	.785	10	.010
	2% finishing agent	.208	10	.200*	.941	10	.567
	4% finishing agent	.132	10	.200*	.965	10	.843
	6% finishing agent	.120	10	.200*	.968	10	.869
Air Permeability	Reference	.347	5	.048	.857	5	.217
	2% finishing agent	.249	5	.200*	.844	5	.177
	4% finishing agent	.252	5	.200*	.943	5	.685
	6% finishing agent	.294	5	.183	.822	5	.121
Thickness	Reference	.300	5	.161	.833	5	.146
	2% finishing agent	.243	5	.200*	.894	5	.377
	4% finishing agent	.300	5	.161	.833	5	.146
	6% finishing agent	.246	5	.200*	.956	5	.777

When Table 15 is examined, it is seen that some data groups aren't distributed normally. Since there are groups with an abnormal distribution within the groups and the number of samples is insufficient, it is deemed appropriate to perform the Kruskal Wallis test among non-parametric tests. Bending length and crease recovery values are used in statistical analysis in warp and weft directions. The following hypothesis are established.

H₀: There is no difference between the groups that are treated with different concentrations of finishing agent

H₁: There is a difference between the groups that are treated with different concentrations of finishing agent

Kruskal Wallis test results are given in Table 16.

It is seen that comparison of groups treated with different concentrations of the finishing agent in Table 16. A

statistically significant difference isn't found between the groups (the reference group, the group dyed with 2% finishing agent, the group dyed with 4% finishing agent and the group dyed with 6% finishing agent) in terms of the bending length values (weft direction) ($p = 0.137 > 0.05$) and the thickness values ($p = 0.177 > 0.05$). A statistically significant difference is found between the groups for the other fabric performance values, such as the air permeability values ($p = 0.016 < 0.05$).

Mann-Whitney U test is used for the pairwise comparison of groups (Table 17). According to Table 20, there is a significant difference in pairwise comparison between groups (especially the group dyed with 4% finishing agent and the group dyed with 6% finishing agent).

Table 16. Kruskal Wallis test results of fabric performance values

	Sample Code	N	p	x ²
Bending Length (Weft Direction)	Reference	16	0.137	5.535
	2% finishing agent	16		
	4% finishing agent	16		
	6% finishing agent	16		
Bending Length (Warp Direction)	Reference	16	0.000	29.006
	2% finishing agent	16		
	4% finishing agent	16		
	6% finishing agent	16		
Crease Recovery (Weft Direction)	Reference	10	0.009	11.557
	2% finishing agent	10		
	4% finishing agent	10		
	6% finishing agent	10		
Crease Recovery (Warp Direction)	Reference	10	0.005	12.688
	2% finishing agent	10		
	4% finishing agent	10		
	6% finishing agent	10		
Air Permeability	Reference	5	0.016	10.371
	2% finishing agent	5		
	4% finishing agent	5		
	6% finishing agent	5		
Thickness	Reference	5	0.177	4.926
	2% finishing agent	5		
	4% finishing agent	5		
	6% finishing agent	5		

Table 17. Mann-Whitney U test results of fabric performance values

	Sample Code	p	Mann-Whitney U	Wilcoxon W
Bending Length (Warp Direction)	Reference-2% finishing agent	0.423	106.500	242.500
	Reference-4% finishing agent	0.128	87.000	223.000
	Reference-6% finishing agent	0.000	14.500	150.500
	2% finishing agent-4% finishing agent	0.445	107.500	243.500
	2% finishing agent-6% finishing agent	0.000	16.000	152.000
	4% finishing agent-6% finishing agent	0.000	16.000	152.000
Crease Recovery (Weft Direction)	Reference-2% finishing agent	0.190	32.000	87.000
	Reference-4% finishing agent	0.009	16.500	71.500
	Reference-6% finishing agent	0.001	9.500	64.500
	2% finishing agent-4% finishing agent	0.853	47.500	102.500
	2% finishing agent-6% finishing agent	0.190	32.000	87.000
	4% finishing agent-6% finishing agent	0.052	24.000	79.000
Crease Recovery (Warp Direction)	Reference-2% finishing agent	0.023	20.000	75.000
	Reference-4% finishing agent	0.029	21.500	76.500
	Reference-6% finishing agent	0.393	38.500	93.500
	2% finishing agent-4% finishing agent	0.035	22.500	77.500
	2% finishing agent-6% finishing agent	0.007	15.000	70.000
	4% finishing agent-6% finishing agent	0.023	20.000	75.000
Air Permeability	Reference-2% finishing agent	0.69	10.500	25.500
	Reference-4% finishing agent	0.056	3.00	18.000
	Reference-6% finishing agent	0.008	0.000	15.000
	2% finishing agent-4% finishing agent	0.421	8.500	23.500
	2% finishing agent-6% finishing agent	0.095	4.000	19.000
	4% finishing agent-6% finishing agent	0.008	0.000	15.000

4. CONCLUSION

In this study, simultaneous dyeing and finishing processes of 100% polyester fabrics are carried out in one bath using exhaust method. A commercial finishing agent is added with different ratios (2%, 4% and 6% owf) in the dyeing bath. Fabrics are evaluated concerning hydrophilicity, volumetric resistivity, colour measurement, colour fastness, soil-releasing test and fabric performance tests like bending strength, crease recovery, air permeability and thickness. Test results are analyzed by Kruskal Wallis test using version 25 of IBM SPSS Statistics. Mann-Whitney U test is used for the pairwise comparison of groups.

The hydrophilicity value of the reference sample (dyed without a finishing agent) is found as 5.87 seconds. It can be said that the addition of a finishing agent to the dyeing bath is improved the hydrophilicity property of the fabric. 71%, 86%, 90% better hydrophilicity is obtained than the reference sample respectively with the addition of 2%, 4% and 6% finishing agent. It is concluded that samples dyed with 6%, 4% and 2% finishing agents are statistically different from each other in terms of hydrophilicity. Samples dyed with 6% finishing agent has the lowest volumetric resistivity value. The increase in the concentration of the finishing agent has decreased the surface resistance, in other words, it has increased the conductivity.

Colour differences between the group dyed with 2% finishing agent, the group dyed with 4% finishing agent, the group dyed with 6% finishing agent and the reference sample are calculated as 0.58, 0.29 and 1.44 respectively. These colour differences are within acceptable limits for production in the textile industry. As the finishing agent concentration has increased, the colour strength (K/S) values have increased, as expected. No change is observed in the colour of the samples after colour fastness tests to washing and water. When the values of colour staining on the multifiber is examined, it is observed that the values are generally at the level of 4/5 and 5. Colour staining values in the weft and warp directions are found to be at the level of 5 for all samples in the dry rubbing fastness test. When the wet rubbing fastness test results are examined, it is seen that the fastness values of all samples are at the level of 4/5. It can be said that the increase in finishing agent concentration has not affected the colour fastness of the fabric.

The group dyed with 4% finishing agent also has the lowest colour difference after the soil release test which is done with soil 1 (%75 Tomato paste +%25 Pure olive oil). The group dyed with 2% finishing agent and the group dyed with 4% finishing agent have the lowest and acceptable colour difference values after the soil release test which is done with soil 2 (mustard). It can be said that 2% finishing agent impregnation is enough to get soil release effect for mustard. As the concentration of the finishing agent has increased, the colour difference has increased. The minimum colour difference with the reference sample is observed in the sample which added 6% finishing agent to dyeing bath for soil 3.

When the fabric performance properties are examined, the reference sample has the highest bending strength. As the concentration of the finishing agent has increased, the bending strength has decreased so that the softness of the samples has increased. Generally, it can be said that increased finishing agent concentration has increased the crease recovery angles of the samples compared with the reference sample. It means that the addition of a finishing agent to the dyeing bath is improved the crease recovery property of the fabrics. When air permeability values are examined, a certain volume of air has passed through the reference sample in the shortest time. As the concentration of the finishing agent has increased, the air permeability of the fabrics has decreased and the thickness values have increased.

The finishing agent gives softness, slipperiness, anti-static and dirt/stain resistant and hydrophilic properties to the polyester fabric. The addition of a finishing agent to the dyeing bath has no effect on the colour fastness of the fabrics. The difference in colour values with finishing agent application is within the acceptable range. The addition of a finishing agent to the dyeing bath has improved the soil-release properties of the fabrics. When the fabric performance properties are examined, the addition of a finishing agent to the dyeing bath improves crease recovery and bending strength properties of the fabrics.

Future Works: Similar to this study, the results can be compared by making a similar application in fibre and yarn form. It can be observed how the performance properties of the fabric are affected by trying different finishing processes after dyeing. It can be compared by applying chemicals produced by different manufacturers for similar purposes.

REFERENCES

1. Özen İ. 2013. Effects of pre- and intermediate causticisation on pattern formation and fastness properties of three- and two-bath dyeings of woven polyester/cationic dyeable polyester/rayon fabrics. *Textile and Apparel* 23(4), 369-373.
2. İbrahim NA, Youssef MA, Helal MH, Shaaban MF. 2003. Exhaust dyeing of polyester - based textiles using high - temperature-alkaline conditions. *Journal of Applied Polymer Science* 89(13), 3563-3573.
3. Dong Y, Wang J, Liu P. 2001. Dyeing and finishing of cotton fabric in a single bath with reactive dyes and citric acid. *Coloration Technology* 117(5), 262-265.
4. Aspland JR. 1992. Disperse dyes and their application to polyester. *Textile Chemist and Colorist* 24(18), 18.
5. Leaver AT, Glover B, Leadbetter PW. 1992. Recent advances in disperse dye development and applications. *Textile Chemist and Colorist* 24(1), 18.
6. Ristić N, Jovančić P, Canal C, Jocić D. 2009. One-bath one-dye class dyeing of PES/cotton blends after corona and chitosan treatment. *Fibers and Polymers* 10(4), 466-475.
7. Najafi H, Assefipour R, Hajilari M, Movahed HR. 2009. One bath method dyeing of polyester/cotton blend fabric with sulphatoethylsulphonyl disperse/reactive dyes treatment by chitin biopolymer. *African Journal of Biotechnology* 8(6), 1127.
8. Maeda S, Kunitou K, Hihara T, Mishima K. 2004. One-bath dyeing of polyester/cotton blends with reactive disperse dyes in supercritical carbon dioxide. *Textile Research Journal* 74(11), 989-994.
9. Afifi TH, Sayed AZ. 1997. One-bath dyeing of polyester/wool blend with disperse dyes. *Journal of the Society of Dyers and Colourists* 113(9), 256-258.
10. Fan L, Tan Y, Amesimeku J, Yin Y, Wang C. 2020. A novel functional disperse dye doped with graphene oxide for improving antistatic properties of polyester fabric using one-bath dyeing method. *Textile Research Journal* 90(5-6), 655-665.
11. Cao J, Meng C, Cheng X, Pan X. 2018. Surface alkali deweighting and dyeing of polyester fabric by one-bath and one-step process. *Surface Innovations* 7(2), 104-111.
12. Touhid SSB, Shawon MRK, Deb H, Khoso NA, Ahmed A, Fu F, Liu XD. 2020. Nature inspired rGO-TiO₂ micro-flowers on polyester fabric using semicontinuous dyeing method: A binder-free approach towards durable antibacterial performance. *Synthetic Metals* 261, 116298.
13. "Laboratory-type dyeing machine", <https://www.atacmakina.com.tr/>, accessed 10 may 2020.
14. TS 866:1985. Absorbency of bleached cotton textile materials, Turkish Standards Institution, <https://en.tse.org.tr>.
15. ASTM D257-14. Standard test methods for dc resistance or conductance of insulating materials, ASTM International, <https://www.astm.org>.
16. TS EN ISO 105-X12. Textiles - Tests for colour fastness - Part X12: Colour fastness to rubbing, Turkish Standards Institution, <https://en.tse.org.tr>.
17. TS EN ISO 105-C06. Textiles - Tests for colour fastness - Part C06: Colour fastness to domestic and commercial laundering, Turkish Standards Institution, <https://en.tse.org.tr>.
18. TS EN ISO 105-E01. Textiles - Tests for colour fastness - Part E01: Colour fastness to water, Turkish Standards Institution, <https://en.tse.org.tr>.
19. ASTM D4265-14. Standard guide for evaluating stain removal performance in home laundering, ASTM International, <https://www.astm.org>.
20. TS 1409: 1973. Stiffness determination of woven textiles, Turkish Standards Institution, <https://en.tse.org.tr>.
21. TS 390 EN 22313: 1996. Textile fabrics -Determination of the recovery from creasing of a horizontally folded specimen by measuring the angle of recovery, Turkish Standards Institution, <https://en.tse.org.tr>.
22. TS 391 EN ISO 9237: 1999. Textiles - Determination of permeability of fabrics to air, Turkish Standards Institution, <https://en.tse.org.tr>.
23. TS 7128 EN ISO 5084: 1998. Textiles-Determination of thickness of textiles and textile products, Turkish Standards Institution, <https://en.tse.org.tr>.
24. Gülşen G, Ala DM. 2015, June. An investigation about relation between comfort features and selected structural parameters of knitted fabrics. 15th Autex World Textile Conference, 10-12 June, Bucharest, Romania.



A New Objective Method for Comfort Assessment of Sportswear Knitted Fabrics

Esin Babalık¹  0000-0001-5775-1524

Sinem Güneşoğlu²  0000-0002-8270-6546

Burçin Ütebay³  0000-0002-1551-2450

Ayşegül Çetmeli³  0000-0003-1267-7310

Cem Güneşoğlu⁴  0000-0002-8796-9679

¹Adiyaman University, Besni Vocational School, Adiyaman, Turkey

²Gaziantep University, Technical Vocational School, Gaziantepi Turkey

³Uniteks R&D Center, İzmir, Turkey

⁴Gaziantep University, Textile Engineering Department, Gaziantep

ABSTRACT

The aim of this study is to develop a new approach for objective comfort assessment of knitted fabrics used in sportswear industry. The method is based on measurement of various mechanical and heat / mass transfer properties and converting the test results into the axis values to draw multi-axial graphics. The graphic area is used to calculate unitless Total Comfort Value (TCV); the higher the TCV the higher the clothing comfort performance the fabric has.

1. INTRODUCTION

Clothing comfort which influences buyers' choices is complex effect of mechanical and heat/moisture transfer properties of fabrics and garments. As described before, heat/moisture transfer properties of fabrics could be primarily listed as air permeability, water vapor permeability, moisture management and thermal conductivity [1-3] and they are used to assess the thermal comfort; whereas mechanical properties could be described variously as tactile, low-stress, appearance, and durability consisting abrasion resistance, pilling tendency, and wrinkle recovery; used to assess the mechanical comfort [4-8]. There have been various attempts to obtain "comfort indexes" by the objective measurements of those properties since textile industry lacks objective approaches for determining level of comfort and objective measurements of fabric properties allow close prediction of observed comfort [8,9].

This paper introduces a new method using multi-axial graphics to assess the comfort properties of knitted fabrics used in sportswear clothing. The method used the test results of various mechanical and heat /moisture transfer properties. The results were converted to multi-axial graphics for mechanical and heat/moisture transfer properties separately, and the calculated graphic areas (unitless numerical values) were used in comfort index calculation which is named as *Total Comfort Value* (TCV). The higher the TCV, the higher clothing comfort performance the fabric has. The study led to compare clothing comfort of different types of fabrics and the reliability has been confirmed by subjective wear trials.

ARTICLE HISTORY

Received: 10.02.2021

Accepted: 15.09.2021

KEYWORDS

Knitted fabric, clothing comfort, multi-axial graphic

To cite this article: Babalık E, Güneşoğlu S, Ütebay B, Çetmeli A, Güneşoğlu C. 2021. A new objective method for comfort assessment of sportswear knitted fabrics. *Tekstil ve Konfeksiyon*, 31(4), 318-328.

2. MATERIAL AND METHOD

2.1 Material

Knitted fabrics were prepared using ring spun cotton (Ne 20/1, Ne 30/1, Ne 40/1), staple polyester (Ne 20/1, Ne 30/1, Ne 40/1) and polypropylene filament (140/72 Denier, 180/72 Denier, 280/72 Denier) yarns. The constructional parameters including yarn arrangements and stitch diagrams are given in Table 1 and 2. All samples were produced on separate circular knitting machines with 22 gauge and 32 " diameter for single jersey, 22 gauge and 34 " diameter for cross miss, 18 gauge and 34 " diameter for double-face and 16 gauge and 34 " diameter for stitch transferred knits. The samples were subjected to pretreatment including scouring and rinsing in an uncontrolled industry environment.

2.2 Method

Since many studies related mechanical comfort to different fabric properties which influence formability of fabric, aesthetic appeal, flexibility, wearer's dynamic movements, well-being using the product, visual and tactile quality we used the following properties to assess the mechanical comfort which are also in accordance with earlier studies [4,6,9-11]: the fabric weight and thickness, the wrinkle recovery, the spirality, the bursting behavior, the pilling tendency and the fabric extension under stress (fabric growth). Considering heat / moisture transfer performance we used the followings: capability of the fabric to manage the transport of liquid moisture, water vapor permeability, air permeability, thermal conductivity and thermal absorbtivity; all of were described in details elsewhere [12-15]. Table 3 shows the mechanical and heat / mass transfer properties measurements taken from the samples with the relevant standards at a glance. All the measurements were completed in the standard laboratory climatic conditions and run for five times.

2.2.1. Multi-axial graphics

The tests were used as the axis and before converting the test results to graphics, we have made following assumptions:

1. For mechanical comfort: The lower fabric density (the combination of lower fabric weight and higher thickness) would led to better comfort. The higher wrinkle recovery and fabric growth was related to flexibility; thus related to better comfort. The higher bursting strength and distension, the lower pilling tendency, spirality and dimensional change after laundry were as matter of appearance and quality, thus they were related to better mechanical comfort.

2. For thermal comfort: The higher air permeability, the better transport of liquid moisture, the higher water vapor

permeability, the higher thermal conductivity and thermal absorbtivity would give better thermal comfort.

3. All parameters had same contribution on comfort, so any weighting factor is not used

The test results were at different scales so some of them were converted to the same scale (between 0.1 – 10) by using different coefficients prior using as axis value to make them have similar contributions on graph areas: Bursting strength results were divided by 100, bursting distension by 10, air permeability by 200, relative water vapor permeability by 10, thermal conductivity by 10, thermal absorbtivity by 20 and overall moisture management capability values were multiplied by 10.

The pilling and wrinkle recovery rating scores were used as axis value; if the score was an intermediate value like 2-3, it was used as number with a half, like 2,5.

The reciprocal of the fabric density values were used as axis value. This not only led to convert the value to the mentioned scale but also to associate the low fabric density with better comfort since the reciprocal of lower fabric density gave higher value and that increased the calculated graph area which was used in comfort value calculation. Similarly, the spirality and the dimensional change testing results were converted to axis value by using following Equation (1):

Axis value for spirality and

$$\text{dimensional change: } \frac{1}{\lceil \text{Test result} \rceil + 0,1} \quad (1)$$

so that 0 as test result was converted to 10 which is the maximum in selected scale; and the lower test results were converted to higher axis values. Then, unitless multi-axial graph area was calculated by Equation (2):

$$\text{Graph area} = \frac{1}{2} * \left(\sum_{1}^n [\text{Axis value } (n-1) * \text{Axis value } n] \right) * \sin((360/n * \pi) / 180) \quad (2)$$

and Total Comfort Value (TCV) was calculated by Equation (3) as offered before [16]:

$$\text{TCV} = \frac{1}{3} C_{\text{mechanical}} + \frac{2}{3} C_{\text{thermal}} \quad (3)$$

where, $C_{\text{mechanical}}$ is the area of multi-axial graphic of mechanical properties (mechanical comfort) and C_{thermal} is the area of multi-axial graphic of heat/mass transfer properties (thermal comfort).

Table 1. Sample plan

Sample Code	Knit type	Face Side		Back side	
		Fiber Combination	Yarn Count	Fiber Combination	Yarn Count
1	Single Jersey	100% PP	140/72 Denier		-
2		100% PES	Ne 20/1		-
3		100% CO	Ne 20/1		-
4		100% PP	180/72 Denier		-
5		100% PES	Ne 30/1		-
6		100% CO	Ne 30/1		-
7		100% PP	280/72 Denier		-
8		100% PES	Ne 40/1		-
9		100% CO	Ne 40/1		-
10		25/75% PP/CO	180/72 Denier / Ne 30/1		-
11		50/50% PP/CO	180/72 Denier / Ne 30/1		-
12		75/25% PP/CO	180/72 Denier / Ne 30/1		-
13		25/75% PES/CO	Ne30/1 Ne 30/1		-
14		50/50% PES/CO	Ne30/1 Ne 30/1		-
15		75/25% PES/CO	Ne30/1 Ne 30/1		-
16	Cross miss	100% PP	180/72 Denier	100% PP	180/72 Denier
17		100% PP	180/72 Denier	100% CO	Ne 30/1
18		100% PP	180/72 Denier	50/50% PP/CO	180/72 Denier / Ne 30/1
19		100% CO	Ne 30/1	100% PP	180/72 Denier
20		100% CO	Ne 30/1	100% CO	Ne 30/1
21		100% CO	Ne 30/1	50/50% PP/CO	180/72 Denier / Ne 30/1
22		50/50% PP/CO	180/72 Denier / Ne 30/1	100% PP	180/72 Denier
23		50/50% PP/CO	180/72 Denier / Ne 30/1	100% CO	Ne 30/1
24		50/50% PP/CO	180/72 Denier / Ne 30/1	50/50% PP/CO	180/72 Denier / Ne 30/1
25		100% PES	Ne 30/1	100% PES	Ne 30/1
26		100% PES	Ne 30/1	100% CO	Ne 30/1
27		100% PES	Ne 30/1	50/50% PES/CO	Ne30/1 / Ne 30/1
28		100% CO	Ne 30/1	100% PES	Ne 30/1
29		100% CO	Ne 30/1	50/50% PES/CO	Ne30/1 / Ne 30/1
30		50/50% PES/CO	Ne30/1 / Ne 30/1	100% PES	Ne 30/1
31		50/50% PES/CO	Ne30/1 / Ne 30/1	100% CO	Ne 30/1
32		50/50% PES/CO	Ne30/1 / Ne 30/1	50/50% PES/CO	Ne30/1 / Ne 30/1
33	Double-Face	100% PP	180/72 Denier	100% PP	180/72 Denier
34		100% PP	180/72 Denier	50/50% PP/CO	180/72 Denier / Ne 30/1
35		100% CO	Ne 30/1	100% PP	180/72 Denier
36		50/50% PP/CO	180/72 Denier / Ne 30/1	100% CO	Ne 30/1
37		50/50% PP/CO	180/72 Denier / Ne 30/1	50/50% PP/CO	180/72 Denier / Ne 30/1
38		100% PES	Ne 30/1	100% PES	Ne 30/1
39		100% PES	Ne 30/1	50/50% PES/CO	180/72 Denier / Ne 30/1
40		100% CO	Ne 30/1	100% PES	Ne 30/1
41		100% CO	Ne 30/1	100% CO	Ne 30/1
42		50/50% PES/CO	Ne30/1 / Ne 30/1	100% CO	Ne 30/1
43		50/50% PES/CO	Ne30/1 / Ne 30/1	50/50% PES/CO	Ne30/1 / Ne 30/1
44	Stitch transferred knit (1 st report)	100% PP	180/72 Denier		-
45		100% PES	Ne 30/1		-
46		100% CO	Ne 30/1		-
47	Stitch transferred knit (2 nd report)	100% PP	180/72 Denier		-
48		100% PES	Ne 30/1		-
49		100% CO	Ne 30/1		-
50	Stitch transferred knit (3 rd report)	100% PP	180/72 Denier		-
51		100% PES	Ne 30/1		-
52		100% CO	Ne 30/1		-

Table 2. Stitch diagrams of the samples

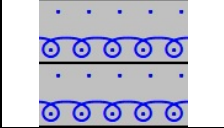
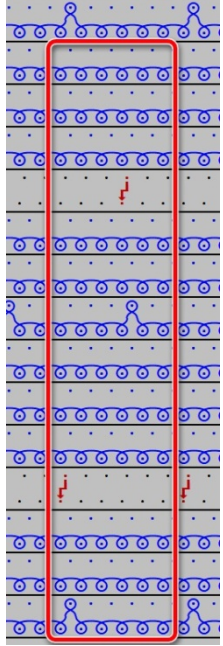
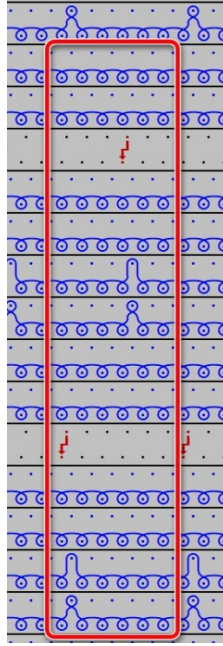
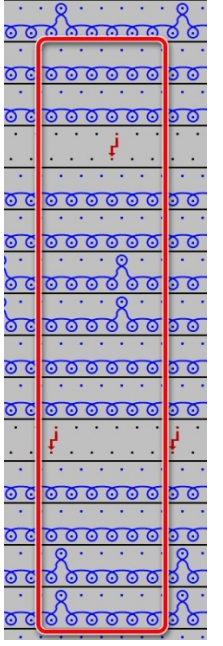
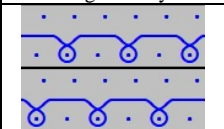
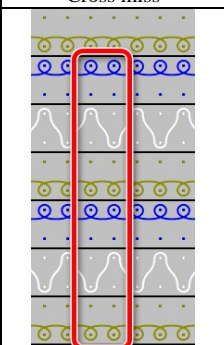
			
			
			
Single Jersey	Stitch transferred knit (1 st report)	Stitch transferred knit (2 nd report)	Stitch transferred knit (3 rd report)
Cross miss			
Double Face			

Table 3. The test and measurements

Mechanical properties (Unit)	Standard / Method
Fabric weight (g/m ²)	TS EN 12127
Fabric thickness (mm)	ISO EN 5084
Fabric density (g/m ³)	Fabric weight / Fabric thickness
Wrinkle recovery (--)	AATCC 128
Spirality (%)	ISO 16322-2
Bursting strength (kPa) and distention (mm)	ISO 13938-2
Fabric growth in wales and courses (%)	ASTM D 2594
Propensity to pilling (--)	ISO 12945-1
Dimensional changes after laundry in wales and courses (%)	AATCC 135
Heat / mass transfer properties	Standard / Method
Air permeability (l/m ² /sec)	ASTM D 737
Overall moisture management capability OMMC (--)	AATCC 195
Thermal conductivity (mW/mK)	The Alambeta instrument standard
Thermal absorbtivity (Ws ^{0.5} / m ⁻² K)	The Alambeta instrument standard
Relative water vapor permeability (%)	The Permetest instrument standard

3. RESULTS AND DISCUSSION

The average of the test results were used at graphics are given in Table 4a, 4b and 5. All the tests gave CV% values lower than 10%.

Table 4a. Mechanical properties of the samples-part 1

Sample Code	Fabric weight (g/m ²)	Fabric thickness (mm)	Fabric density (g/m ³)	Wrinkle recovery (--)	Spirality (%)	Bursting strength (kPa)
1	241,40	0,65	0,37	3,00	0	604,20
2	186,00	0,54	0,34	3,44	0	478,12
3	181,80	0,65	0,28	2,44	0	241,76
4	191,00	0,52	0,37	2,11	0	475,80
5	146,80	0,47	0,31	3,22	0	275,50
6	141,00	0,51	0,28	2,11	0	191,30
7	153,20	0,52	0,29	3,22	0	377,80
8	102,00	0,39	0,26	3,89	0	249,42
9	113,60	0,49	0,23	2,78	0	171,38
10	149,20	0,53	0,24	2,22	4,8	163,96
11	155,20	0,54	0,28	2,78	5,1	201,66
12	169,60	0,54	0,25	3,22	3,5	178,88
13	144,40	0,51	0,29	2,67	0	207,94
14	148,20	0,47	0,26	3,33	0	185,54
15	148,20	0,48	0,32	3,56	0	241,60
16	242,20	0,79	0,24	2,56	4,8	168,54
17	230,60	0,71	0,28	2,00	0	213,40
18	233,60	0,80	0,25	2,44	0	178,14
19	181,40	0,80	0,32	2,33	0	214,52
20	173,80	0,77	0,26	1,67	0	167,50
21	182,60	0,77	0,31	2,11	0	224,60
22	212,40	0,78	0,31	2,67	0	593,66
23	204,60	0,80	0,32	2,89	0	600,44
24	207,40	0,80	0,29	2,44	0	601,92
25	183,80	0,67	0,23	3,44	3,2	205,58
26	176,80	0,72	0,23	3,44	0	188,66
27	177,80	0,72	0,24	3,78	0	206,46
28	171,00	0,67	0,27	2,89	0	224,08
29	173,60	0,71	0,26	2,89	0	206,40
30	179,60	0,75	0,28	3,56	0	362,86
31	178,20	0,72	0,25	3,22	0	367,08
32	175,60	0,71	0,25	3,67	0	360,40
33	395,60	1,22	0,26	3,22	0	188,68
34	368,80	1,23	0,22	3,67	0	189,62
35	335,40	1,12	0,25	3,44	0	191,08
36	312,00	1,07	0,25	2,89	0	211,94
37	327,60	1,19	0,25	3,22	0	213,10
38	279,60	0,99	0,32	4,11	0	596,48
39	278,80	1,00	0,30	4,11	0	453,94
40	284,00	1,16	0,30	3,11	0	422,66
41	269,40	1,06	0,26	3,89	0	241,54
42	272,20	1,03	0,29	3,89	0	213,20
43	270,40	1,10	0,28	3,44	0	274,28
44	127,40	0,56	0,28	3,56	0	463,84
45	196,60	0,85	0,28	3,78	0	355,74
46	189,60	0,85	0,25	2,89	0	324,78
47	122,60	0,64	0,25	3,00	0	233,42
48	194,60	0,89	0,26	3,44	0	317,24
49	198,40	0,95	0,25	3,78	0	237,88
50	125,00	0,66	0,23	3,00	0	328,88
51	206,00	0,79	0,23	3,22	0	419,00
52	194,60	0,88	0,22	3,67	7,6	206,20

Table 4b. Mechanical properties of the samples-part 2

Sample Code	Bursting distention (mm)	Fabric growth in wales (%)	Fabric growth in courses (%)	Pilling tendency (--)	Dimensional changes in wales (%)	Dimensional changes in courses (%)
1	52,68	4,36	2,05	4-5	-0.2	+0.2
2	37,36	1,79	1,03	1-2	+0.6	-0.8
3	40,28	10,26	4,62	3-4	+4.1	-6.7
4	44,22	2,82	2,05	4-5	+0.6	-0.6
5	32,50	1,28	1,28	1-2	+1.8	+1
6	38,86	8,46	2,82	3	+6.2	-12.2
7	51,88	2,82	1,28	4-5	+1	-0.9
8	41,02	1,03	0,77	2	0	-1.9
9	41,40	4,87	1,54	2	+3	-4
10	39,00	8,21	3,33	4-5	+2.4	-9.6
11	30,38	8,46	3,33	4	+2.3	-7.3
12	33,38	4,10	0,51	4	+2.8	-6.8
13	39,28	7,18	1,54	4	+2.8	-5.7
14	36,92	3,85	1,03	4-5	+0.8	-3.5
15	33,80	3,85	2,05	4	+0.4	-3.1
16	37,30	5,38	2,31	2	+3.6	-11.1
17	31,32	6,92	2,05	2-3	+11.7	-8.5
18	29,66	4,10	0,77	2	+3.5	-4
19	30,50	3,59	1,28	2	+2.1	-6
20	32,24	1,28	0,00	2	+1.8	-5.5
21	37,88	0,77	0,00	2	-0.6	-3
22	48,84	5,13	1,03	4-5	0	-0.2
23	45,02	3,85	1,79	4-5	-0.3	-1.5
24	52,44	4,36	0,77	4-5	+0.6	-0.9
25	38,64	7,95	2,82	4	+1.7	-10.1
26	31,94	10,77	2,56	3	+6.9	-12.7
27	29,72	7,95	3,59	4	+4.8	-10.7
28	37,20	4,36	3,33	4	+2.2	-3.8
29	36,24	7,69	1,79	4-5	+1.4	-5.3
30	39,04	3,08	1,03	2	+0.5	-0.4
31	32,76	4,36	0,26	2	+1.3	-1.3
32	33,30	2,56	0,51	1-2	-0.4	-0.9
33	36,14	6,92	2,82	3-4	+8.8	-10.3
34	35,76	9,23	3,08	4	+6.5	-13.7
35	37,00	7,95	3,85	4	+4.9	-10.2
36	35,50	7,18	1,79	2-3	+2.4	-7.7
37	36,36	3,85	1,03	2-3	+3.6	-5.3
38	49,16	4,10	2,31	4-5	+0.7	-0.9
39	45,98	6,41	2,56	2	+2.1	-2.1
40	37,88	5,64	0,77	2-3	+2	-7.1
41	38,10	7,69	3,33	2-3	+7.8	-15.1
42	29,76	7,44	2,31	2-3	+3.6	-9.8
43	39,18	5,13	2,31	2	+3.2	-5.8
44	39,52	2,31	0,00	4-5	-0.9	-1.3
45	40,12	2,05	0,77	2	+1.5	-1.3
46	33,24	4,87	2,05	4-5	+2.7	-4.8
47	36,56	4,87	3,33	2	+3.6	-11
48	36,50	3,08	2,31	2	+0.7	-6.2
49	33,02	0,77	0,26	2	+1.7	-8.6
50	49,06	5,90	3,08	4-5	+1.9	-2.1
51	43,02	1,54	0,51	2-3	-1.1	-2.6
52	39,46	4,87	2,56	3-4	+7.3	-14.6

Table 5. Heat / mass transfer properties of the samples

Sample Code	Air permeability (l/m ² /sec)	OMMC (--)	Thermal conductivity (mW/mK)	Thermal absorbtivity (Ws ^{0.5} / m ² K)	Relative water vapor permeability (%)
1	421,80	0,5790	32,36	160,24	54,90
2	1106,00	0,4630	29,12	105,14	57,29
3	383,00	0,2684	32,48	113,48	53,44
4	507,00	0,6344	29,66	141,12	55,07
5	1374,00	0,4725	28,28	97,72	54,45
6	356,20	0,6392	28,16	112,76	65,79
7	961,40	0,2681	29,24	122,20	74,88
8	2042,00	0,4003	24,16	94,70	74,57
9	941,20	0,2949	29,40	93,06	67,10
10	1048,00	0,4202	24,52	131,34	68,45
11	668,40	0,6235	25,10	138,32	66,21
12	1437,50	0,6445	26,12	138,94	67,54
13	611,00	0,4566	23,50	130,96	61,30
14	1096,00	0,6251	22,80	123,28	65,70
15	620,00	0,8692	22,48	124,74	62,11
16	1474,00	0,3101	32,90	132,30	67,64
17	583,00	0,4936	33,14	135,14	65,70
18	1672,00	0,3171	34,48	138,62	67,11
19	821,80	0,4395	30,98	115,02	63,58
20	2294,00	0,8146	31,58	116,08	66,50
21	1136,00	0,2402	31,34	120,08	65,49
22	222,40	0,4514	32,98	138,34	58,78
23	331,80	0,5911	33,42	124,30	58,16
24	267,60	0,4978	36,88	109,22	60,69
25	322,00	0,4716	31,86	110,40	59,86
26	402,40	0,6002	33,40	108,94	62,43
27	369,00	0,7075	28,14	105,50	63,36
28	271,20	0,6057	27,76	119,86	59,02
29	361,40	0,3876	34,92	117,00	58,70
30	1021,20	0,3063	35,36	107,94	62,51
31	864,40	0,7784	30,70	110,56	59,24
32	1016,20	0,2034	35,02	111,62	61,52
33	591,40	0,1517	53,34	156,42	66,14
34	387,40	0,7455	46,82	160,72	68,86
35	456,80	0,7558	48,74	148,86	68,34
36	639,60	0,1891	44,24	152,18	64,02
37	701,80	0,7081	44,94	148,58	67,71
38	339,00	0,7559	38,42	126,38	53,77
39	372,40	0,6742	38,80	117,98	54,03
40	483,60	0,6907	39,38	118,90	54,63
41	619,00	0,6686	39,92	124,38	53,16
42	970,60	0,7732	38,32	115,38	53,75
43	537,40	0,7098	40,70	137,60	53,23
44	1042,40	0,6741	29,50	109,46	56,66
45	968,20	0,7582	34,94	111,18	56,58
46	712,60	0,7500	39,06	125,90	53,65
47	859,40	0,2897	27,80	113,84	57,37
48	1048,00	0,6708	35,20	107,70	54,20
49	927,80	0,6175	27,56	119,60	55,96
50	1972,00	0,0456	29,02	107,58	68,78
51	2167,60	0,7756	34,88	107,60	62,21

The multi-axial graphics are given in Figure 1-4; calculated graphic areas and TCV of the samples are given in Table 6.

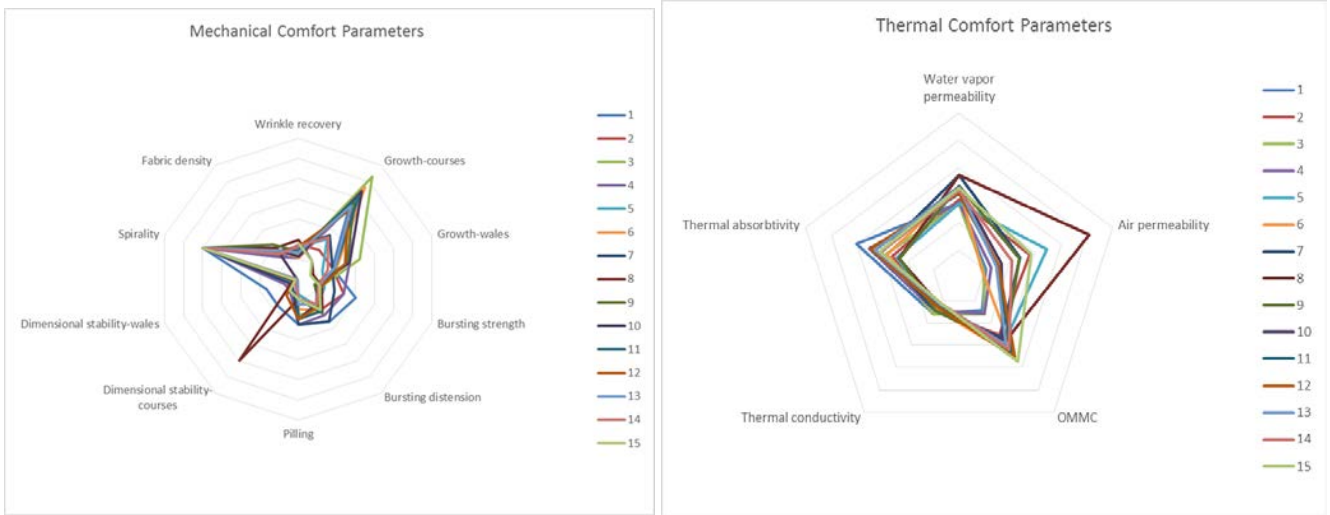


Figure 1. Multi-axial graphics for single jersey samples

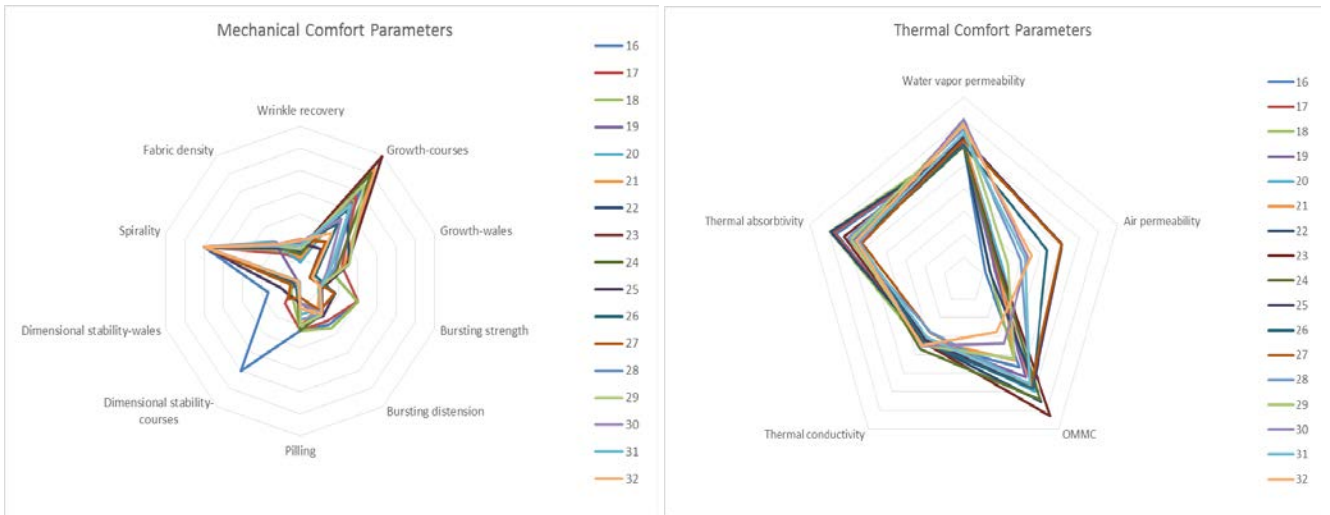


Figure 2. Multi-axial graphics for cross miss samples

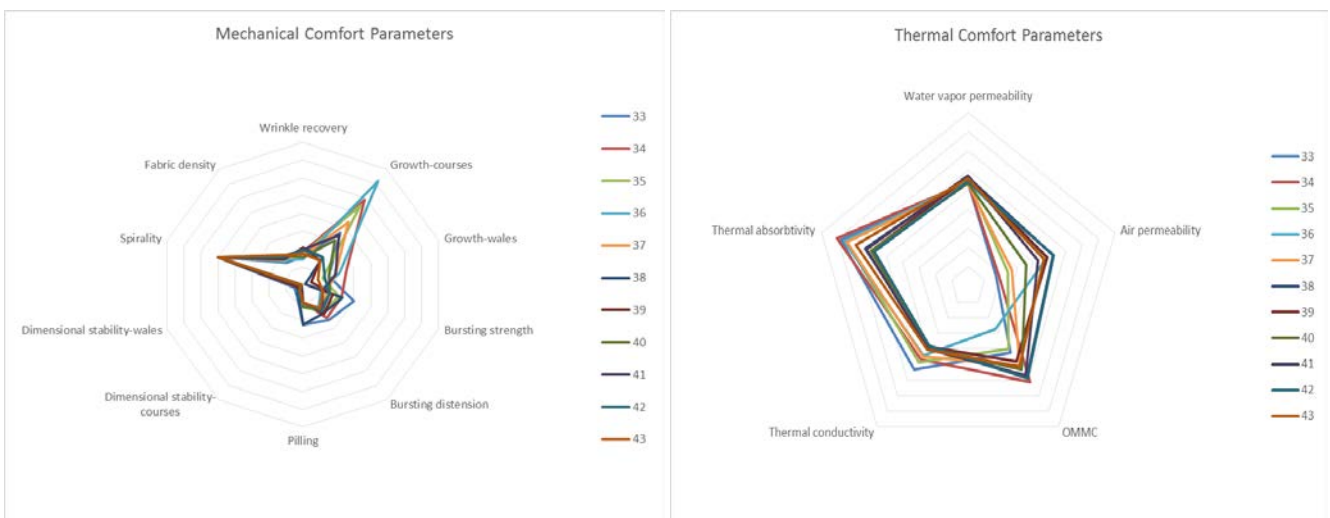


Figure 3. Multi-axial graphics for double-face samples

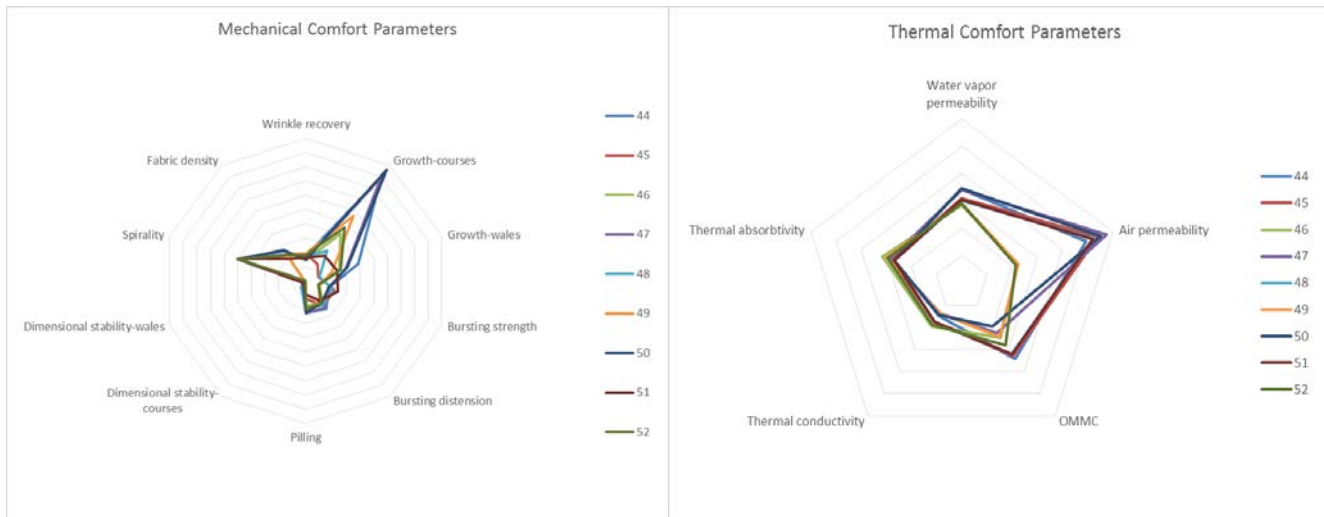


Figure 4. Multi-axial graphics for stitch transferred samples

Table 6. Comfort values of the samples

Knit Type	Sample Code	Graphic Area (Mechanical Properties)	Graphic Area (Thermal Properties)	Total Comfort Value (TCV)
Single Jersey	1	66,84	46,11	53,02
	2	35,28	57,14	49,85
	3	57,98	35,99	43,32
	4	55,67	43,37	47,47
	5	29,96	63,55	52,35
	6	41,78	46,03	44,61
	7	45,09	66,68	59,48
	8	34,57	92,85	73,42
	9	46,14	57,52	53,73
	10	35,68	54,26	48,07
	11	43,28	54,70	50,89
	12	45,69	57,53	53,58
	13	37,41	51,85	47,03
	14	28,41	56,98	47,46
	15	23,63	71,99	55,87
Cross miss	16	82,18	41,75	55,23
	17	55,81	47,50	50,27
	18	53,96	44,81	47,86
	19	28,32	41,07	36,82
	20	49,41	46,55	47,50
	21	48,42	42,75	44,64
	22	43,41	48,49	46,80
	23	56,87	50,82	52,83
	24	47,10	46,63	46,79
	25	34,47	62,88	53,41
	26	35,18	57,35	49,96
	27	32,99	58,56	50,04
	28	39,02	51,35	47,24
	29	50,66	47,72	48,70
	30	36,32	49,17	44,89
31	38,74	51,13	47,00	
32	30,63	47,74	42,03	
Double-Face	33	50,73	58,32	55,79
	34	61,18	62,49	62,05
	35	42,94	56,85	52,21
	36	50,81	59,86	56,85
	37	41,45	58,89	53,07
	38	34,22	67,68	56,53
	39	30,07	59,66	49,80
	40	36,34	54,44	48,40
	41	39,59	63,05	55,23
	42	32,00	64,36	53,57
43	27,34	65,22	52,59	
Stitch transferred	44	97,70	99,72	99,05
	45	34,67	102,77	80,07
	46	32,25	60,63	51,17
	47	86,10	93,70	91,17
	48	41,11	97,16	78,47
	49	39,52	53,34	48,74
	50	88,86	87,51	87,96
	51	40,59	97,49	78,53
	52	51,55	60,37	57,43

From the method used we had the following statements:

1. It is known that synthetic fibers are widely preferred in sportswear market it is contributed to better comfort sensations. The study showed that the TCV value of 100% polyester (PET) and polypropylene (PP) fabrics were higher than that of 100% cotton samples in all knit type in accordance with the sportswear market choice. Within the samples, high TCV values were obtained by PP and PET fabrics with stitch transferred patterns, which also fits well with the latest recent sportswear trends on mesh-structured synthetic fabrics. As observed in single jersey fabrics, TCV

value increased as the synthetic fiber portion in the fabric increases and that is induced greatly by thermal properties. Also as the yarn fineness increased, single jersey fabrics gave better heat/mass transfer (thermal comfort) property but worse mechanical performance (mechanical comfort) which also agrees with the literature [17, 18].

2. For cross miss and double-sided fabrics, the samples with the synthetic face side, which in touch with human skin had higher TCV for cotton face. Also, fabrics with polypropylene face introduced better TCV for polyester face and polypropylene / cotton blends had higher TCV than polyester / cotton blends among double-face knitted samples. As the transferred stitch length increases (from 1st report stitches to 3rd report) an important change at TCV was not observed.

3. Among the results, it was also stated that polyester, as a widely used fiber type in sportswear may be replaced with polypropylene fiber with highly acceptable comfort performance.

4. The findings were also revealed with wear trials [19] where 12 male and 12 female volunteers with similar BMI (Body Mass index) have worn shirts produced by 100% polypropylene, polyester and cotton single-jersey (Samples 7-9) and stitch transferred fabrics (Sample 44-46). The volunteers were asked to complete a questionnaire for comfort assessment rating the comfort level of 1 – 5 (5 is the most comfortable) after low and high level physical activity. The stitch transferred shirts were rated as “more comfortable” especially after high activity level; and the shirts which were rated more comfortable by the questionnaire after the wear trials have been produced by high TCV fabrics. It was also noted that the differences

between TCV values of synthetic and cotton stitch transferred samples was higher than single jersey fabrics which is concluded that the wearer’s subjective perception on separating the comfort level of synthetic and cotton would be easier for stitch transferred fabrics. Wear trials also pointed the same result with higher comfort level rating differences among stitch transferred shirts (lower for cotton).

4. CONCLUSION

This study focused on introducing a new approach on objective comfort assessment of sportswear knitted fabrics. The method comprised various test and analysis of mechanical and thermal (heat / mass transfer) properties of the samples; then the results were converted to axis values to draw multi-axial graphics. The attempt for converting the results was to draw any possible larger area since the area was used to calculate a new value called Total Comfort Value (TCV). It was found that comfort assessment based on TCV agreed with literature findings and latest trend in sportswear industry. The TCV was also verified by wear trials, the study of which is prepared for publication. The future work will be on determining any weighting factors to better understand the effect of fabric parameters on comfort that may be strengthen the method proposed but the current method seems to be satisfying.

Acknowledgement

This work was supported by the TUBITAK under Grant number 5150091 and by Gaziantep University under Grant number MF.ALT.18.03. The authors also wish to thank Mr. Gassan Asker and Akarca Mensucat / K.Maraş for pre-treatment process of the samples.

REFERENCES

1. Gunesoglu S, Meric B. 2006. Heat and mass properties of 2-yarn fleece knitted fabrics. *Indian Journal of Fibre & Textile Research* 31, 415-421.
2. Tastan E, Meric B. 2015. Thermophysiological comfort properties of different knitted fabrics used in cycling clothes. *Textile Research Journal* 85(1), 62-70.
3. Hes L, Gunesoglu C, Gunesoglu S. 2015. Analysis of heat transfer in inflatable sleeping pads. *Tekstil ve Konfeksiyon* 25(4), 289-292.
4. Iftikhar F, Zulfiqar A, Hussain T, Nazir A, Adolphe DC. 2019. Influence of yarn count and cover factor on mechanical, comfort, aesthetic and hand properties of ladies’ summer apparel fabrics. *Journal of Natural Fibers* DOI: 10.1080/15440478.2019.1692322
5. Behera BK, Mishra J. 2007. Comfort properties of non-conventional light weight worsted suiting fabrics. *Indian Journal of Fibre & Textile Research* 32, 72-79.
6. Sztandera LM, Cardello AV, Winterhalter C, Schutz H. 2013. Identification of the most significant comfort factors for textiles from processing mechanical, handfeel, fabric construction, and perceived tactile comfort data. *Textile Research Journal* 83(1), 34-43.
7. Uren N, Okur A. 2019. Analysis and improvement of tactile comfort and low-stress mechanical properties of denim fabrics. *Textile Research Journal* 89(23-24), 4842-4857.
8. Taieb AH, Msahli S, Sakli F. 2010. A new index for evaluating the mechanical comfort of linen fabric. *Journal of Natural Fibers* 7, 251-266.
9. Mehrtens DG, McAlister KC. 1962. Fiber properties responsible for garment comfort. *Textile Research Journal* 32(8), 658-665.
10. Uddin MH, Hassan A, Nesa MI, Sharmin Z, Bhuiyan SH. 2019. Effects of different count and stitch length on spirality, shrinkage and gsm of knit fabrics. *IOSR Journal of Polymer and Textile Engineering* 6(6), 33-39.
11. Behera BK. 2007. Comfort and handle behaviour of linen-blended fabrics. *AUTEX Research Journal* 7(1), 33-47.
12. Gunesoglu S, Meric B, Gunesoglu C. 2005. Thermal contact properties of 2-yarn fleece knitted fabrics. *Fibres & Textiles in Eastern Europe* 13(2), 46-50.
13. Bedek G, Salaun F, Martinkovska Z, Devaux E, Dupont D. 2011. Evaluation of thermal and moisture management properties on knitted fabrics and comparison with a physiological model in warm conditions. *Applied Ergonomics* 42, 792-800.
14. Oglakcioglu N, Marmarali A. 2007. Thermal comfort properties of some knitted structures. *Fibres & Textiles in Eastern Europe* 155-62), 64-65.

-
15. Selli F, Turhan Y. 2017. Investigation of air permeability and moisture management properties of the commercial single jersey and rib knitted fabrics *Tekstil ve Konfeksiyon* 27(1), 27-31.
 16. Geraldes MJ, De Araujo M, Hes L. 2001. High Performance Functional Knit Structures. Proceedings of the Tecnitex 2001 Autex Conference, 227-235, Minho, Portugal
 17. Yang Y, Yu X, Chen L, Zhang P. 2020. Effect of knitting structure and yarn composition on thermal comfort properties of bi-layer knitted fabrics. *Textile Research Journal* DOI: 10.1177/0040517520932557
 18. Tyagi GK, Bhattacharya S, Kherdekar G. 2011. Comfort behaviour of woven bamboo-cotton ring and MJS yarn fabrics. *Indian Journal of Fibre & Textile Research* 36, 47-52.
 19. Babalık E, Gunesoglu S, Gunesoglu C. A survey study on subjective clothing comfort assessment of a sportswear clothing, Manuscript in preparation